

**FINITE ELEMENT MODELING OF IMMISCIBLE
HYDROCARBONS IN GROUNDWATER
SYSTEMS**

By

JAMES EDWARD MARTELL

Bachelor of Science in Arts and Sciences

Oklahoma State University

Stillwater, Oklahoma

1986

**Submitted to the Faculty of the
Graduate College of the
Oklahoma State University
in partial fulfillment of
the requirements for
the Degree of
MASTER OF SCIENCE
July 1989**

FINITE ELEMENT MODELING OF IMMISCIBLE
HYDROCARBONS IN GROUNDWATER
SYSTEMS

Thesis Approved :

Antyari

Thesis Adviser

William F. McManis

Manu Bato

Nauman N. Dushan

Dean of the Graduate College

ACKNOWLEDGEMENTS

I wish to express my deep gratitude to the many people who have made my graduate work at Oklahoma State University a rewarding experience.

Foremost, I am grateful to Dr. A. K. Tyagi for his support, encouragement, and his constructive criticism. I wish also to thank Dr. William McTernan and Dr. Marcia Bates for their service on the graduate committee and assistance during the course of this study. I am also grateful for all of the support that I have received from the faculty and staff of the Civil Engineering Department. Without the love and support of my parents, Paul and Patricia Martell I would have never made it to where I am now. They have been a great inspiration in my life and words can not express my great love and respect for each of them. I would also like to thank my brothers Craig and Paul and my sister Mary Ann for their humor, friendship and belief in me.

Finally, I would like to thank the many friends that I have made here at Oklahoma State University over the years and I wish them much luck in their future endeavors.

TABLE OF CONTENTS

Chapter	Page
I. INTRODUCTION	1
Behavior of Immiscibles	2
Immiscible Compounds	4
Hydrocarbons	4
Three Phase System	6
MOFAT 2-D Model Introduction	9
II. REVIEW OF LITERATURE	11
Petroleum Industry Models -1950's	11
Hydrocarbon Contaminants Models-1970's	12
Hydrocarbon Contaminant Studies-1970's	17
Modeling in the Late 1970's and 1980's	22
Casulli and Greenspan	23
Charles Faust	23
Hochmuth and Sunada	24
Abriola and Pinder	26
Corapcioglu and Baehr	27
Overview	30
III. MATERIALS AND METHODS	32
Computer Equipment	32
Model Theory	33
Multiphase Flow Equations	34
Finite Element Formulation	36
Addressing Element Matrices	37
Treatment of Non-Linearity	38
Mass Conservation and Capacity	39
Updating of Nodal Pressure Heads	39
Description of Sensitivity Analysis	40
Discussion of Parameters	44
IV. RESULTS AND DISCUSSION	50
Oil and Water Saturations (Node 116)	50
Alpha Parameter	50
N Parameter	57

Chapter	Page
Porosity Parameter	57
Permeability (Ksw) Parameter	62
Density Parameter	71
Viscosity Parameter	71
Oil Heads at Node 116	78
Alpha Parameter	78
N Parameter	82
Porosity Parameter	82
Permeability (Ksw) Parameter	84
Density Parameter	84
Viscosity Parameter	86
Oil Velocities	88
Alpha Parameter	88
N Parameter	88
Porosity Parameter	90
Permeability (Ksw) Parameter	90
Density Parameter	92
Viscosity Parameter	92
Plume Configuration	93
Alpha Parameter	93
N Parameter	93
Porosity Parameter	94
Permeability (Ksw) Parameter	94
Density Parameter	94
Viscosity Parameter	94
Central Processing Unit (CPU) Time	95
Time For Total Oil Infiltration	95
 V. CONCLUSIONS	 102
REFERENCES	108
APPENDICIES	113
APPENDIX A - RECOMMENDED JCL SAMPLE FOR IBM 3081K	 114
APPENDIX B - INPUT DATA USED FOR MOFAT-2D SIMULATION	 115
APPENDIX C - PLOTS OF HYDROCARBON PLUMES FOR MOFAT 2-D SIMULATIONS.	 124
APPENDIX D - CURVE EQUATIONS FOR INFILTRATION TIME VS PARAMETER	 148

LIST OF TABLES

Table	Page
I. Van Genuchten Soil Equations	41
II. Sensitivity Analysis Parameters	42
III. Soil and Fluid Properties Used in MOFAT 2-D Runs	46
IV. Characteristic Values of Alpha and N For Soils	48
V. CPU Times and Computer Costs For Parameters	97

LIST OF FIGURES

Figure	Page
1. Transport of Low Density Immiscible Hydrocarbons	3
2. Transport of High Density Immiscible Hydrocarbons	3
3. Generalized View of the Three Phase System	8
4. MOFAT-2D Finite Element Grid	45
5. Saturation vs Time $\alpha = .05/m$	52
6. Saturation vs Time $\alpha = .2/m$	52
7. Saturation vs Time $\alpha = .3/m$	53
8. Saturation vs Time $\alpha = .4/m$	53
9. Saturation vs Time $\alpha = .5/m$	54
10. Saturation vs Time $\alpha = .6/m$	54
11. Saturation vs Time $\alpha = .7/m$	55
12. Saturation vs Time $\alpha = .8/m$	55
13. Saturation vs Time $\alpha = .9/m$	56
14. Saturation vs Time $\alpha = 1.0/m$	56
15. Saturation vs Time $N = 1.2$	58
16. Saturation vs Time $N = 1.4$	58
17. Saturation vs Time $N = 1.6$	59
18. Saturation vs Time $N = 1.8$	59

Figure	Page
19. Saturation vs Time N=2.0	60
20. Saturation vs Time N=2.2	60
21. Saturation vs Time N=2.4	61
22. Saturation vs Time N=2.6	61
23. Saturation vs Time Porosity=5%	63
24. Saturation vs Time Porosity=10%	63
25. Saturation vs Time Porosity=20%	64
26. Saturation vs Time Porosity=25%	64
27. Saturation vs Time Porosity=30%	65
28. Saturation vs Time Porosity=40%	65
29. Saturation vs Time Porosity=45%	66
30. Saturation vs Time Porosity=50%	66
31. Saturation vs Time Ksw=.2	68
32. Saturation vs Time Ksw=.4	68
33. Saturation vs Time Ksw=.5	69
34. Saturation vs Time Ksw=.6	69
35. Saturation vs Time Ksw=1.0	70
36. Saturation vs Time Density=.4	72
37. Saturation vs Time Density=.6	72
38. Saturation vs Time Density=.8	73
39. Saturation vs Time Density=1.0	73
40. Saturation vs Time Density=1.2	74
41. Saturation vs Time Density=1.6	74
42. Saturation vs Time Density=1.8	75

Figure	Page
43. Saturation vs Time Viscosity=.7	76
44. Saturation vs Time Viscosity=1.0	76
45. Saturation vs Time Viscosity=1.5	77
46. Saturation vs Time Viscosity=1.7	77
47. Saturation vs Time Viscosity=2.0	79
48. Saturation vs Time Viscosity=2.3	79
49. Saturation vs Time Viscosity=2.5	80
50. Oil Head vs Time For Alpha Parameter	81
51. Oil Head vs Time For N Parameter	81
52. Oil Head vs Time For Porosity Parameter	83
53. Oil Head vs Time For Ksw Parameter	83
54. Oil Head vs Time For Viscosity Parameter	85
55. Oil Head vs Time For Density Parameter	85
56. Horizontal Oil Velocity Alpha Parameter	87
57. Horizontal Oil Velocity N Parameter	87
58. Horizontal Oil Velocity Porosity Parameter	89
59. Horizontal Oil Velocity Ksw Parameter	89
60. Horizontal Oil Velocity Density Parameter	91
61. Horizontal Oil Velocity Viscosity Parameter	91
62. Total Time of Oil Infil. vs Alpha	99
63. Total Time of Oil Infil. vs N	99
64. Total Time of Oil Infil. vs Porosity	100

Figure	Page
65. Total Time of Oil Infil. vs Ksw	100
66. Total Time of Oil Infil. vs Density	101
67. Total Time of Oil Infil. vs Viscosity	101

CHAPTER I

INTRODUCTION

The contamination of groundwater aquifers by hydrocarbons is a rapidly growing environmental problem. Until recently, contamination of public and private drinking water supplies by residual oil, leaking storage tanks, or leaking oil pipe lines was rarely thought of as a serious environmental problem. Besides leaky storage tanks and petroleum pipe lines, oils and gasolines can be introduced into the subsurface by land application of refinery waste by-products (Baehr 1984) and through urban runoff. In order for a hydrocarbon contaminant in the subsurface to be removed effectively by the various removal techniques, the contaminants' position and concentration must be understood. Often it is useful to predict the movement of hydrocarbon contaminants by means of mathematical computer models. Because hydrocarbons are immiscible (i.e. incapable of being mixed with water) with the exception of some soluble fractions, they behave differently from other contaminants. Their subsurface movement is subsequently difficult to predict. One problem in the prediction of hydrocarbon

movement is that of multi-phase transport. According to Baehr (1984), hydrocarbon contaminants may undergo transport as four separate phases: 1. as solutes in water, 2. as vapors in air, 3. as unreacted constituents in an immiscible phase, and 4. as adsorbed constituents onto soil surfaces. Each of these phases and its behavior in the subsurface as well as its behavior with other hydrocarbon phases must be addressed by the computer models.

Behavior of Immiscibles

According to Baehr (1984) the density of contaminants that are immiscible in water is either less than or greater than that of water. This difference in density produces two distinct scenerios. If the density of the contaminant is less than that of water, the hydrocarbon contaminant will, if it reaches the saturated zone, move along the top of the water table (Figure 1). If the plume reaches the saturated zone and its density is greater than that of water, it will proceed down to the lower regions of the water table (Figure 2). Besides hydrocarbon density and phase relationships, Kovski (1970) suggests that viscosity, release rate, release volume, water table gradient, depth to water table, permeability and the amount of water flushing the vadose zone play an important role in hydrocarbon transport. Viscosity, which is dependent on temperature,

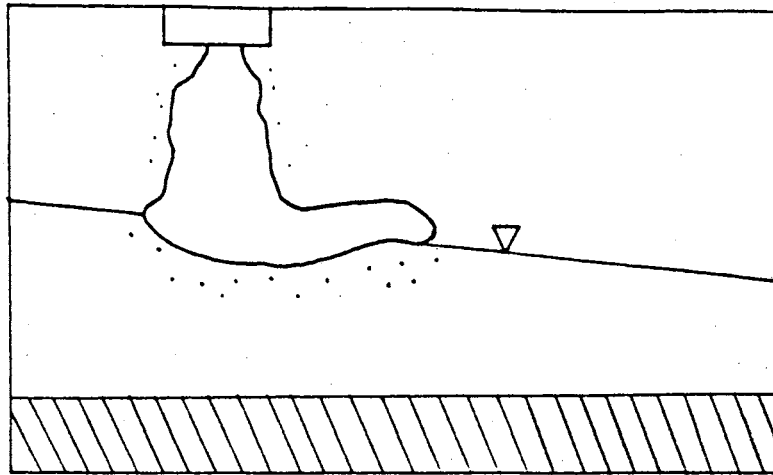


Figure 1. Transport of Low Density
Immiscible Hydrocarbons

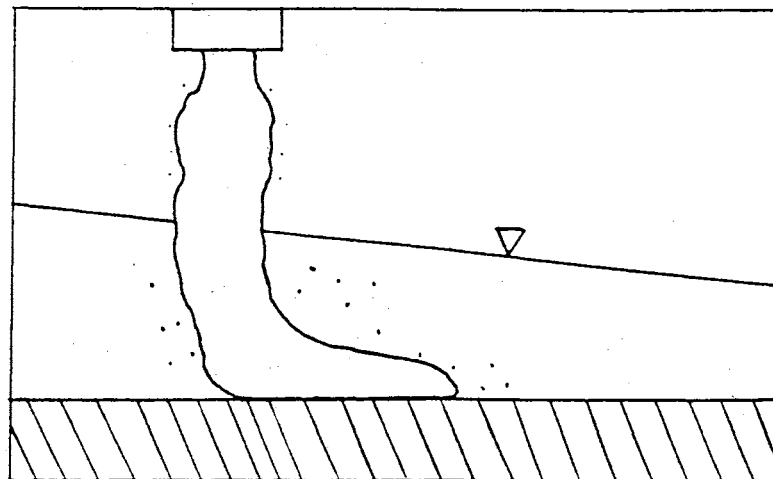


Figure 2. Transport of High Density
Immiscible Hydrocarbons

acts to slow down migration rates both vertically and horizontally. Therefore, migration potential for less viscous hydrocarbons is greater than that for viscous hydrocarbons. Release rate and volume will often dictate whether the hydrocarbon plume will reach the water table or remain at residual saturation in the unsaturated zone. High release rates and volumes will allow the plume to overcome capillary forces and flow downward under gravitational forces.

Immiscible Compounds

There are two types of immiscible compounds. These are heterogeneous and homogeneous immiscibles. Heterogeneous immiscible compounds contain more than one molecular constituent. An example of a heterogeneous immiscible compound is gasoline. Homogeneous immiscible compounds consist of only one molecular constituent. 1,1,1-trichloroethylene is an example of a homogeneous compound (Baehr 1984). Heterogeneous immiscible hydrocarbon contaminants are the primary focus of this research.

Hydrocarbons

Hydrocarbons is a broad term for a unlimited number of hydrogen-carbon bonded molecules. Carbon can combine with itself covalently in single, double and triple bonds.

These bonds may form long carbon chains and rings that lead to the nearly two million hydrocarbon compounds that have been identified (Goodger 1975). Hydrocarbons are considered to be saturated if they contain all of the hydrogen possible for bonding. Unsaturated hydrocarbons are those that do not have enough hydrogen for complete carbon to hydrogen bonding to occur at every bond site. Unsaturation causes the carbon compounds to form double and triple bonds (Burcik 1961). Two general hydrocarbon molecular structures can be described. The carbon-hydrogen molecules can form open chain type structure, known as the alkanes, or closed chain ring-type structure, known as the cyclanes. Open chain hydrocarbons can also be delineated into straight chains and attached side chains. According to Goodger (1975) there are five main hydrocarbon groups. The alkanes, also known as the paraffins, are a saturated open chained group having a general structure of C_nH_{2n+2} . Because they are saturated, they are stable and chemically unreactive. Some examples of the common alkanes are methane, ethane, propane, and butane. The cyclanes, also known as the cycloparaffins, are single ring saturated hydrocarbons having a general structure of C_nH_{2n} . The cyclanes because of their saturation state, are very stable and have very similar properties to the alkanes. The cyclanes are very important constituents in crude oils (Burcik 1961).

The alkenes, sometimes referred to as the olefins, are unsaturated double bonded open chain hydrocarbons.

Although the alkenes have the same general molecular formula as the cyclanes, they are unstable because of their unsaturated state. The alkenes are formed during refining processes and are not formed naturally. Another unsaturated hydrocarbon group is the alkynes also known as the acetylenes. The alkynes are open chained hydrocarbons containing one carbon to carbon triple bond. The alkynes are very unstable and have a high combustion temperature and flame speed. Finally the last group of unsaturated hydrocarbons having a low hydrocarbon to carbon ratio is the aromatics.

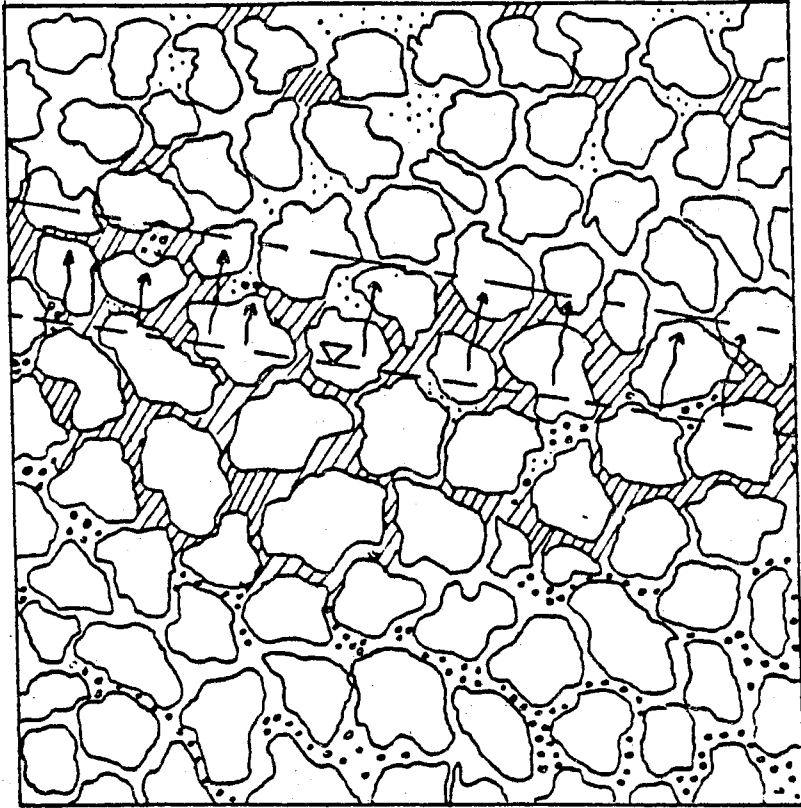
Aromatic hydrocarbons are often distinguishable because of their pleasant smell. The aromatic hydrocarbons are cyclical and are considered to be derivatives of the benzene ring. The benzene ring is comprised of alternating single and double bonds which suggests that it should be unstable, yet it is fairly stable. Benzene, a clear liquid, has been proven to be a human carcinogen and is therefore a considerable environmental threat.

Three Phase System

When hydrocarbons are introduced to a porous medium, they are often transported as three separate phases (see

figure 3). The immiscible phase, known as the non-aqueous phase liquid, travels as a unreacted constituent separate from the water. As stated earlier, the non-aqueous phase may travel along the top of the water table or along the bottom of the aquifer depending on its density as compared to water. The non-aqueous phase travels as a separate entity from water yet it is influenced in part by its fluctuations (in the case of floating hydrocarbons) and velocity. Therefore, mathematical prediction of non-aqueous phase transport is difficult to achieve. Hydrocarbon transport also may involve a gas phase. Volatile hydrocarbon constituents will occupy pore spaces as a gaseous phase as the hydrocarbon plume moves downgradient. The gaseous hydrocarbons will often displace air and water in the pores themselves. The gaseous phase travels upward in order to achieve pressure equilibrium with the atmosphere. Finally, hydrocarbons are also transported in the solute phase. Soluble fractions of the hydrocarbon are transported within the flowing groundwater as a miscible contaminant. Soluble hydrocarbon fractions often appear in downstream water wells long before the non-aqueous phase reaches the same wells.

Mathematical prediction for the transport of each of these phases and their interactions together has





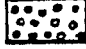


-  Gas Phase
-  Nonaqueous Phase Liquid
-  Soluble Phase
-  Water Table
-  Capillary Fringe

Figure 3. Generalized View of the Three Phase System

long been a difficult problem for modelers.

MOFAT 2-D Model Introduction

One model that attempts mathematical prediction of hydrocarbon contaminant transport is the MOFAT-2D Model. Developed in 1988 by J.J. Kaluarachchi and J.C. Parker, MOFAT-2D simulates flow and transport of three phase fluids in a two dimensional vertical domain. The model itself is a finite element FORTRAN code developed for use on a mainframe computer. The 309000 byte FORTRAN program consists of a main program and 37 individual subroutines.

For the purposes of this research, a sensitivity analysis was performed on the MOFAT-2D model in order to determine the effect of soil retention curve shape parameters alpha and N, porosity, permeability, oil viscosity and oil density on the overall output of the program. The output of the program consists of an initial summary of the input parameters and a summary at various time steps of oil and water heads, oil, water and total saturations values as well as x and y velocities for each node point in the finite element mesh. Simulations were run for a grid size of 15m X 23m. A hydrocarbon spill occurs on the land surface along a 5 meter strip of land and is allowed to infiltrate downward into the unsaturated

zone. Numerous computer runs were performed in order to assess the effect of the various input parameters on the process of infiltration and flow as predicted by the model.

CHAPTER II

REVIEW OF LITERATURE

Countless research publications on hydrocarbon contamination have appeared in the scientific community over the last thirty years. Starting with adaptations of hydrocarbon displacement models developed in the petroleum industry, groundwater hydrocarbon contaminant models have developed to a high level of sophistication and complexity. Numerous researchers have made significant contributions to the study and understanding of immiscible hydrocarbon fluid flow. The following review of some of these important authors and researchers and their contributions to the development of competent models is by no means a complete one.

Petroleum Industry Models -1950's

Studies performed within the petroleum industry on the migration of hydrocarbons, gas, and water often provided useful information for the prediction of hydrocarbon contaminant movement in groundwater systems. Jim Douglas Jr., D.W. Peaceman and H.H. Rachford Jr. in the article " A Method for Calculating Multi-Dimensional Immiscible Displacement" (1959) presented a model that simulates

movement of water in oil saturated reservoir rocks. The model was a two dimensional finite difference solution of differential equations which involve relative permeabilities, viscosity, density, capillary pressure and gravity. Comparisons of Douglas, Peaceman and Rachfords' model with other reservoir engineering models and sand tank models, showed that there was good agreement in the models results. The model was originally intended for use in the petroleum industry to describe displacement of oil by water and gas migration but, has been one of the first models applied to immiscible hydrocarbon flow.

Hydrocarbon Contaminant Models -1970's

R. Mull (1970), presented a group of equations that describe migration of hydrocarbons both vertically and horizontally under the assumption of 'piston flow'. Starting out with a generalized version of Darcy's law, Mull derived first an equation for the oil front velocity as a function of distance between source and position of the front. Vertical velocity equations were then derived and a method of predicting the outline of the whole oil body was presented.

Mull described capillary zone movement and fluid displacement by migrating oil in a set of simple equations. An equation describing migration of oil from a non-

continuous small volume source based on piston flow was also presented. As well as developing an analytical solution for predicting hydrocarbon movement, Mull carried out laboratory investigations on the various parameters that effect oil migration. Relative permeabilities for different fluid saturations and pore size distributions as well as soil moisture-capillary pressure relationships were investigated. Mull found that oil migrates to a greater distance in the capillary fringe than in the "seepage zone" (i.e. upper unsaturated zone) and that oil contaminant movement in the subsurface is an exceptionally slow process. John R. Kovski, in the early 1970's examined the physical processes for hydrocarbon contaminant movement in the subsurface. According to Kovski, the rate at which hydrocarbons are transported in an aquifer and their areal extent is dependent^{on} the following important factors:

1. Viscosity, density, release rate, and release volume of the hydrocarbon
2. Gradient of the water table
3. Water table depth and fluctuations
4. Pore size distribution of the subsoil
5. Amount of Rainfall

The work that Kovski did in his paper was taken chiefly from J. Van Dam's work (1967) on hydrocarbon transport.

Two types of infiltration rates were described by

Kovski: Fast infiltration, which produces a hydrocarbon mound thick enough to depress the water table and, slow infiltration which will not result in a mound building up. For both types of infiltration rates, the hydrocarbons, once released, will flow downward under the influence of gravity taking up the pore spaces. The oil permeability will increase and the oil taking up the pore space will be unable to take up the total pore space due to the residual concentrations of air and water. Lateral migration also occurs due to capillary forces. In slow infiltration, the hydrocarbon released is generally stopped before it reaches the capillary fringe. Air fills the pores as the oil front passes and the oil is left behind at residual saturation defined as the saturation state where suction force in the pore space prohibits further movement by gravitational forces. Lateral thinning will occur according to Kovski, until the oil reaches residual saturation everywhere. With fast infiltration, the release of hydrocarbons is enough to reach the water table and create a hydrocarbon mound.

According to Kovski, the area over which the oil will spread can be estimated by specific formulas. Kovski, indicated that the water table gradient has a distinct effect on the rate and extent of lateral movement.

B. Hoffmann (1971) addressed the problem of soluble hydrocarbon dispersion. As Hoffmann stated, oil trapped in the capillary fringe acts as a potential source of soluble

hydrocarbons which can then be transported into groundwater. Hoffmann presented a mass rate of exchange equation which was later utilized by Fried, Muntzer, and Zilliox (1979). Soluble movement through porous media can be described by the differential equations used to describe heat flow. Hoffmann described the dispersion of a soluble substance by means of the theory of probability. The probability distribution of the occurrence of an element at a particular point in a homogeneous isotropic medium is a normal distribution. Hoffman suggested that if a number of elements originate from the same point, the concentration distribution can be derived by superimposing the probabilities. The coefficient of dispersion is essentially a measure of the distribution.

Hoffmann, taking into account chemical and biological effects (absorbtion, reduction) on the concentrations, presented a dispersion equation. Considering the assumptions of a point source of pollution, Hoffmann solved the differential dispersion equation for: a continuous point source, a finite point source, and an instantaneous point source. The solutions of these equations give an area in which lines of equal concentration could be plotted allowing the plume to be defined.

Hoffmann, with the aid of a soil column, performed experiments to determine the dispersion coefficients for

various soils. Dispersion was, according to Hoffmann, affected by the pore size distribution and therefore a parameter that is related to it must be found. Through evaluation of field tests and laboratory tests, Hoffmann suggested the use of an "effective" mixing parameter. This parameter took into account microbial and chemical effects on dispersion. Four soils were investigated successfully by Hoffmann for an "effective" mixing parameter.

M. Van Der Waarden, W.M. Groenewoud and A.L.A.M. Birdie in a well known article written in 1971 presented their work on transport of soluble hydrocarbon components in soils. In the article "Transport of Mineral Oil Components to Groundwater - I", an explanation of the authors experiments performed as well as the results were presented. Experiments were done using a cylindrical glass tube with a diameter of 4.8 cm and a glass particle pack of 80 cm in height. The apparatus was built as simple as possible in order that other investigators can duplicate it for verification or other purposes. A residual oil zone was created so that the trickling water may pass through it. Tests were performed to measure 2-isopropylphenol in an aromatic free gas oil, o-xylene in the same gas oil, components of a gasoline fraction, components of a kerosine, and various components of a gas oil. From the

experiments performed, the authors found that the rates of dissociation for water soluble components in hydrocarbons are determined by the partition coefficients of the components and the water/oil ratios. It was also found that oil zones do not perceptibly move when fluctuations in the groundwater table occur. No adsorption was seen in the experiments carried out because the medium used was glass particles. Preliminary experiments that were carried out on natural dune sands indicated that adsorption effects were slowing down the extraction of the soluble components. No biodegradation occurred due to the short residence time in the simulated soil column. Evaporation of lower molecular weight hydrocarbons was also suggested by the authors but no further study was performed.

Hydrocarbon Contaminant studies -late 1970's

In 1977 M. Van Der Waarden, W.M. Gronewoud and A.L.A.M. Bridié published a second article entitled "Transport of Mineral Oil Components To Groundwater II". This paper examined the adsorption of hydrocarbons onto various soil types. Using the same soil column apparatus in their earlier experimentation, the authors used glass particles, dune sand, a sand containing clay, limestone and sterilized natural compost as the soil medium. The oil used in the

experiment was 2-Isopropylphenol (IPP) which is miscible with gas oils and fairly soluble in water.

Results indicated that pure sand, limestone, and clay do not have a high adsorptive power. Adsorption onto the compost was two to three times higher. It was found that the IPP did not desorb totally. When the IPP solution was percolated through dune sand, retardation in the breakthrough curve and lower maximum hydrocarbon concentrations were observed. When the compost was used as the column media no IPP appeared in the drain water during the experimental period. Studies with kerosine in the various soil packs backed up the previous conclusion that limestone acts as a very weak adsorbent material and the other media acts to lower the peak concentrations and delays appearance of the soluble fractions.

Differentiation of the soluble fractions based on their boiling range temperatures was studied. High temperature fractions are less soluble and more readily adsorbed. Lower temperature fractions (<175°C) tended to evaporate from their aqueous state rapidly. It was found that fractions with a boiling range of 175 to 350°C were most likely to dissolve and produce odors in drinking water.

J.J. Fried, P. Muntzer and L. Zilliox (1979) studied the transport of lighter hydrocarbons. According to the authors, an oil entering into the soil will meet the water

and air phases and will flow as a polyphasic immiscible fluid. Depending on the saturations of the various fluids and their movement, the parameters considered should be the soil and fluid parameters, relative permeabilities, and capillary pressures. Fried, Muntzer and Zilliox indicated that three phase flow equations are difficult to deal with due to the complex boundary conditions and hysteresis effects in the relationships between capillary pressure relative permeabilities, and saturation. The authors described the process of hydrocarbon contamination as follows: When oil enters into the soil as a massive spill it will infiltrate down under the influence of gravity. The oil will reach the capillary fringe if the amount of the spill is greater than that of the retention capacity of the soil (assuming a somewhat heterogeneous soil). Spreading will occur on the water table horizontally and with water table fluctuations. If the oil body does not reach the water table, dissolved fractions may still reach it and travel with its flow.

A mass rate of exchange equation (i.e. the quantity of product dissolved per unit time) was presented. The quantity of exchange increases with increased flow velocity but also decreases with time. The authors used the partition coefficient assumption that had been developed earlier by Van der Waarden et al.(1971) with the

stipulation that an oil body undergoes chemically selective and progressive flushing. The assumption developed by Fried, Muntzer and Zilliox was that in a soil which contains oil at a concentration less than that of residual saturation, the concentration of dissolved hydrocarbon fractions does not vary significantly with water flow velocity. Experiments on toluene, isooctane and a gas oil were performed in order to verify this assumption. The results supported the assumption that water flow velocity is not significant in effect with the usual ranges of velocities found in an aquifer.

Besides the well known physical effect of dispersion, Muntzer and Zilliox suggested that the mechanisms of adsorption, evaporation, and biochemical degradation can effect the dissolved fraction as well as the undissolved fraction. Evaporation, according to the authors, causes a greater area of potential exchange with infiltrating precipitation water. Adsorption can cause separation of the compounds as well as act to delay or hold the contaminant on the soil grains. Biochemical degradation acts also to slow down or stop the transport of hydrocarbons. The main parameters that effect the level of biodegradation is pH, humidity, temperature and the availability of free oxygen.

Three separate approaches were taken by J.J Duffy,

E. Peake and M.F. Mohtadi (1979) in their evaluation of the effects of an oil spill on groundwater quality. In the first part, they developed and applied a theoretical model that can predict oil concentrations in ground water. Secondly, they described laboratory experiments designed to assess exact oil concentrations and types of hydrocarbons remaining in the subsoil. Finally actual field measurements were examined at specific oil spill sites.

Based on the work of Hoffmann (1971) and others working with miscible contaminant transport, a model was developed to predict oil concentrations in water as a function of distance and time. The model took into account such abstractions as convective transport, dispersion -diffusion, adsorption-desorption and biochemical reactions. The authors supported Muntzer and Zilliox's' conclusions that Biochemical reactions were dependent on type of microorganisms, oxygen availability, moisture content, pH and others parameters. Biochemical degradation in the adsorbed phase was neglected in the model. The model was adaptable to two and three dimensional cases and boundary conditions were assumed to be constant oil concentrations entering into the unsaturated zone. Soil trough experiments were performed to study soluble fraction concentrations for a crude oil spilled over the top of a

uniform sand. The experiments supported Van der Waarden's (1971) conclusion that equilibrium concentrations of soluble hydrocarbons can be reached with percolation. Concentrations of the soluble fractions changed with the water volume percolated. Some compounds were more readily reduced in concentration while others persisted in the soil after extensive percolation of water. Fertilizer and soil inoculum were added to the soil zone containing oil in order to accelerate biodegradation. Biodegradation was found to have increased. Irrigation was continued and water samples were analyzed for soluble fractions. The results showed that there was a significant increase in soluble hydrocarbons after fertilizer was added. Therefore the hypothesis was formed that the biochemical breakdown of insoluble to slightly soluble hydrocarbons will yield soluble compounds.

Modeling in the Late 1970's and 1980'S

Finite difference and finite element analysis used in the design and testing of structures and in heat flow analysis was easily adapted for the prediction of contaminant movement. In the late 1970's and early 1980's numerous modelers utilized finite difference and finite element methods in the design of their increasingly complex models.

Casulli and Greenspan

V. Casulli and D. Greenspan (1982) developed two separate finite-difference models dealing with immiscible and miscible fluid flow. The governing equations of conservation of momentum, conservation of volume and conservation of mass were approximated using a finite difference method. Boundary conditions for the governing equations were given by either the pressure or the normal velocity components of the two fluids. For purposes of testing the immiscible model, computer runs were for different cases of differing pressure values, time increments, and outflow discharge rates. Casulli and Greenspan developed the model for use in the petroleum industry as well as the groundwater industry. They were successful in presenting a fast, efficient, and accurate way of numerical prediction.

Charles Faust

Charles R. Faust in 1985, presented a simplistic comprehensive model for both unsaturated and saturated flow. Faust's model was a derivation of petroleum reservoir engineering models that had been used consistently within the petroleum industry. The model presented was based on conservation of mass equations for

three phase fluid flow derived by Peaceman (1977). Simplification of these equations using the assumption that pressure gradients are negligible and air pressure is at atmospheric pressure, allowed for less complex equations and fewer unknowns, saving time and money. Another simplifying assumption used by Faust was that at shallow depths, densities and viscosities are not dependent on pressure. Two nonlinear equations were produced and solved using a finite-difference scheme. For verification purposes, Faust addressed two separate problems. One problem involved a 1500 day waterflood of a petroleum reservoir. This problem had an analytical solution with which Faust could compare. The second problem simulated by the model was that of two-dimensional flow problem in the unsaturated zone. Although a analytical solution was not available for comparison, the model results were compared against results from the SATURN (Huyakorn et al., 1983) and UNSAT2 (Neuman et. al.,1974) models. Good agreement in both scenerios was observed. The model was found to be stable stable and can be applied to numerous cases.

Hochmuth and Sunada

David P. Hochmuth and Daniel K. Sunada (1985) presented a numerical model to simulate two phase

immiscible fluid flow in a groundwater environment. Hochmuth and Sunada in the development of their model, which is applicable only to unconfined aquifers under transient flow conditions, examined the relationships between the air, water and oil systems in the aquifer materials. The most important relationship according to the authors is that between the capillary pressure and saturation. According to Hochmuth and Sunada, the capillary pressure is equal to the pressure of the non-wetting fluid minus the wetting fluid (the fluid which is more readily absorbed onto the soil grains). As is the case of any two-phase immiscible system, saturation decreases with increasing capillary pressure. Also permeability of a porous media to either wetting or non-wetting fluids is dependent on the saturation. Saturation of the fluid must be above residual saturation in order to be mobile under normal ground-water conditions. According to Hochmuth and Sunada, the oil pressure must be greater than the entry pressure (value of capillary pressure in which water saturation decreases rapidly) in order for the oil to travel. With downward migration of the oil due to gravity, air and some residual hydrocarbons will remain in the pore spaces in which the front moved through. The oil will strive for residual saturation by spreading. Once on the water table, the oil usually forms

a mound and travels down-gradient until residual saturation is achieved. Hochmuth and Sunada do not address the problem of dissolved fractions that travel in the water itself.

Formulas dealing with fresh/salt water interfaces were essentially adapted by Hochmuth and Sunada for the purpose of developing the model although capillary pressure could not be ignored as it is in fresh/saline water interface formulations. Partial differential equations used in the model were solved by means of a Galerkin finite-element method. Non-steady flow in a horizontal direction for both oil and water (joined by a sharp interface) is simulated by the model.

Two means of verification were applied to the model. One being a approximate analytical solution and the other a laboratory investigation. Although an exact analytic solution for the two-phase immiscible flow problem had not been developed, an approximate analytical solution based on the theory of Hantush (1968) on fresh water lenses in saline aquifers was used. Both the analytical solution and the laboratory solution showed good agreement when compared to the models results.

Abriola and Pinder

Recently in 1985, Linda Abriola and George Pinder

presented a one dimensional implicit model for multiphase flow in their papers "A Multiphase Approach to the Modeling of Porous Media Contamination by Organic Compounds" parts 1 and 2. In the first paper, equations based on conservation of mass principles were developed for the model. The equations took into account an immiscible phase as well as a soluble phase. Adsorption of water onto the soil as well as migration or formation of water vapor was not addressed. Equation development proceeded by developing the mass balance equations for the soil phase, water phase, soluble phase and immiscible phase. According to the authors, these equations have included in them such things as matrix and fluid compressibility, gravity, capillarity, diffusion and dispersion. Part 2 of the paper explained the procedure used to solve the three nonlinear partial differential equations. Using a Newton-Raphson iteration method, a one-dimensional finite difference system is used to solve the equations. The model after verification was shown to be workable and useful for the prediction of three phase flow.

Corapcioglu and Baehr

In 1987, M. Yavuz Corapcioglu and Arthur L. Baehr presented a comprehensive finite-difference model for hydrocarbon contamination from sources such as storage

tanks and petroleum pipelines in the unsaturated zone. The model developed by Baehr and Corapcioglu incorporated thermodynamic theory to quantify mass partitioning between phases of each individual constituent. The model addressed transport of hydrocarbons as solutes in the water phase, vapors in the air phase and unaltered constituents in the immiscible phase. Baehr and Corapcioglu addressed various phase and chemical transformations occur after the petroleum contaminant has entered the soil.

The first assumption made by Baehr and Corapcioglu is that of the continuum hypothesis. This hypothesis states that continuous variables are used to quantify movement and composition of the mass in each phase. To begin with, the three fluid phases (oil, water and gas) were characterized by volumetric contents, densities and mass flux vectors. Individual constituents of each of these phases (oil, water and gas phases) are characterized by phase specific concentrations and phase specific mass flux vectors. The solid phase is assumed to be incompressible and is described by its bulk density and its amount of adsorbed concentrations of each constituent.

For the governing equations, Baehr and Corapcioglu started with 3 - dimensional macroscopic conservation of mass equations for each phase. Transformation of the constituents due to abiotic chemical reactions were

addressed by the model. The conservation of mass equations for the gas phase were also included. Adsorption rates, desorption rates, biodegradation rates and abiotic transformation rates were also considered. Although gas phase biotic and abiotic decomposition of hydrocarbons is unlikely they were also included for a complete formulation. Adsorption - desorption for the gas and oil phase was neglected.

Equations of state describing capillary pressures, relative permeabilities, densities and viscosities were developed. Along with this, Baehr and Corapcioglu developed equilibrium concentration equations for the relationships between the gas and oil phase, the oil and water phase and the oil adsorbed phase. This was accomplished by use of thermodynamic principles, Raoult's law and Henry's law.

For this model Baehr and Corapcioglu considered aerobic decay with *Nocardia* group and *Pseudomonas* group being the principal bacteria. From case studies of hydrocarbon contamination, evidence suggests that oxygen rather than the supply of hydrocarbons is the limiting factor on biodegradation. Biodegradation was therefore estimated by setting it equal to the equivalent of available O₂. The availability of oxygen was modeled by using a conservation of mass equation for total free

oxygen.

Overview

As one can see, the growth of immiscible hydrocarbon contaminant models has come about in the 1970s and 1980s. With the start of Immiscible flow models developed for the petroleum industry in the late fifties, Van Dam (1967) and Mull later in the early 1970s developed ways to study hydrocarbon infiltration and lateral migration ignoring capillary pressure. Hoffmann almost at the same time addressed the problem of soluble components that may leach out into the groundwater. Hoffmann presented a mass rate of exchange equation for the soluble fractions in hydrocarbon contamination. That same year Van Der Waarden, Groenewoud and Birdié presented the results of their work on soluble hydrocarbon fractions. Later in 1977 they presented their research on the effect of soils and their adsorptive properties on hydrocarbons. In the late 1970s Fried, Muntzer and Zilliox also addressed the problem of soluble fractions with the presentation of their own mass rate of exchange equation. Duffy, Peake and Mohtadi at the same time presented a tested and proven model for hydrocarbon contamination of groundwater. The model took into account convective transport, dispersion-diffusion, adsorption-desorption, and biological degradation. In the

1980s numerous researchers developed increasingly more complex models for immiscible flow. Cassulli and Greenspan in 1982 developed a model using a finite difference scheme. In 1985 Faust presented a finite difference model, derived from previous equations used in the petroleum industry, and useful for both saturated and unsaturated conditions. During that same year Hochmuth and Sunada developed a finite element model describing two-phase hydrocarbon contaminant flow in an unconfined aquifer. Also in 1985, Abriola and Pinder presented a one dimensional finite difference model which incorporated some assumptions allowing for efficiency and accuracy. Recently in 1987, Baehr and Corapcioglu presented a finite difference model for the prediction and fate of immiscible organics in the unsaturated zone.

Of all the models that had been developed over the history of immiscible contaminant modeling, there are very few that take into account the whole scenario of contamination from the point of leakage to the point of discovery in a contaminated well but, as one can see, hydrocarbon contaminant modeling has come a long way in a relatively short period of time.

CHAPTER III

MATERIALS AND METHODS

The purpose of this study is to evaluate the sensitivity of individually selected input parameters used in the MOFAT-2D computer program. The MOFAT-2D model was developed by J.J. Kaluarachchi and J.C. Parker of the Center for Environmental and Hazardous Materials Studies at Virginia Polytechnic Institute and State University. In order to complete this study, numerous computer runs were performed to simulate hypothetical situations involving hydrocarbon spill events. The selected parameters chosen for this study were each varied across a chosen spectrum of values while all other input values were kept constant. The models output was then analyzed in order to assess the effect of the individual parameters on the overall output. The importance of each parameter can then be defined.

Computer Equipment

The MOFAT-2D computer model used for this research required the use of a mainframe computer due to its size and complexity. The mainframe computer used was the IBM

model 3081K. The IBM 3081K is a member of the 3081X high performance mainframe computer family. The system runs on the MVS/SP, Version 1, Release 3.1 operating system, and can process 10.5 million instructions per second (UCC Users Manual 1985). The WYLBUR fortran 77 system application was used for compilation and linking purposes.

An IBM personal computer was used for the development of graphs and for reading input data and example problems from the 5.25 inch computer disk onto which the program was stored. IBM personal computers were used for the purpose of transferring the program onto the IBM 3081K mainframe computer.

Model Theory

The model MOFAT-2D is an immiscible hydrocarbon contaminant flow model that simulates one or two dimensional three phase flow in a porous medium. The three phases being the water phase, the non-aqueous phase liquid (NAPL) and the gas phase. MOFAT-2D utilizes a weighted upstream finite element method based on Galerkin's principle in order to get approximate solutions for the models governing equations. Assuming the gas pressure to be constant and at atmospheric pressure, the model uses the equations that follow.

Multiphase Flow Equations

Under the assumption of constant fluid properties and an incompressible porous media, the 2-dimensional cartesian flow equations used by the model are as follows

(Kaluarachchi and Parker 1988):

$$L_w(h_w) = \frac{\partial}{\partial x_i} (Kw_{ij} (\frac{\partial h_w}{\partial x_j} + u_j)) - C_{ww} \frac{\partial h_w}{\partial t} - C_{wo} \frac{\partial h_o}{\partial t} = 0 \quad (\text{EQ. 1})$$

$$L_o(h_o) = \frac{\partial}{\partial x_i} (Ko_{ij} (\frac{\partial h_o}{\partial x_j} + \rho_{ro} u_j)) - C_{oo} \frac{\partial h_o}{\partial t} - C_{ow} \frac{\partial h_w}{\partial t} = 0 \quad (\text{EQ. 2})$$

where (w) is water and (o) is oil and :

x_{ij} = cartesian spatial coordinates (i=1,2)

Kw_{ij} = conductivity tensor for water

Ko_{ij} = conductivity tensor for oil

h_w = water height equivalent pressure heads for water

h_o = water height equivalent pressure heads for oil

ρ_{ro} = oil to water density ratio

u_j = unit gravitational vector

$$C_{pq} = \phi \frac{\partial s_p}{\partial h_q} \quad p, q = o, w \text{ (fluid capacities)} \quad (\text{EQ. 3})$$

ϕ = porosity

S_p = saturation of phase p

h_q = q-phase head

Darcy velocities along the cartesian coordinates (i) for oil and water are:

$$V_{wi} = -K_{wi} \left(\frac{\partial h_w}{\partial x_j} + u_j \right) \quad (\text{EQ. 4})$$

$$V_{oi} = -K_{oi} \left(\frac{\partial h_o}{\partial x_j} + \eta_{ro} u_j \right) \quad (\text{EQ. 5})$$

Phase conductivities are described by:

$$K_{wi} = k_{rw} K_{swi} \quad (\text{EQ. 6})$$

$$K_{oi} = k_{ro} K_{swi} / \eta_{ro} \quad (\text{EQ. 7})$$

k_{rw} = relative permeability of water

k_{ro} = relative permeability of oil

η_{ro} = oil to water viscosity ratio

K_{swi} = saturated conductivity tensor for water

Initial and Boundry conditions for each phase p are as follows:

$$h_p(X_i, 0) = h_{p1}(X_i) \quad \text{over entire region for } t=0$$

$$h_p(X_i, t) = h_{p2}(X_i, t) \quad \text{type-1 along boundary segment}$$

$$V_{pi}(n_i) = q_{p1}(X_i, t) \quad \text{type-2 along boundary segment}$$

Finite Element Formulation

Exact solutions for water head and oil head values were approximated for use in the model by upstream weighting functions and Galerkin's weighted residual method. Also using this method and Green's theorem, equations 1 and 2 was written in matrix form as:

$$[A^w] \{hw\} + [B] \left\{ \frac{dhw}{dt} \right\} + [E^w] \left\{ \frac{dho}{dt} \right\} = \{F^w\} \quad (\text{EQ. 8a})$$

$$[A^o] \{ho\} + [B] \left\{ \frac{dho}{dt} \right\} + [E^o] \left\{ \frac{dho}{dt} \right\} = \{F^o\} \quad (\text{EQ.8b})$$

Where the matrices are as follows and S_e refers to the segment of the surface element e , where there are flux type boundry conditriions prevailing and R_e is the element volume and n is the total number of elements:

$$A_{IJ}^w = \sum_{e=1}^n \int_{R_e} K_{wij} \frac{\partial W_I}{\partial x_i} \frac{\partial N_J}{\partial x_i} dR \quad (\text{EQ. 8c})$$

$$A_{IJ}^o = \sum_{e=1}^n \int_{R_e} K_{oij} \frac{\partial W_I}{\partial x_i} \frac{\partial N_J}{\partial x_i} dR \quad (\text{EQ. 8d})$$

$$B_{IJ}^w = \sum_{e=1}^n \int_{R_e} C_{ww} N_I N_J dR \quad (\text{EQ. 8e})$$

$$B_{IJ}^o = \sum_{e=1}^n \int_{R_e} C_{oo} N_I N_J dR \quad (\text{EQ. 8f})$$

$$E_{IJ}^w = \sum_{e=1}^n \int_{R_e} C_{wo} N_I N_J dR \quad (\text{EQ. 8g})$$

$$E_{IJ}^o = \sum_{e=1}^n \int_{R_e} C_{ow} N_I N_J dR \quad (\text{EQ. 8h})$$

$$F_I^w = \sum_{e=1}^n \left[- \int_{R_e} K_{wij} \frac{\partial W_I}{\partial x_i} u_j dR - \int_{S_e} W_I q_{w1} dS \right] \quad (\text{EQ. 8i})$$

$$F_I^o = \sum_{e=1}^n \left[- \int_{R_e} K_{oij} \rho_{ro} \frac{\partial W_I}{\partial x_i} u_j dR - \int_{S_e} W_I q_{o1} dS \right] \quad (\text{EQ. 8j})$$

Addressing Element Matrices

According to Kalurachichi and Parker (1988), a system based on Gauss point pressure heads in place of the commonly used nodal heads was used. The purpose for using Gauss

point pressure heads was to lessen the instability and convergence problems encountered when dealing with sharp oil fronts and non-homogeneous mediums.

Treatment of Nonlinearity

In order to achieve computational accuracy not common in previously developed immiscible hydrocarbon models, Kaluarachchi and Parker (1988) developed a system by which finite element approximation can be achieved through either the Picard method or the Newton-Raphson method.

The Picard method, according to Kaluarachchi and Parker, is useful for moderately non-linear flow and transport problems. The Picard method is a finite difference approximation technique used on finite element formulations and is often the choice of many modelers because of its relative simplicity as compared to other more sophisticated methods.

However, Kaluarachchi and Parker (1988), through an input variable, allow for the use of the Newton-Raphson method. The Newton-Raphson method is the recommended method for problems that are highly non-linear. Although the Newton-Raphson method is computationally more complex, it provides faster convergence where the Picard method may fail in highly non-linear cases.

Mass Conservation and Capacity

Three separate methods to prescribe the capacity computation for each problem are allowed by MOFAT-2D. These include the time weighted scheme, the mean head analytic scheme and the modified chord-slope scheme (Kaluarachchi and Parker 1988). In the time weighted scheme, capacities are computed from pressure saturation relationships and weighted between individual time steps. In the mean head analytic scheme, previous time step and current iteration values of oil and water heads are averaged and the resulting capacity values are used. The modified chord slope method, according to Kaluarachchi and Parker, is a modified version of the chord-slope scheme which had been shown to have poor convergence under highly non-linear conditions. The modified chord-slope method uses time weighting and has been shown to have good convergence under non-linear conditions.

Updating of Nodal Pressure Heads

In order to keep nodal heads updated for each iteration, Kaluarachchi and Parker employed a scheme to account for the maximum convergence error for the whole finite element mesh. The system is based on an allowable absolute convergence error that is included in the input. Time steps are adjusted by the program so that non-linear

convergence is achieved depending on the maximum and minimum number of iterations that are prescribed by the programmer.

Description of Sensitivity Analysis

For the purposes of the sensitivity analysis, a total of six parameters were chosen to be analyzed. These include curve shape parameters alpha and n, porosity of the medium, water saturated permeability in the x and y directions, oil/water viscosity ratios, and the oil/water density ratios. The analysis of these parameters was performed using Van Genuchten soil relationship equations within the model (see Table I) and was performed solely for infiltration and flow problems only. Redistribution after infiltration was not addressed. P-cymene, a colorless relatively insoluble hydrocarbon having a formula of $[CH_3C_6H(CH_3)_2]$, was chosen as the immiscible fluid utilized in this analysis.

Simulations were run involving hypothetical problems. Initially a "base run" was performed in order to determine if any input data errors had occurred and also to determine the expected central processing unit (CPU) time required for each simulation. Once the "base run" was completed, specific parameters were altered through a pre-set range of values while all other parameters were kept constant. Table II indicates the range and increments through which

TABLE I
VAN GENUCHTEN SOIL EQUATIONS

$$\bar{S}_w = \frac{S_w - S_m}{1 - S_m}$$

$$\bar{S}_t = \frac{S_t - S_m}{1 - S_m} \quad S_o = S_t - S_w$$

$$\bar{S}_w = \left[1 + (\alpha \beta_{ow} h_{ow})^n \right]^{-m}, \quad h_o > h_o^{cr}$$

$$\bar{S}_w = \left[1 + (\alpha h_{aw})^n \right]^{-m}, \quad h_o \leq h_o^{cr}$$

$$\bar{S}_t = \left[1 + (\alpha \beta_{ao} h_{ao})^n \right]^{-m}, \quad m (=1-1/n)$$

$$k_{rw} = \bar{S}_w^{1/2} \left\{ 1 - \left[1 - \bar{S}_w^{1/m} \right]^m \right\}^2$$

$$k_{ro} = (\bar{S}_t - \bar{S}_w)^{1/2} \left\{ \left[1 - \bar{S}_w^{1/m} \right]^m - \left[1 - \bar{S}_t^{1/m} \right]^m \right\}^2$$

where

- h_o^{cr} = critical oil head = $\beta_{ow} h_w / (\beta_{ao} + \beta_{ow})$
- h_{ow} = oil-water capillary head (= $h_o - h_w$)
- h_{ao} = air-oil capillary head (= $h_a - h_o$)
- h_{aw} = air-water capillary head (= $h_a - h_w$)
- S_w = water saturation
- S_t = total liquid saturation
- k_{rw} = relative permeability of water
- k_{ro} = relative permeability of oil

TABLE II
SENSITIVITY ANALYSIS PARAMETERS

Parameter	Line	Values	Description
1. PROP	8(1)	.05/m .6/m .2/m .7/m .3/m .9/m .4/m 1.0/m .5/m	Parameter alpha of the VG model.
2. PROP	8(3)	1.2 2.0 1.4 2.2 1.6 2.4 1.8 2.6	Parameter n for the VG model.
3. PROP	8(4)	5% 30% 10% 40% 20% 45% 25% 50%	Total porosity
4. PROP	8(5,6)	.2 m/day 1 m/day .4 m/day 3 m/day .5 m/day 5 m/day .6 m/day 7 m/day	Ksw x-direction Ksw y-direction
5. DENR	9(1)	.4 1.2 .6 1.6 .8 1.8 1.0	Oil/Water Density
6. VISR	9(2)	.7 2.0 1.0 2.3 1.5 2.5 1.7	Oil/Water Viscosity

each parameter was taken. The sensitivity analysis performed for this research entailed approximately 50 computer runs run over a period of three months. Due to the high CPU times required to run the model, the number of computer runs averaged approximately two per day. Six input parameters varied over a pre-set range of values were analyzed for their effect on the overall output of the model.

Initially several example runs were performed on MOFAT-2D in order to determine the correct job control language that allowed the five internal files, utilized by the program, to function properly (Appendix A). The next step was to check if the program was working properly. Several examples supplied with the the model were run in order to compare outputs. Output files that were automatically stored by the program after each run were compared to the results supplied within the manual. Exact agreement between these files was observed.

Besides running example runs, simulations involving leaking storage tanks containing TCE and P-cymene within a finite element grid of 16m x 210 m were modeled in order to become more familiar with the model and the required input.

For Purposes of the sensitivity analysis a hypothetical spill event was simulated for a vertical finite element grid area of 16m x 23m which consists of 345 node points

(Fig 4.). The spill occurs on the land surface along a five meter strip of land. The water table, located at an elevation of five meters on the left side of the grid, has a gradient of 8.7 cm/m. Water saturated boundaries are assumed at both ends at their initial heads. Zero flux is assumed for both p-cymene and water phases (Kaluarachchi and Parker 1988). A total of 7.5 m³/m² of p-cymene was spilled. Once the total amount of p-cymene was infiltrated, the simulation was ended. Homogeneous soil conditions were assumed (see Table III).

Discussion of Parameters

Parameters α , n , porosity and the water saturated permeabilities in the x and y directions are all porous medium dependent parameters while oil/water density ratio and the oil/water viscosity ratio are fluid dependent parameters. What follows is a brief description of each of the parameters and their ranges over which the sensitivity analysis was run.

(1) Alpha and n are curve shape parameters specifically used in the Van Genuchten soil property equations to describe saturation-capillary head relationships. Both alpha and n are soil dependent properties and change with changing soil conditions. Alpha is a non-zero constant used in the V.G. soil equations for

MOFAT 2-D
FINITE ELEMENT GRID

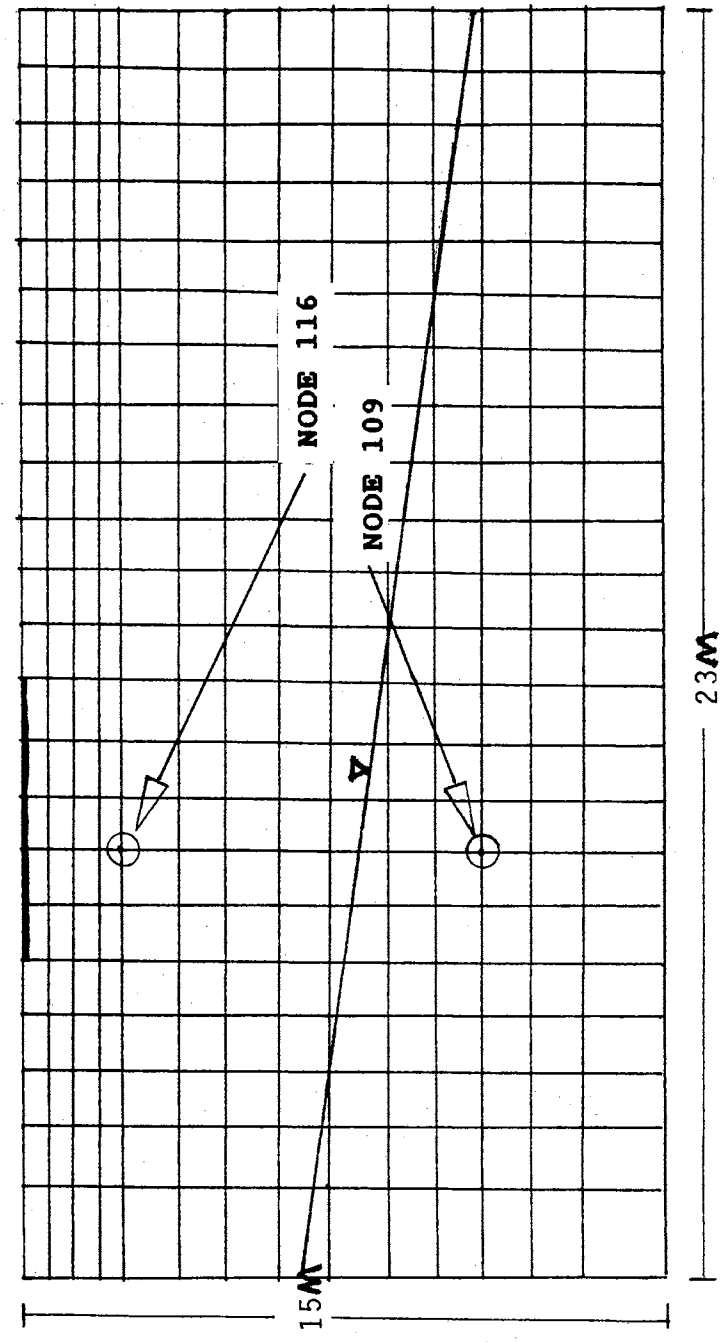


Figure 4. MOFAT 2-D Finite Element Grid (Scale in Meters)

TABLE III
 SOIL AND FLUID PROPERTIES USED
 IN MOFAT-2D RUNS

Parameter	Value
Porosity	.30
Alpha	.7/m
(n) curve parameter	2.1
(Sm) min. wetting fluid sat.	.02
Ksw -x	.4 m/hr
Ksw -y	.4 m/hr
(Bao) Fluid pair scaling factor	1.83
(Bow) Fluid pair scaling factor	2.2
Oil/Water Density	.86
Oil/water Viscosity	2.0

water and total saturations. N is an exponential constant in the same equations (Table II). Alpha was varied over a range from .05/m to 1.0/m while, n a dimensionless unit, was varied over a range of 1.2 to 2.6 for the sensitivity analysis. Representative values of alpha and N can be found in Table IV.

(2) porosity is described as the volume of the void space within the porous media divided by the bulk volume of the media. Porosity is therefore a dimensionless representation of the relative amount of void space within the porous media. Porosity was analyzed over a range from 5% (shale) to 50% which is roughly equivalent to 47.6% or hypothetically the greatest porosity attainable.

(3) The water saturated permeability in both the x and y direction is the flow of a unit volume of water through a unit area normal to flow per unit time under a unit hydraulic gradient. Water saturated permeability is equal to velocity of the water in m/day divided by the hydraulic gradient in m/m for a water saturated medium. The water saturated permeability was varied over a range from .2 m/day, relatively impermeable, to 7 m/day.

(4) Oil/Water density ratios will determine if the oil used in the model will float or sink in the water. Ratios greater than one will sink in water while ratios less than one will float on the water table. Oil to water density ratios used in this study were varied over a range

TABLE IV
 CHARACTERISTIC VALUES OF
 ALPHA AND N FOR SOILS

SOIL NAME	PERMEABILITY	ALPHA	N
Hygiene sandstone	108 cm/day	.0079/cm	10.4
Touchet Silt Loam G.E. 3	303 cm/day	.0050/cm	7.09
Silt Loam	4.96 cm/day	.00423/cm	2.06
Guelph Loam (drying)	31.6 cm/day	.0115/cm	2.03
(wetting)	-	.0200/cm	2.76
Riet Netofa Clay	.082 cm/day	.00152	1.17

(From Van Genuchten 1980)

from .4 to 1.8.

(5) Oil/Water viscosity ratio of a fluid can be described as its resistance to flow relative to water. Low viscosity fluids have a tendency to flow easily while highly viscous fluids flow at slow velocities and with great resistance. Although viscosity is temperature dependent, the model assumes constant temperature in the soil. Oil/Water viscosity was varied over a range from .7 to 2.5 for the sensitivity analysis.

Results and discussion of the sensitivity analysis can be found in the following chapters.

CHAPTER IV

RESULTS AND DISCUSSION

Model outputs were analyzed for parameter effects on oil and water saturation, oil and water heads, oil velocities, and plume configurations. Two separate node points were chosen for this purpose (Fig. 4). Node 116, located within the unsaturated zone directly beneath the spill area, is utilized in order to address the effects of the various parameters in an unsaturated condition. Node 109, located within the saturated zone directly beneath the spill area, was utilized in order to address the effects of the parameters on model output within the saturated zone.

Oil and Water Saturations (Node 116)

Alpha Parameter

When compared to the effects of other parameters on oil and water saturation, the alpha parameter appears to have the most pronounced effect on the saturation of oil and water at nodal points in the unsaturated zone. At alpha = .05/m oil saturation slowly increases from the initial 0% saturation to only 8% saturation over a 60 hour simulation

period at node 116. Water saturation initially starts at a value of 98% and decreases only to 91% over the same 60 hour period (Fig.5). When alpha was increased to .2/m saturation response was also increased (Fig. 6). Water saturation at node 116 initially starts at 80% and decreases 26% to approximately 54% over a 26 hour period. Oil saturation responds in an opposite but equal fashion from 0% to 45% over the same period. At alpha=.3/m water saturation initially begins at 66% and decreases to 45% in 19.4 hours (Fig. 7). Oil saturation for alpha=.3/m increases from an initial value of 0% to 54% over the same period. A similar trend in oil and water saturations is seen as the alpha parameter is increased incrementally up to .7/m (Figs. 8-11). The initial water saturation values continue to decrease to approximately 34.2% while oil saturations increase to 69.5% over increasingly shorter periods of time. At alpha values greater than .7/m, an initial retardation in oil saturation response during the first 4 hours of simulation time is observed (Figs. 12-14). This retardation in the rate of increasing oil saturation becomes more pronounced as alpha increases toward 1.0/m.

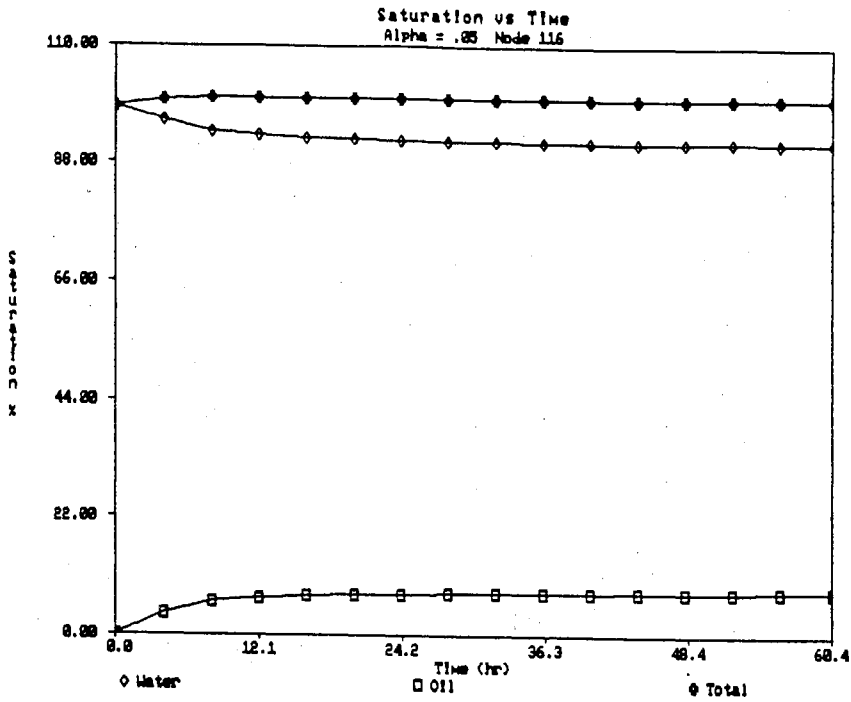


Figure 5. Saturation vs Time
Alpha=.05/m

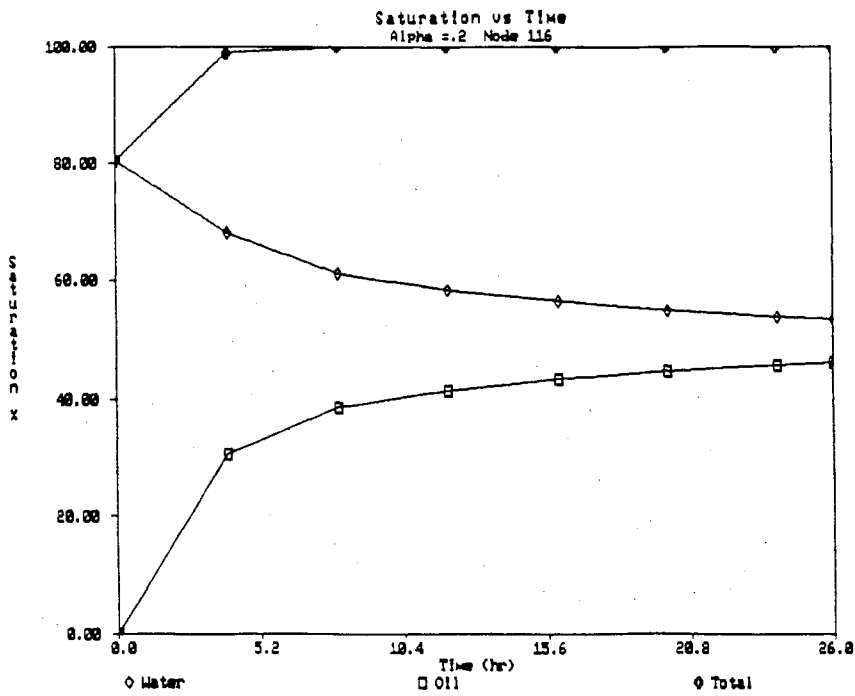


Figure 6. Saturation vs Time
Alpha=.2/m

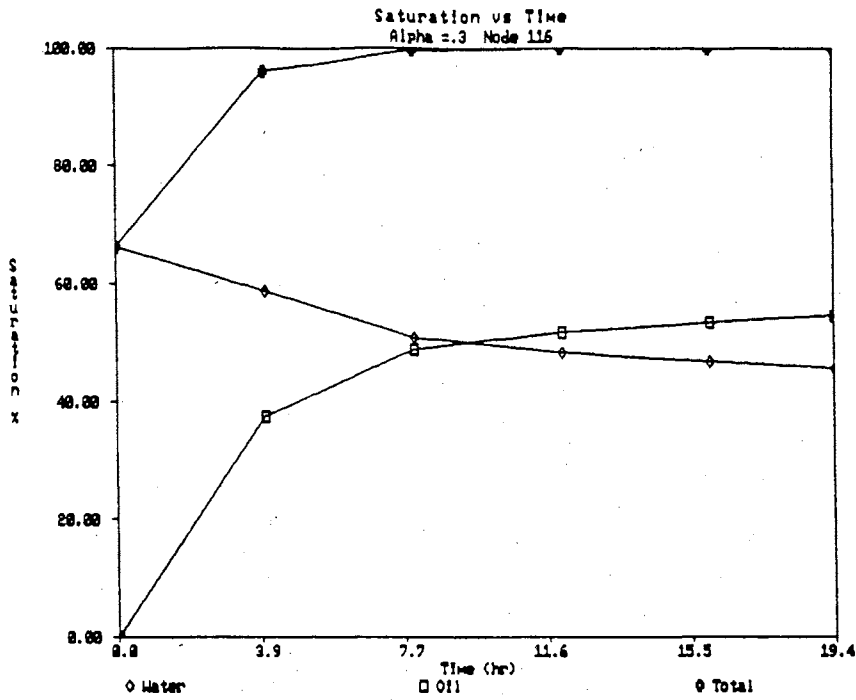


Figure 7. Saturation vs Time
Alpha = .3/m

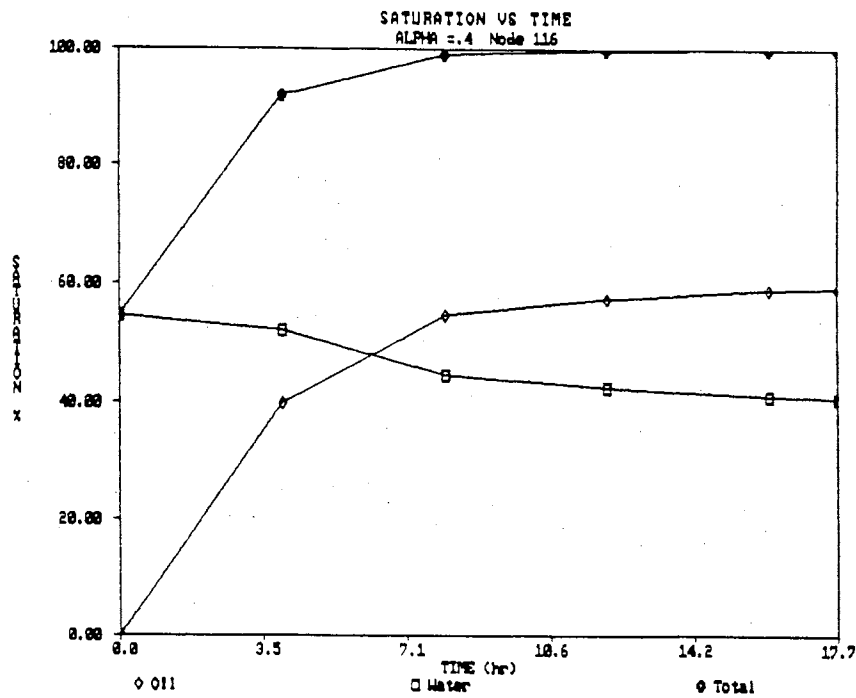


Figure 8. Saturation vs Time
Alpha = .4/m

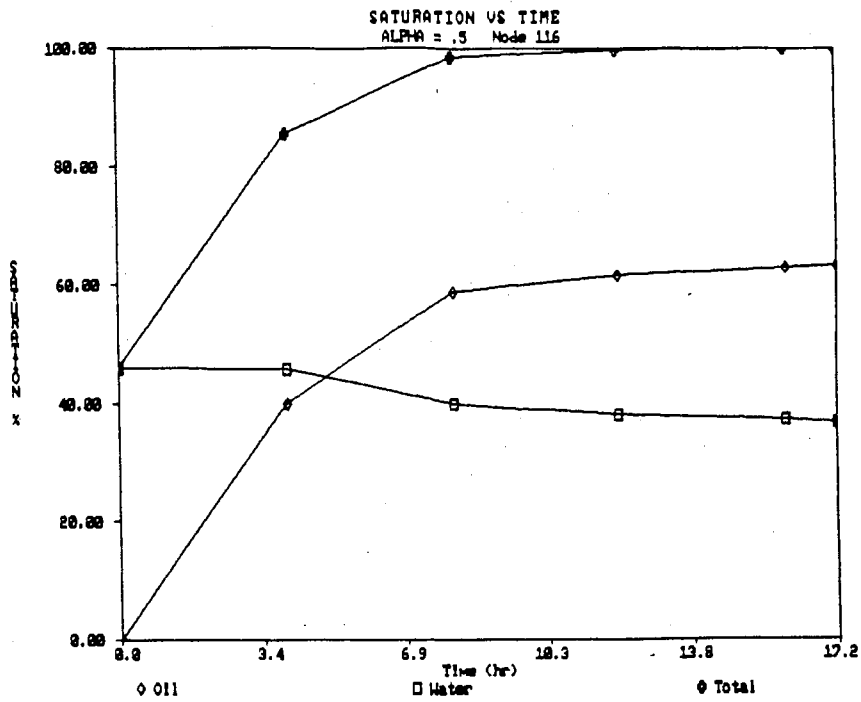


Figure 9. Saturation vs Time
Alpha=.5/m

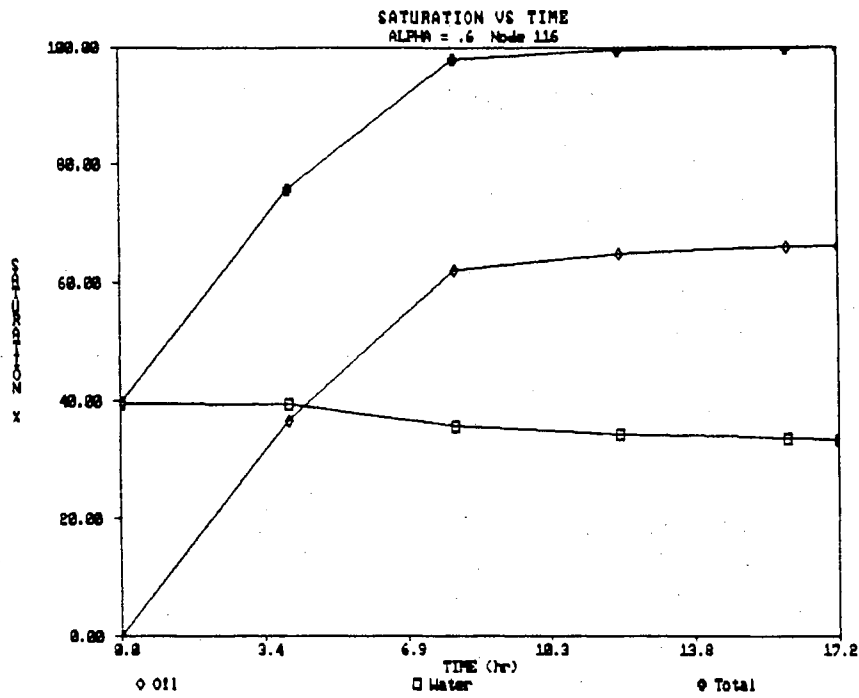


Figure 10. Saturation vs Time
Alpha=.6/m

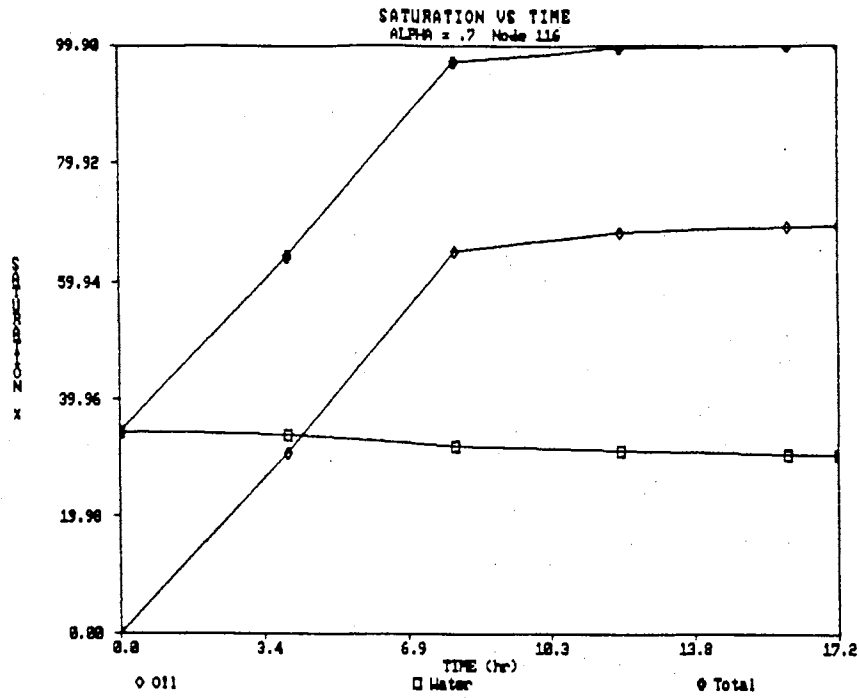


Figure 11. Saturation vs Time
Alpha=.7/m

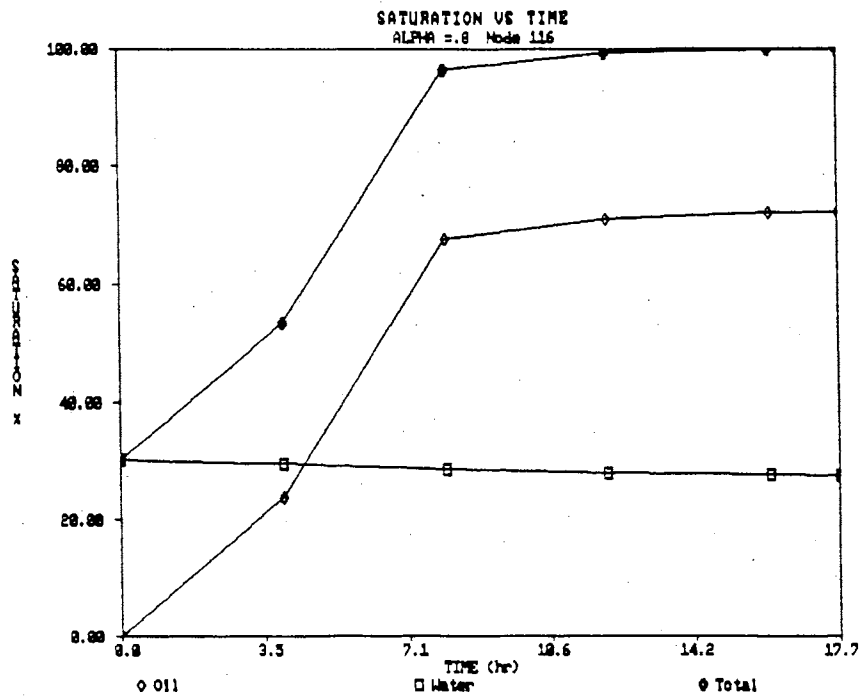


Figure 12. Saturation vs Time
Alpha=.8/m

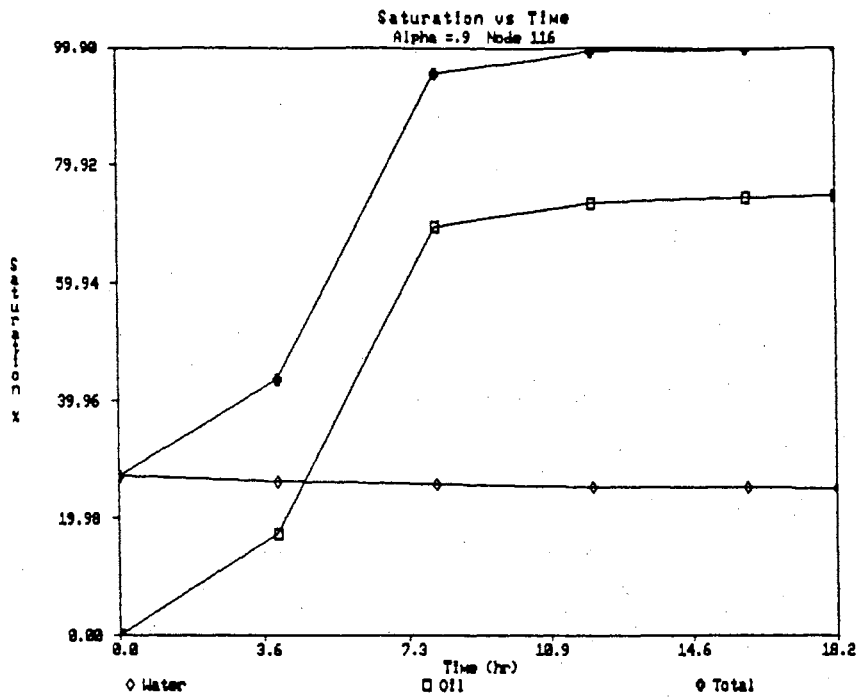


Figure 13. Saturation vs Time
Alpha = .9/m

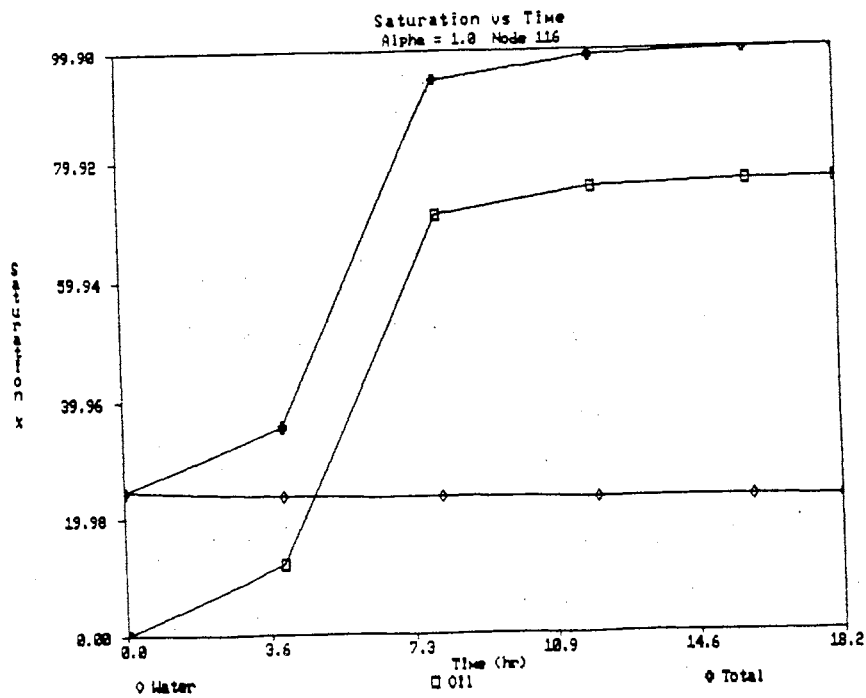


Figure 14. Saturation vs Time
Alpha = 1.0/m

N Parameter

The N parameter effects MOFAT-2D's prediction of oil and water saturations at node 116 in a similar manner as the alpha parameter. As N is increased the initial water saturation values decrease and the initial oil saturation values increase. With N=1.2 initial water saturation is approximately 80% with oil saturation equal to 0% initially and moving up to only 3.8% after 4 hours (Fig. 15). When N is increased to 1.4, initial water saturation values decrease to a value of 65% (Fig. 16). Oil saturation over time nearly doubles over what it was at N=1.2. As N is increased further, oil saturation continues to increase and become the predominant fluid saturating the nodal points over the water. Retardation in the rate of oil saturation increase is observed during the first 4 hours of simulation time for N=1.2 through N=2.0 (Figs. 16-19). At N=2.2 through N=2.6, oil saturations of 40-50% are reached within the first 4 hours of simulation time (Figs 20-22). Water saturations continue to decrease from 31% at N=2.2 and 26% at N=2.4 to 22% at N=2.6.

Porosity Parameter

As with alpha and N, the porosity parameter appears to have a pronounced effect on oil and water saturations at

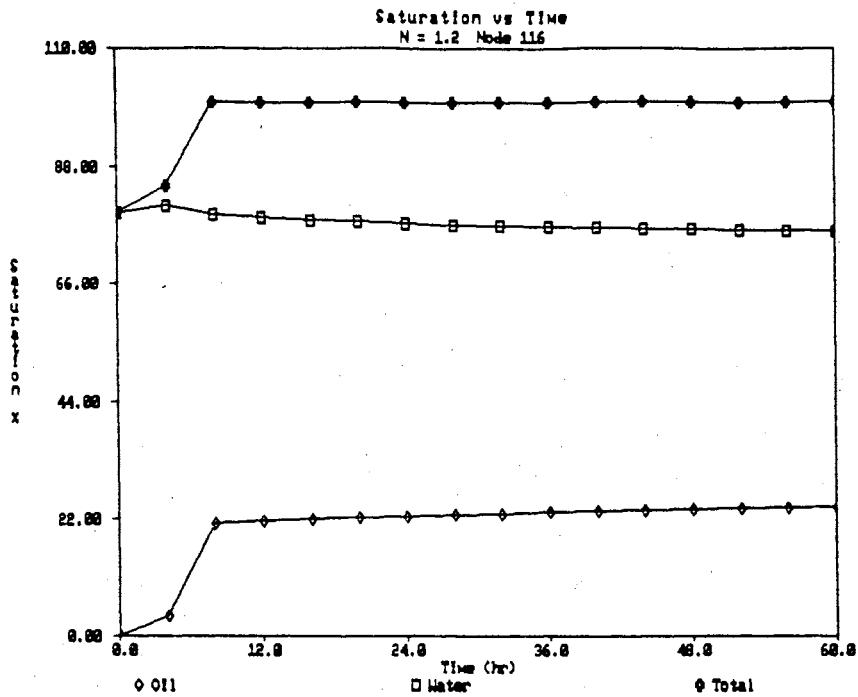


Figure 15. Saturation vs Time
N=1.2

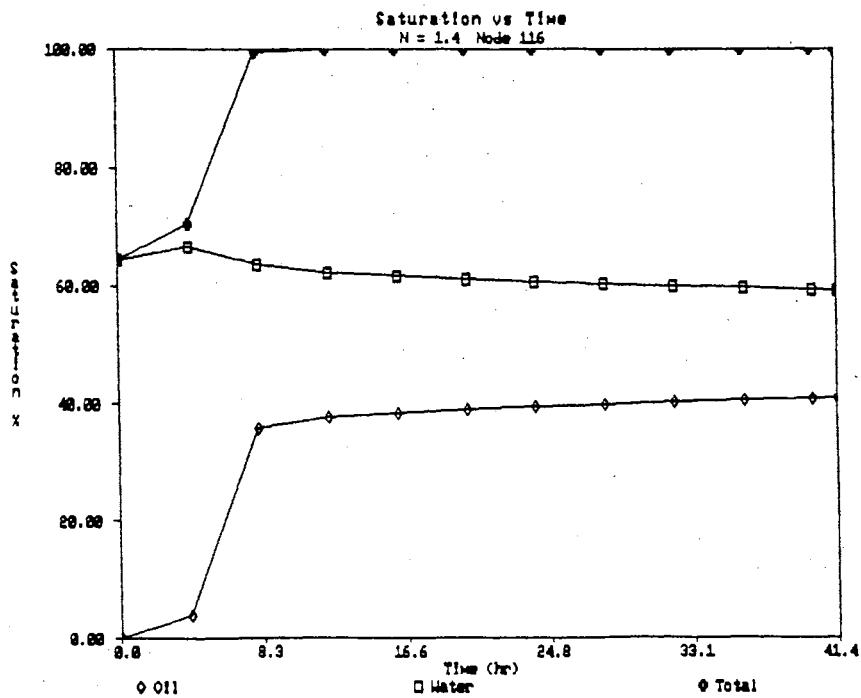


Figure 16. Saturation vs Time
N=1.4

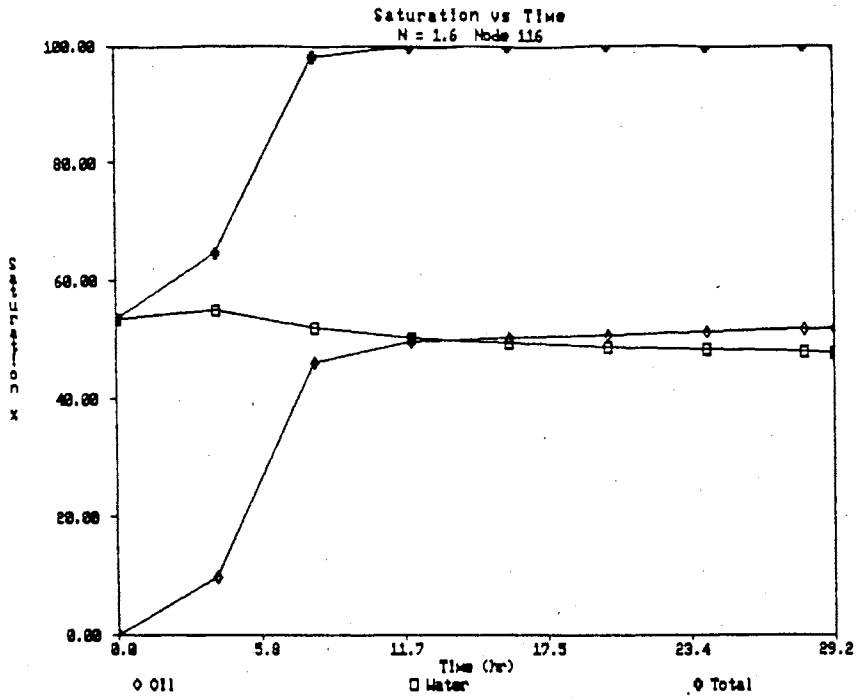


Figure 17. Saturation vs Time
N=1.6

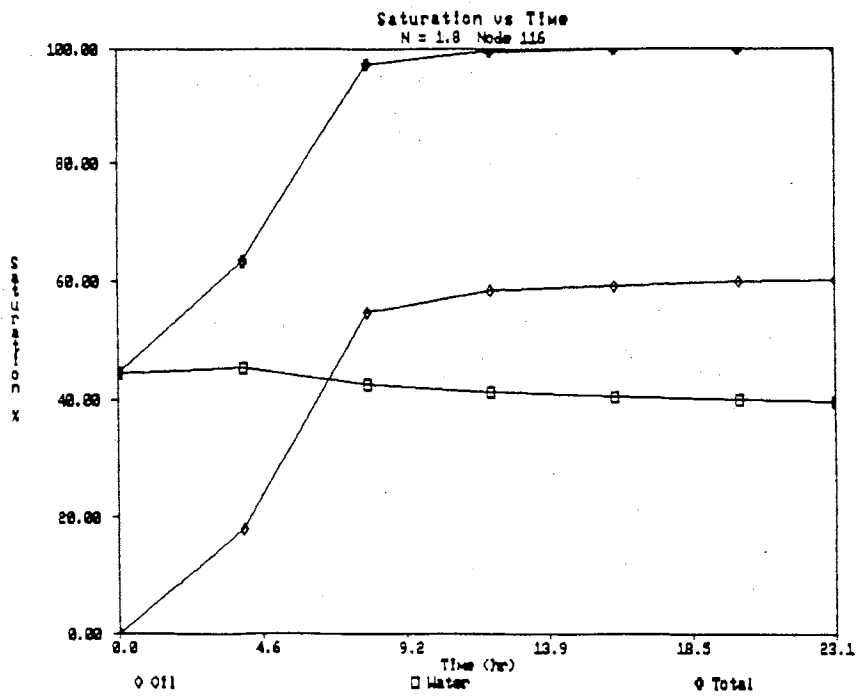


Figure 18. Saturation vs Time
N=1.8

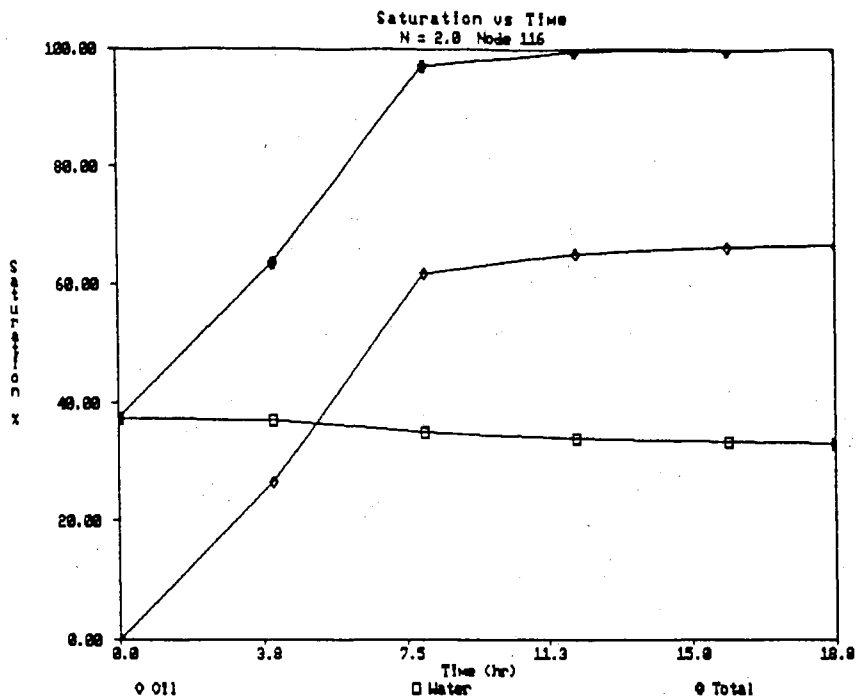


Figure 19. Saturation vs Time
N=2.0

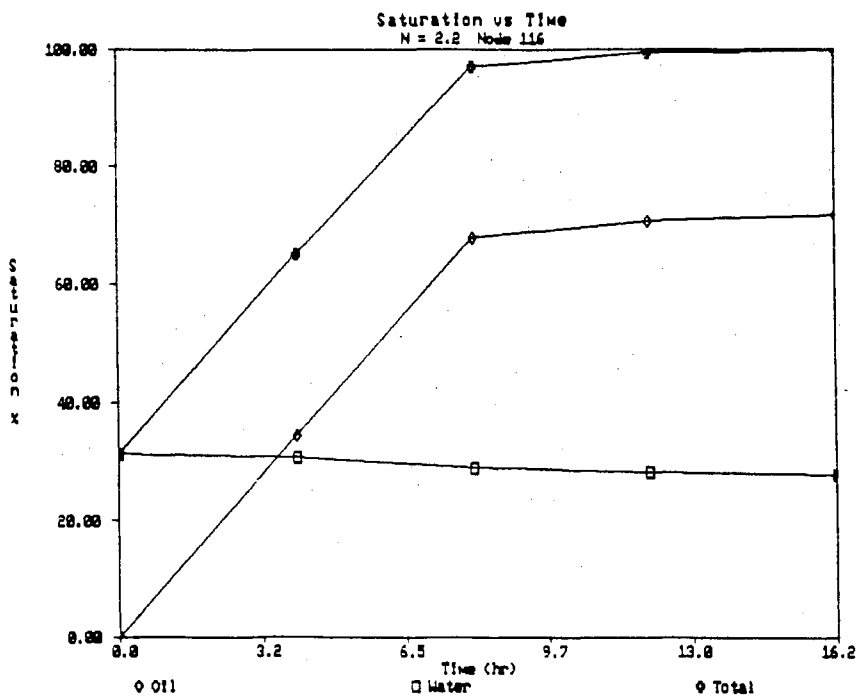


Figure 20. Saturation vs Time
N=2.2

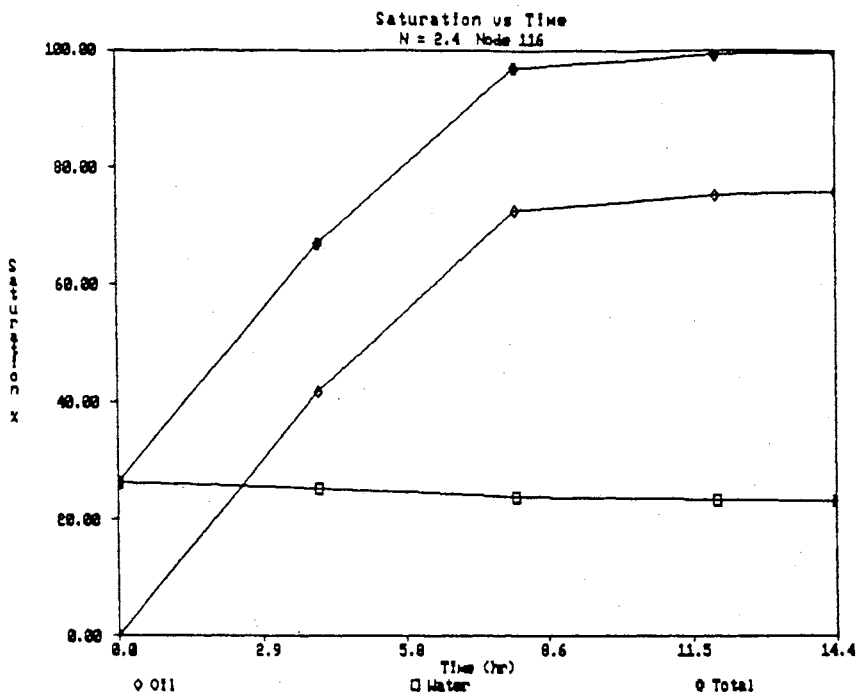


Figure 21. Saturation vs Time
N=2.4

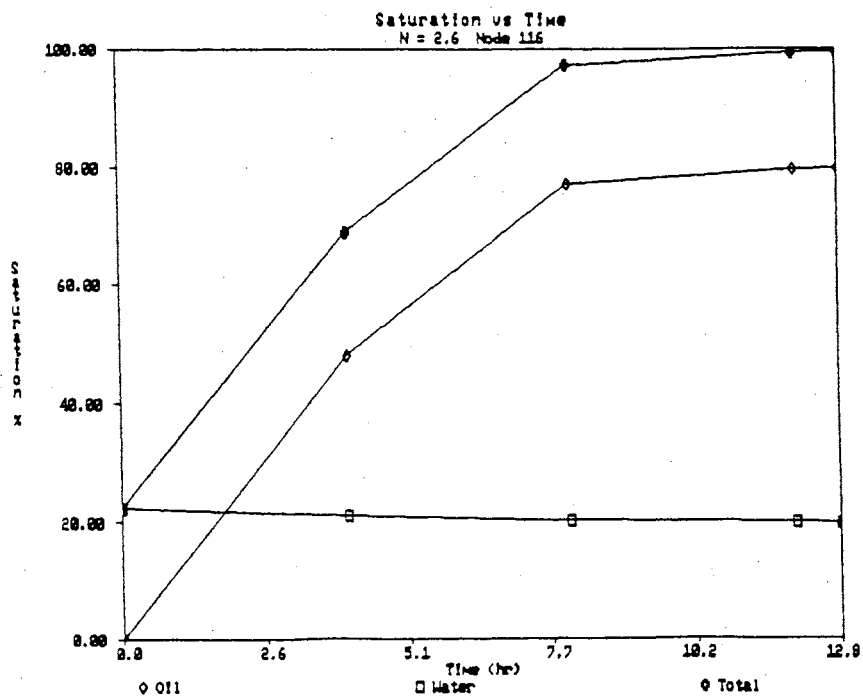


Figure 22. Saturation vs Time
N=2.6

node 116. At porosity = 5%, oil saturation reaches 68% in 2 hours after the simulation starts (Fig. 23). From the 68%, oil saturation increases steadily to 78% at 60 hrs. Water saturation decreases steadily from 34% to 23% over the 60 hour period. At 10% porosity, oil saturation reaches 68% within 4 hours and steadily increases to 74% at 34 hours (Fig. 24). Increasing porosity to 20% a delay in saturation rate is found in the first 2 hours of simulation time. At 20% and 25% porosity 68% oil saturation is found to occur at approximately 6 hours (Figs 25,26). 25% porosity exhibits a substantial delay in oil saturation rate during the first 2 hours of simulation time. At porosity = 30% oil saturation approaches 68% at 8 hours after an initial 2 hour delay in response (Fig. 27) At porosity = 40%, no oil saturation increase is observed until 2 hours (Fig. 28). A slow rate of oil saturation occurs initially in the first four hours but increases after that point. The oil saturation approaches 68% at 10 hours. At porosity = 45% and 50% any significant response of oil beginning to saturate the pore spaces at node 116 begins after 4 hours of simulation time (Figs. 29,30). Oil saturation begins reaching a value of 68% around 10 to 12 hours.

Permeability (Ksw) Parameter

At high Ksw values such as Ksw = 3 m/day , 5 m/day, and

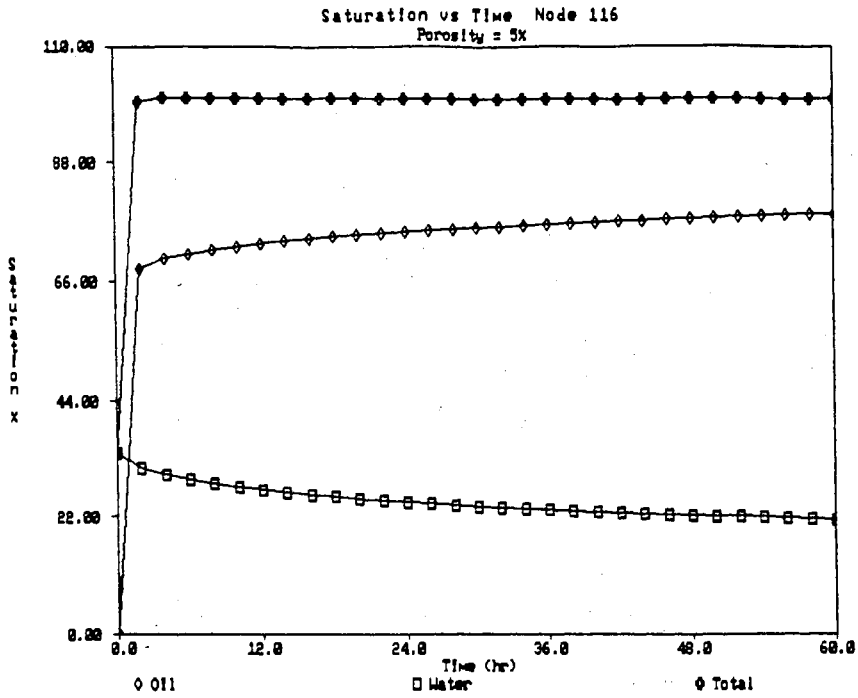


Figure 23. Saturation vs Time
Porosity=5%

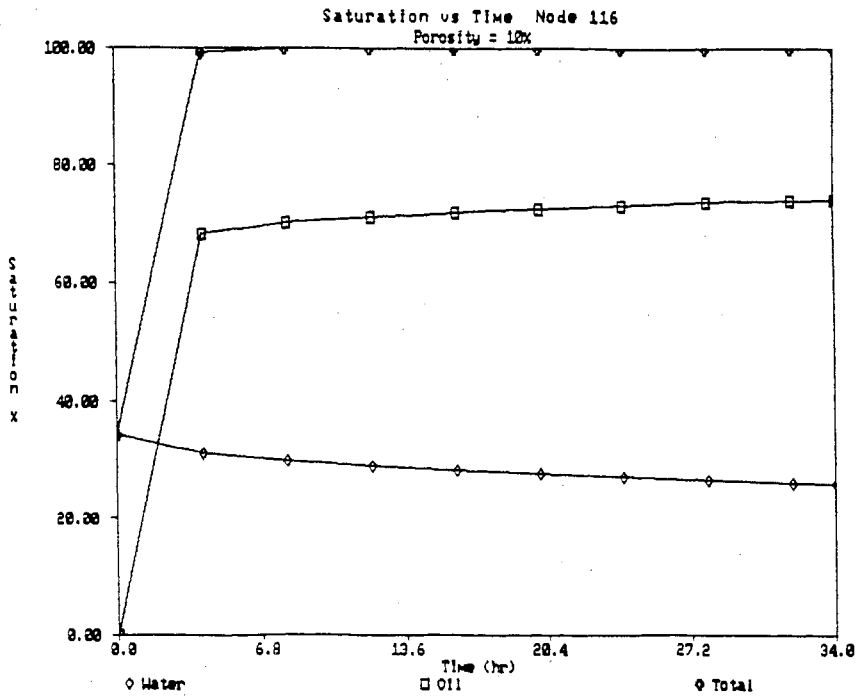


Figure 24. Saturation vs Time
Porosity=10%

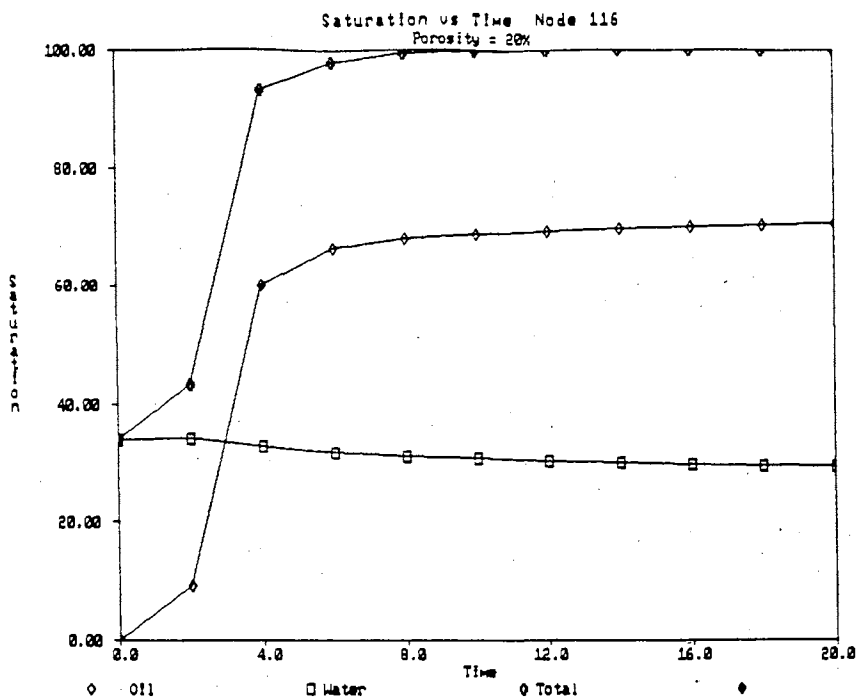


Figure 25. Saturation vs Time
Porosity=20%

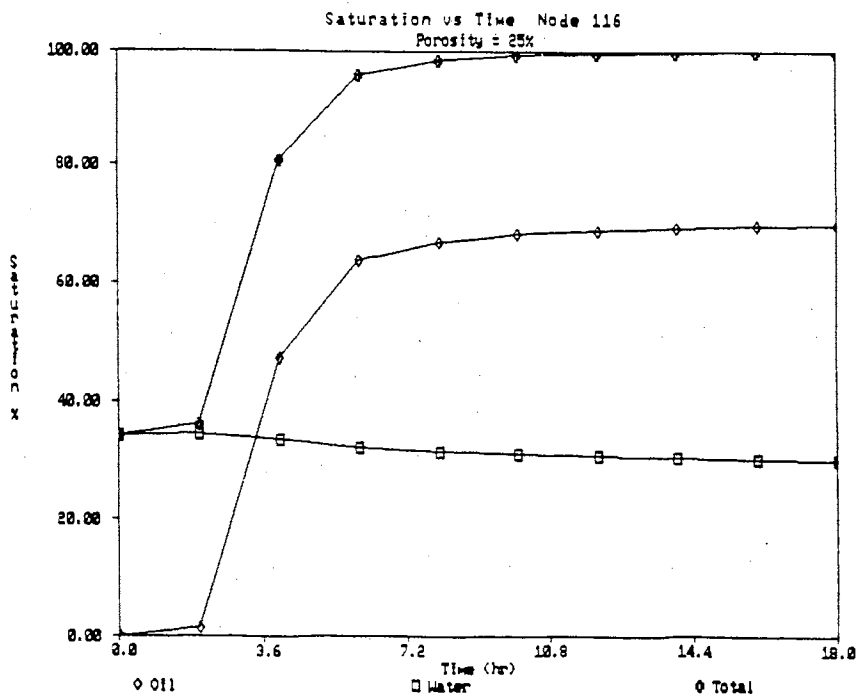


Figure 26. Saturation vs Time
Porosity=25%

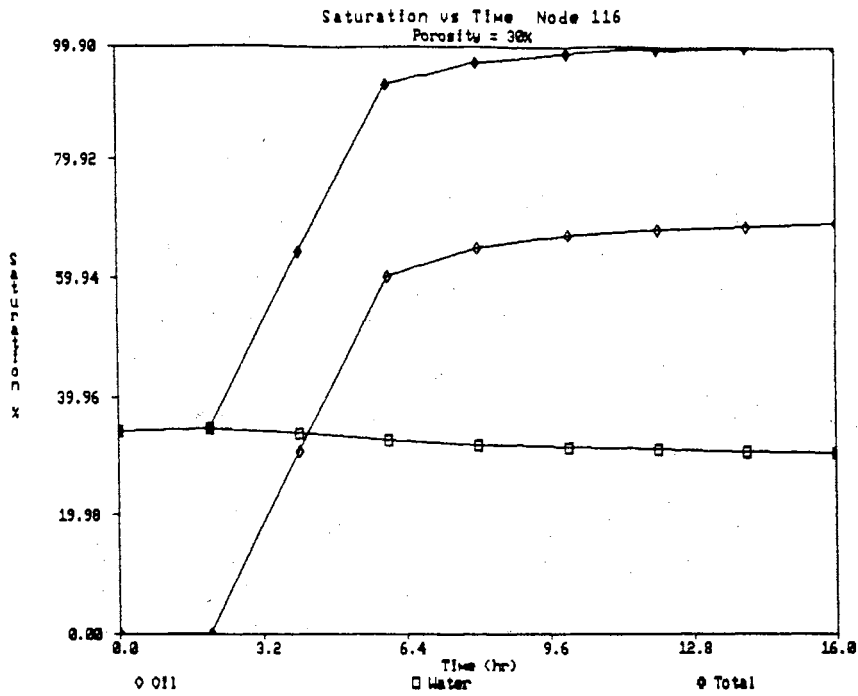


Figure 27. Saturation vs Time
Porosity=30%

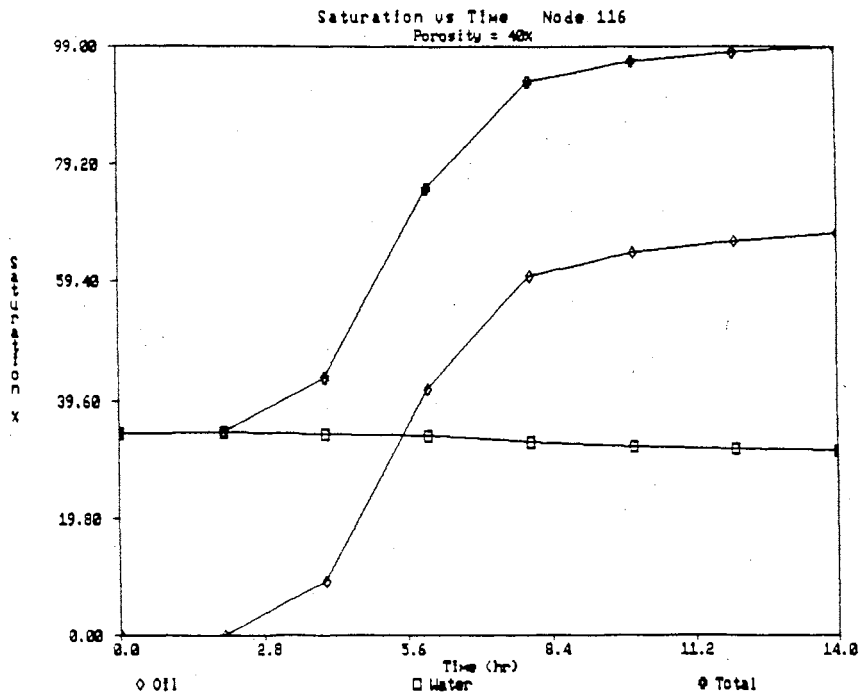


Figure 28. Saturation vs Time
Porosity=40%

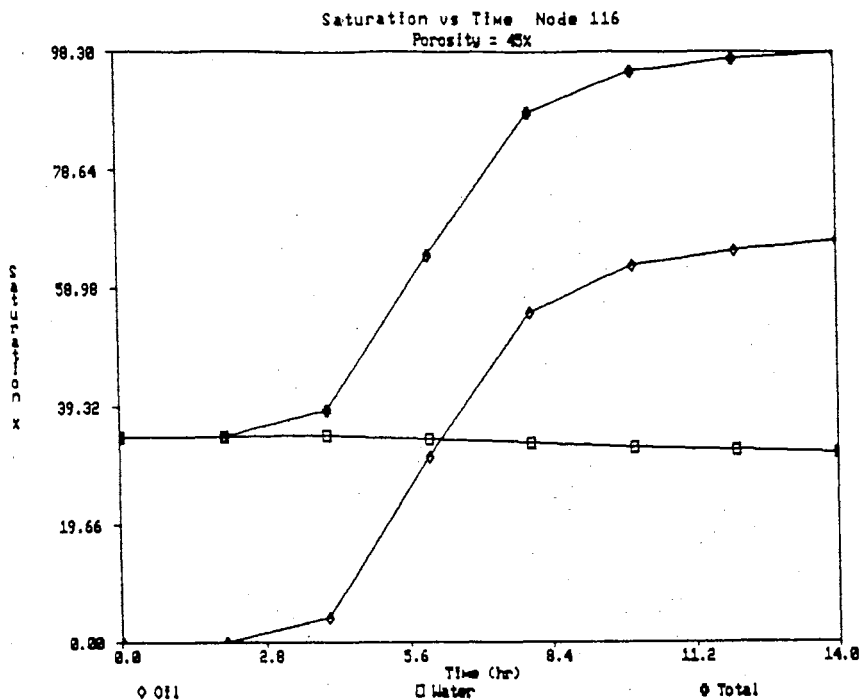


Figure 29. Saturation vs Time
Porosity=45%

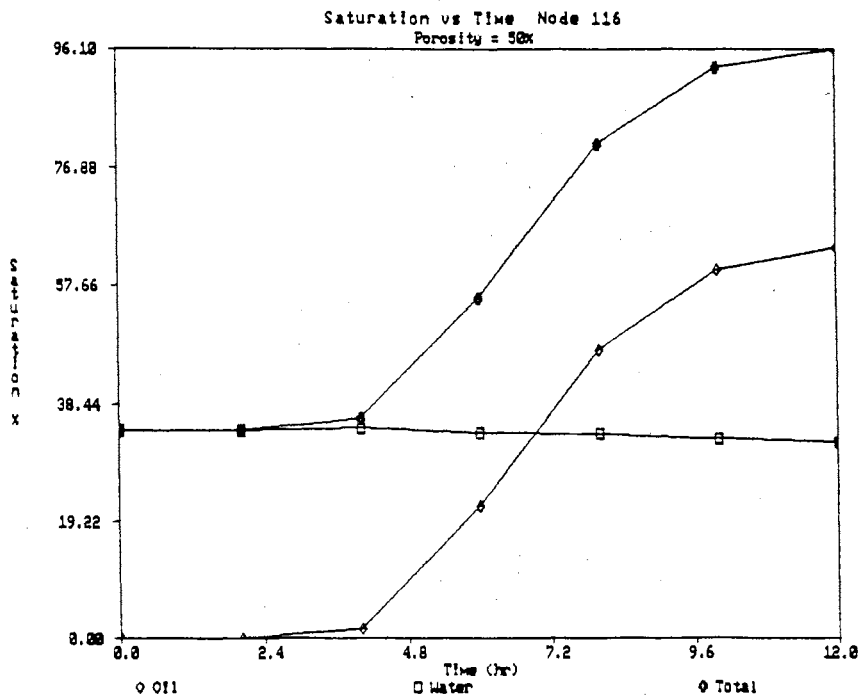


Figure 30. Saturation vs Time
Porosity=50%

7 m/day, oil infiltration from the surface was so rapid that the total 7.5 cubic meters/square meter volume of p-cymene was infiltrated and the simulation was ended before substantial output was calculated. Therefore output data for these values of permeability was very limited.

At low K_{sw} (.2 m/day), oil saturation is slow in reacting when the simulation starts (Fig. 31). After an initial delay, the oil saturation increases slowly eventually leveling off to a near constant saturation value. As K_{sw} is increased the rate of oil saturation also increases. There is a approximate 111% rate of increase in oil saturation per hour from $K_{sw} = .2$ m/day to $K_{sw} = .4$ m/day (Fig. 32). From $K_{sw} = .4$ m/day to .6 m/day there is a 4.3% increase in oil saturation per hour (Figs. 32-34). The percentage of increase in oil saturation is equal to 1% between $K_{sw} = .5$ m/day and .6 m/day. Water saturations all decrease slightly approximately 4% over the time of the simulation from an initial 34% water saturation to 30%. Although no data is available for the high values of permeability, it can be assumed that at these values oil saturation would increase in a very rapid manner over a short period of time as figure 35 indicates for $K_{sw} = 1$ m/day.

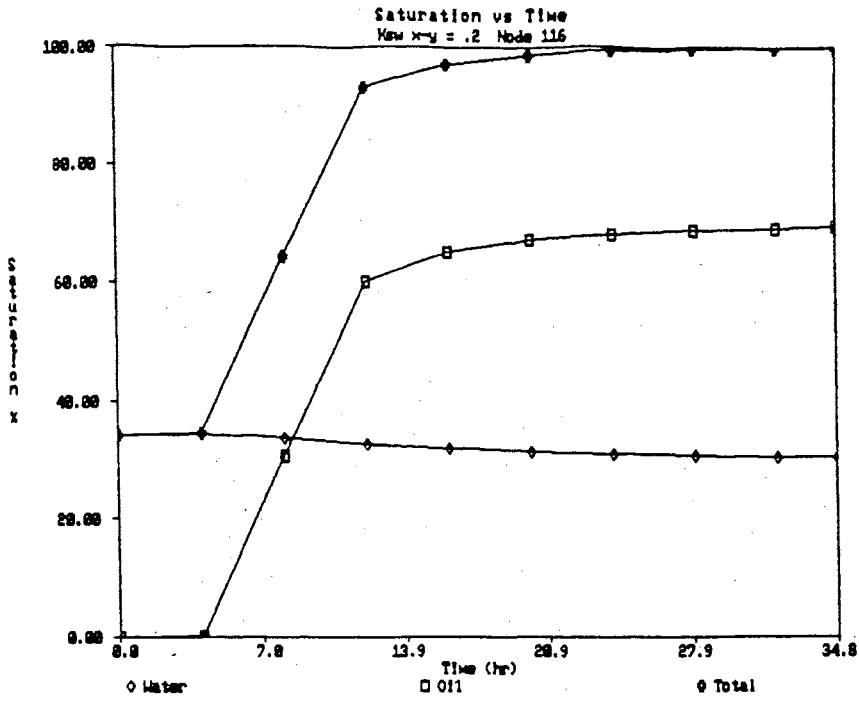


Figure 31. Saturation vs Time
Ksw=.2

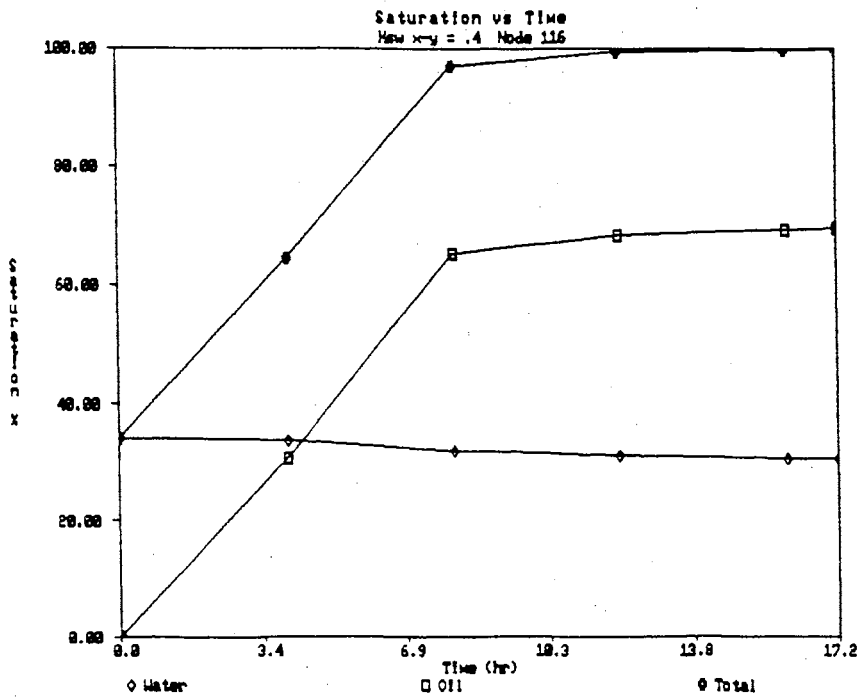


Figure 32. Saturation vs Time
Ksw=.4

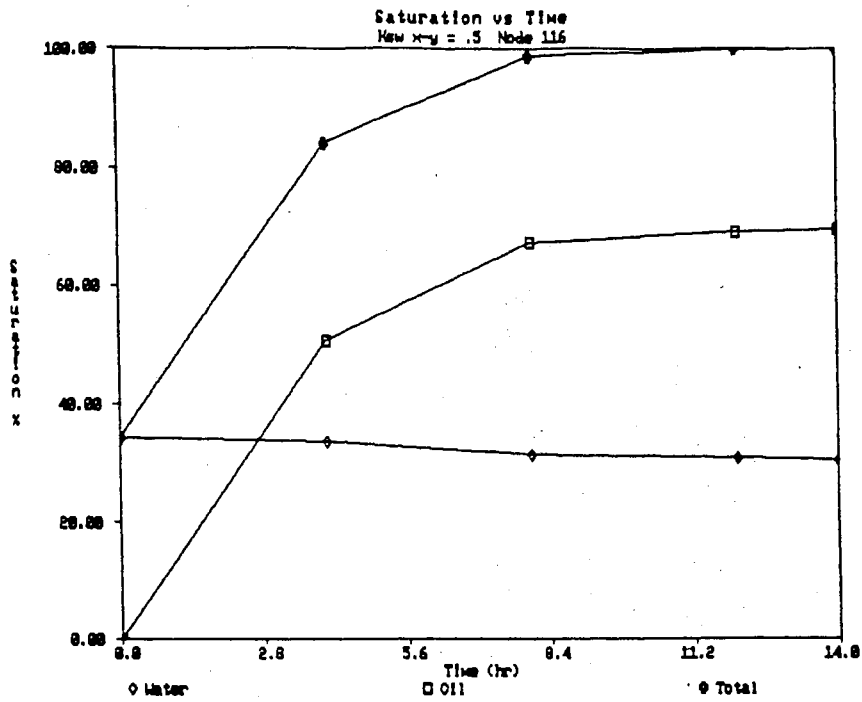


Figure 33. Saturation vs Time
Ksw=.5

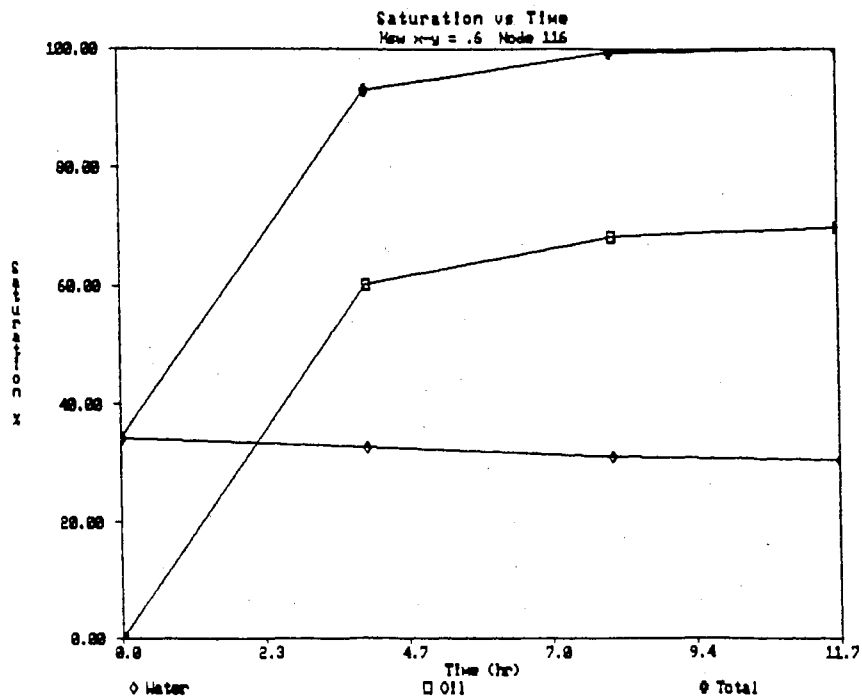


Figure 34. Saturation vs Time
Ksw=.6

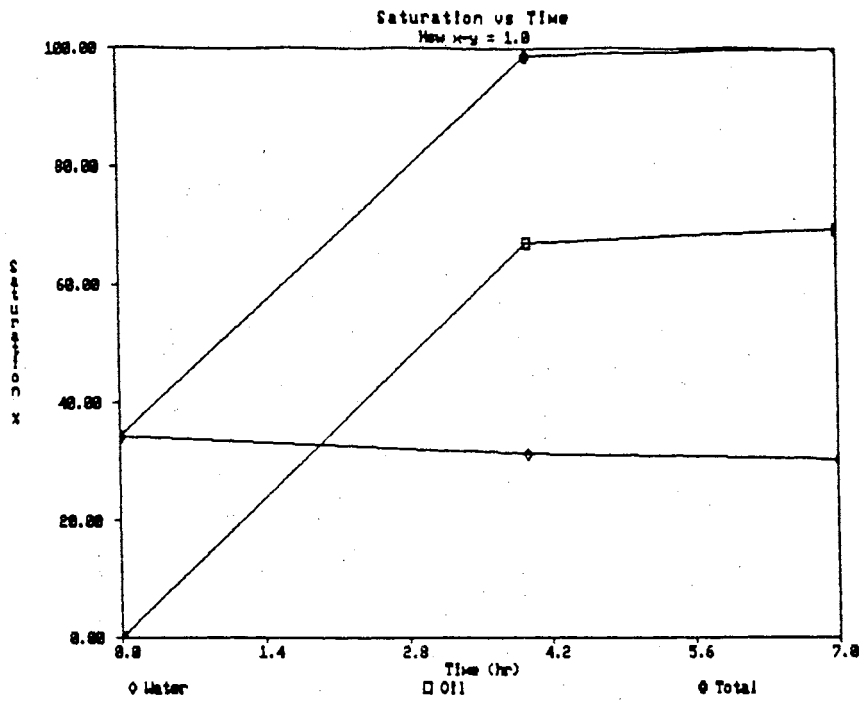


Figure 35. Saturation vs Time
Ksw=1.0

Density Parameter

At densities of .4 and .6 oil saturation shows an initial slow rise (Figs. 36,37). These low values appear to effect the time it takes for the oil to reaches a near equilibrium value of 68% to 69% saturation. At density =.8 the rate of oil saturation increase appears to approach a constant rate (Fig. 38). For densities =1.0 through 1.8 the oil saturation rates increase with each incremental step in oil density (Figs. 39-42). Water saturations over the entire range of density values show little variance. Water saturations decrease uniformly from approximately 34% to 30% saturation.

Viscosity Parameter

The viscosity parameter, expressed as a ratio of oil to water viscosity, has a inverse effect on oil saturation when compared to the other parameters in this study. With increasing values of viscosity, the rate of oil saturation increase decreases. At viscosity =.7 oil saturation approaches equilibrium in approximately 4 hours (Fig. 43). At viscosity =1.0 oil saturation equilibrium is obtained in 6 to 8 hours (Fig. 44) At viscosity =1.5 oil saturation approaches equilibrium in 8 to 10 hours (Fig. 45). At viscosity = 1.7 and 2.0 oil saturation equilibrium is

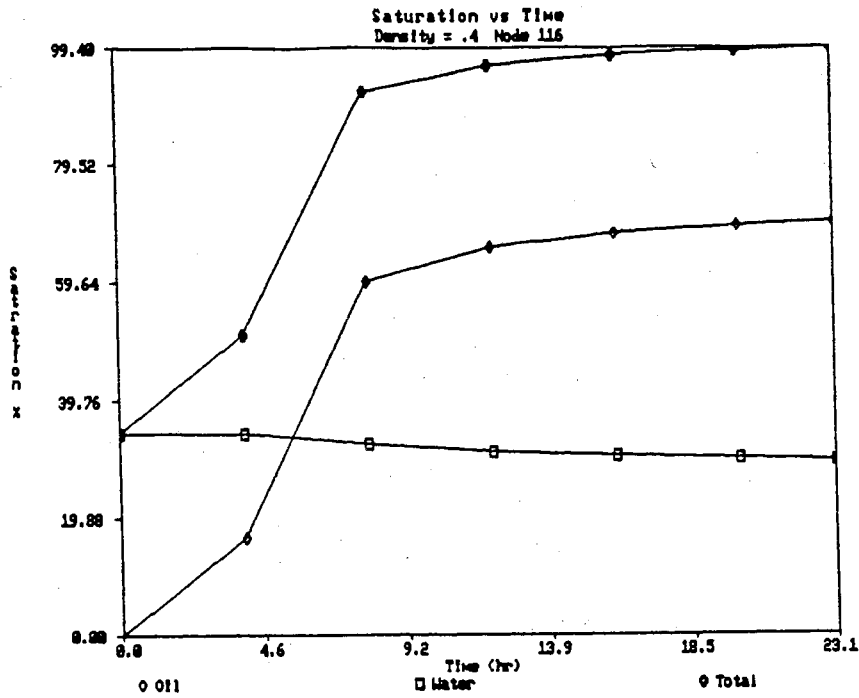


Figure 36. Saturation vs Time
Density=.4

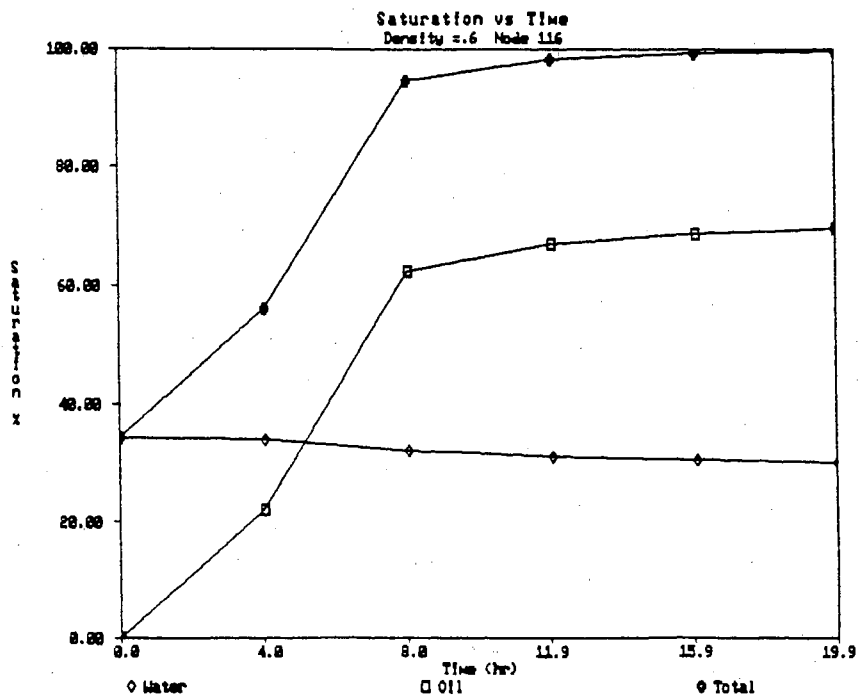


Figure 37. Saturation vs Time
Density=.6

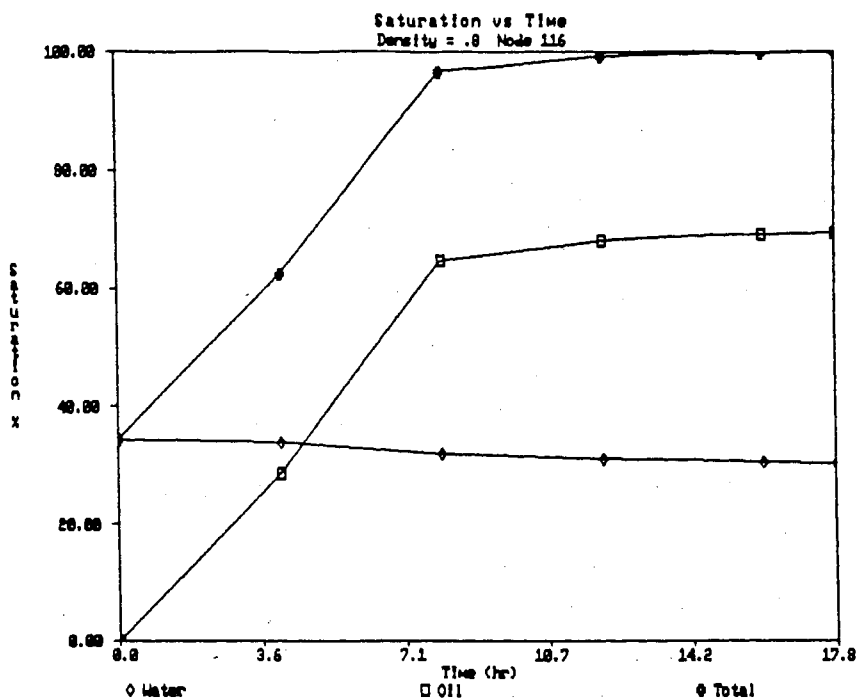


Figure 38. Saturation vs Time
Density=.8

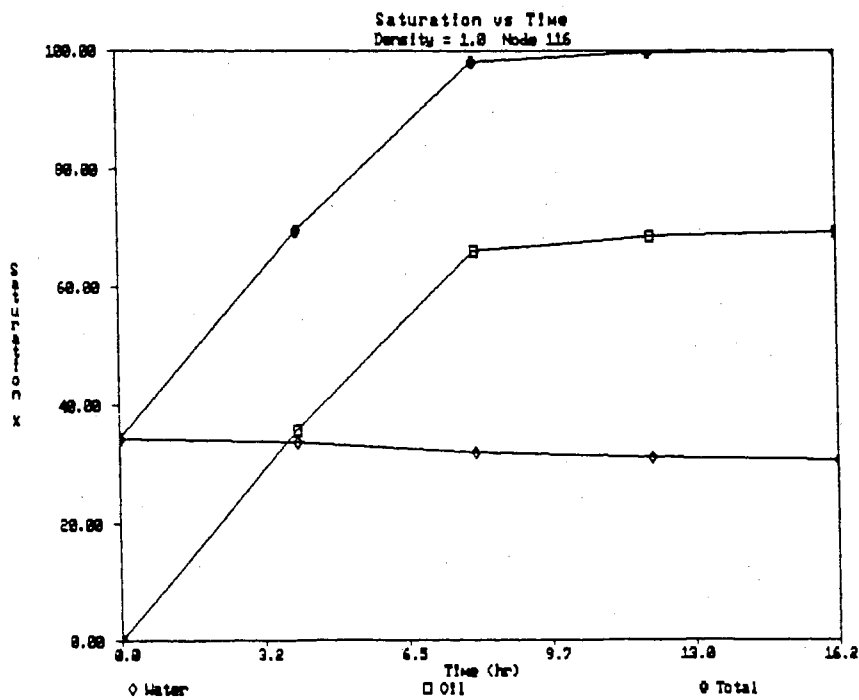


Figure 39. Saturation vs Time
Density=1.0

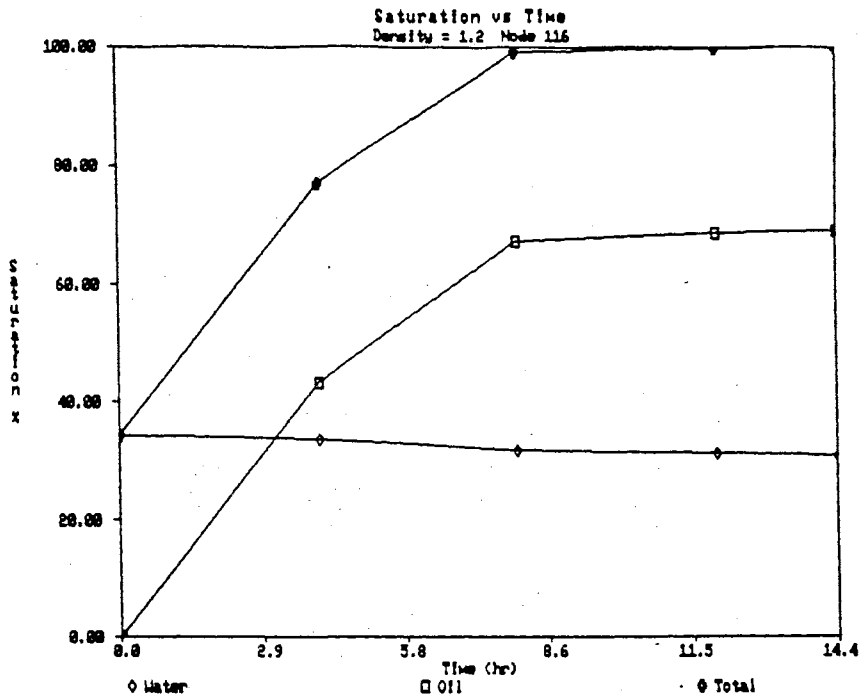


Figure 40. Saturation vs Time
Density=1.2

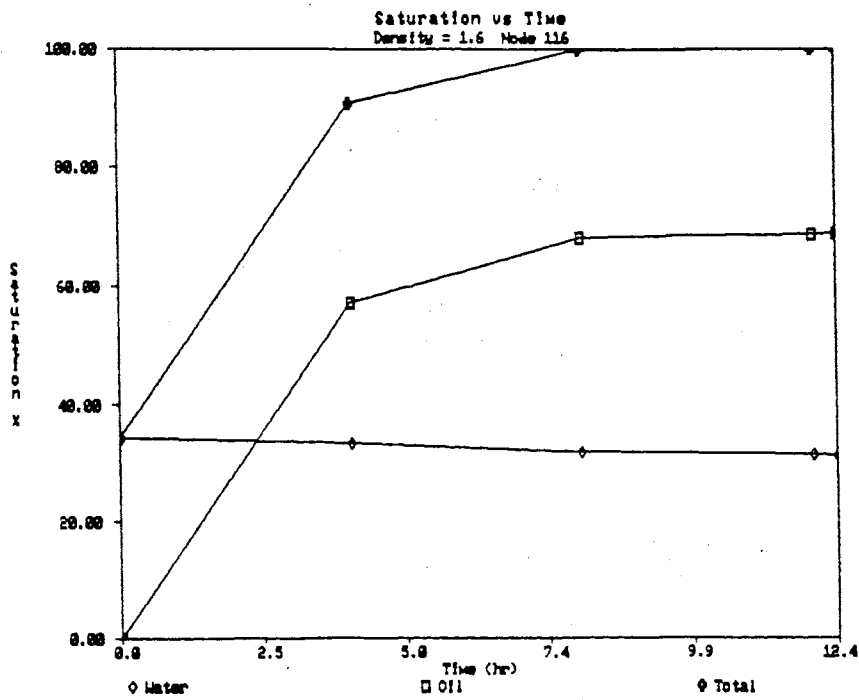


Figure 41. Saturation vs Time
Density=1.6

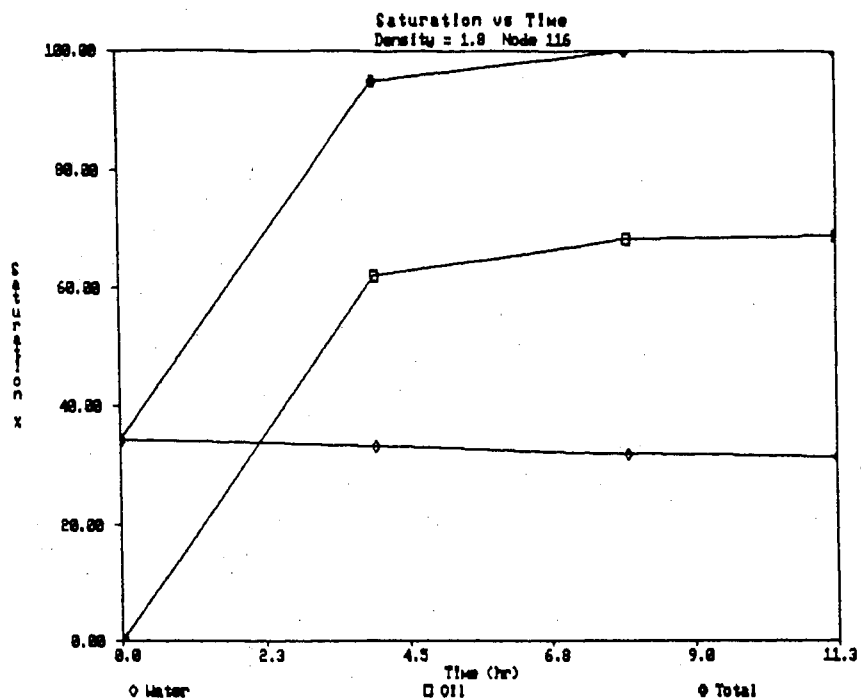


Figure 42. Saturation vs Time
Density=1.8

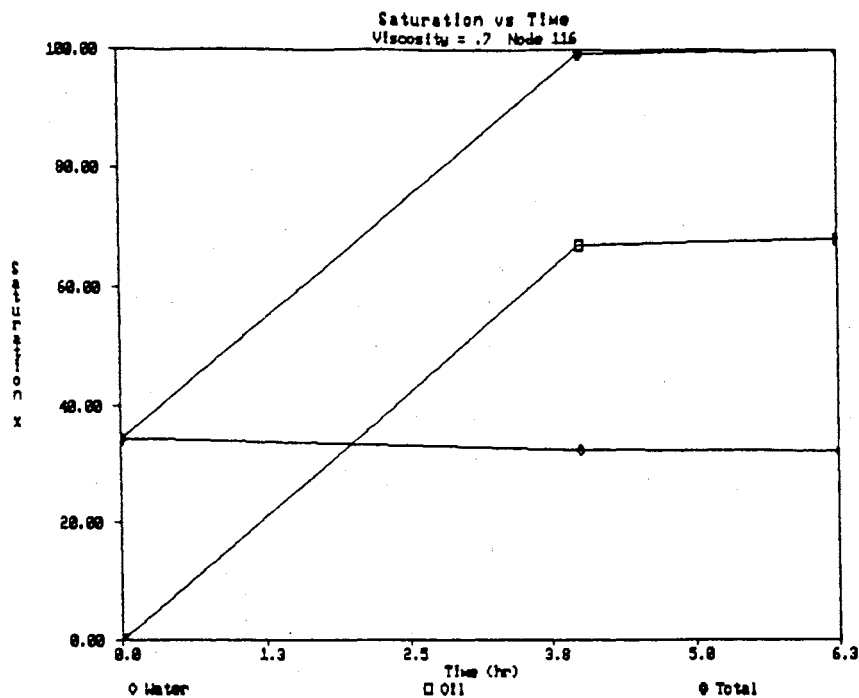


Figure 43. Saturation vs Time
Viscosity=.7

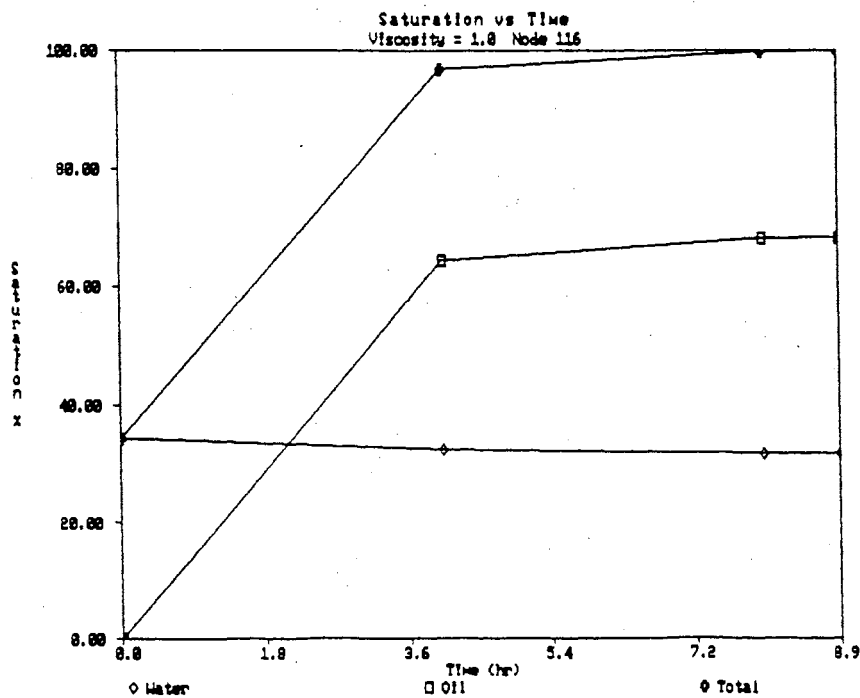


Figure 44. Saturation vs Time
Viscosity=1.0

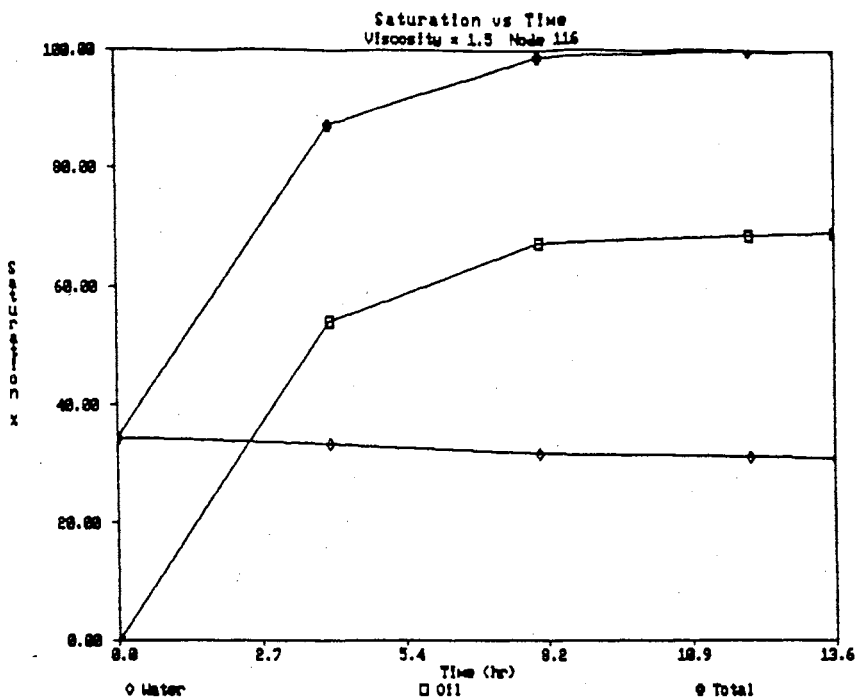


Figure 45. Saturation vs Time
Viscosity=1.5

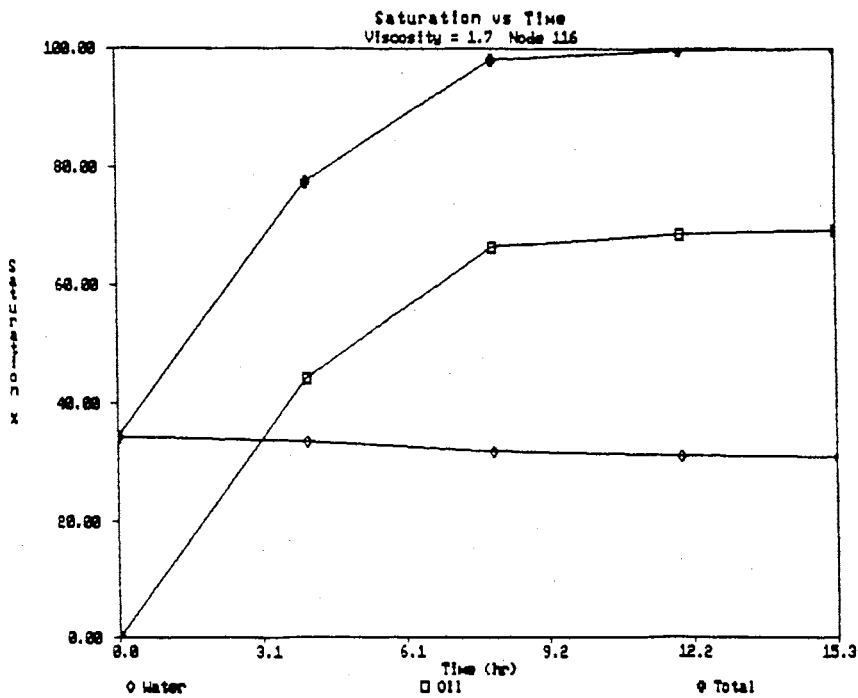


Figure 46. Saturation vs Time
Viscosity=1.7

approached at 10 to 12 hours (Figs. 46,47). At viscosities equal to 2.3 and 2.5 there is an initial delay in the increase of oil saturation during the first 4 hours of simulation time followed by a increase in saturation rate (Figs. 48,49). At viscosity equal to 2.3 and 2.5 oil saturation at node 116 approaches equilibrium in 12 to 16 hours. Water saturations appear not to be affected by changes in oil viscosity and all tend to decrease at a constant rate from 34% to around 30% over the simulation period.

Oil Heads at Node 116

Alpha Parameter

A trend of increasing oil head with time followed by a leveling of head asymptotically towards zero is observed for the alpha parameter as well as the other parameters. Because node 116 is located in the unsaturated zone, nodal pressure heads are expressed as negative values. The rates of oil head increase vary with each parameter as seen in figures 50-55. With increasing increments of the alpha parameter there is a decline in the rate of oil head increase (Fig. 50). At extremely low alpha (.05/m) this decline in oil head rate is not found. Alpha =.05/m shows an initial increase in oil head at a slower rate than alpha = .2/m and .4/m although after 4 hours it exceeds the rates

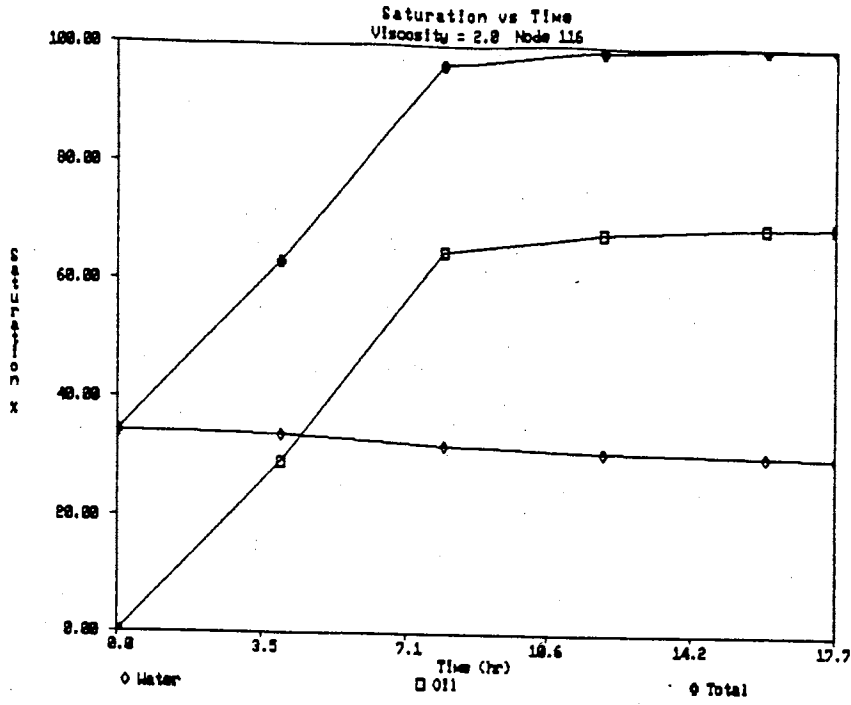


Figure 47. Saturation vs Time
Viscosity=2.0

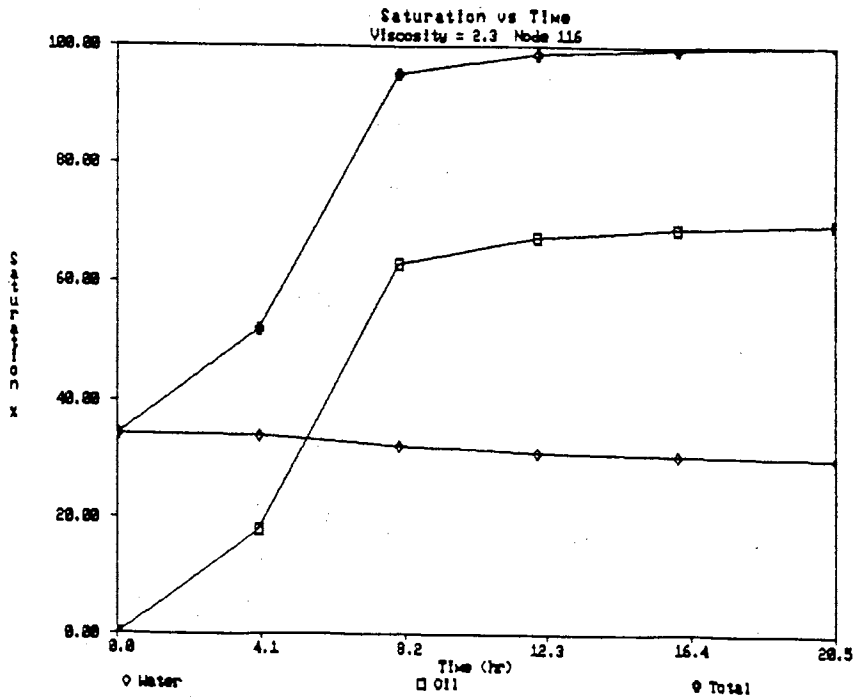


Figure 48. Saturation vs Time
Viscosity=2.3

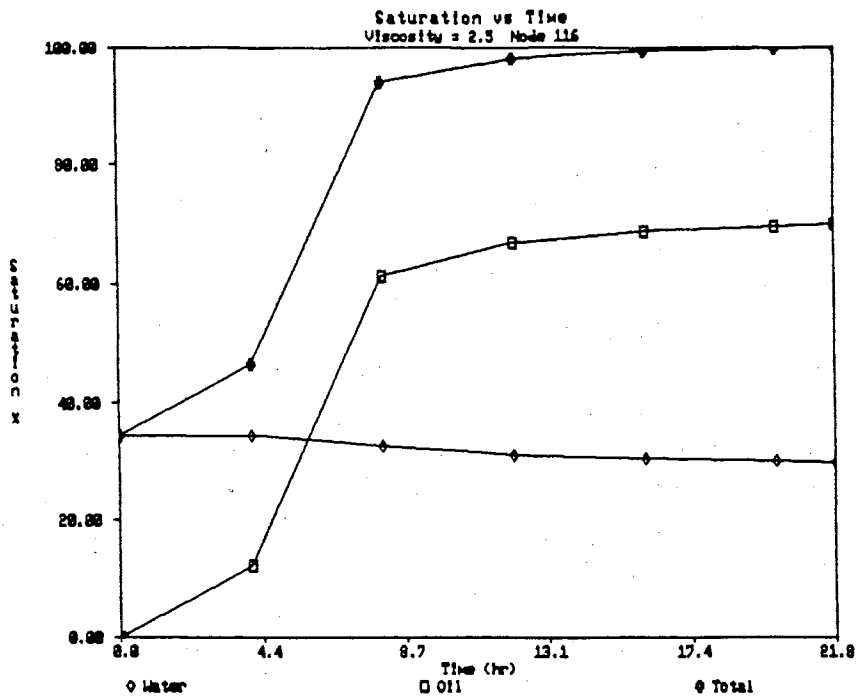


Figure 49. Saturation vs Time
Viscosity=2.5

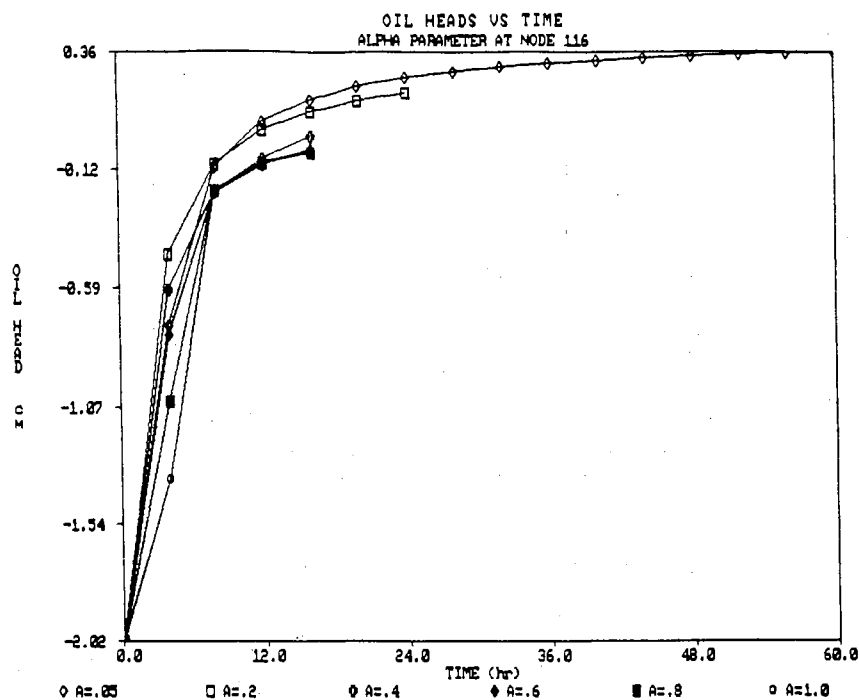


Figure 50. Oil Head vs Time For
Alpha Parameter

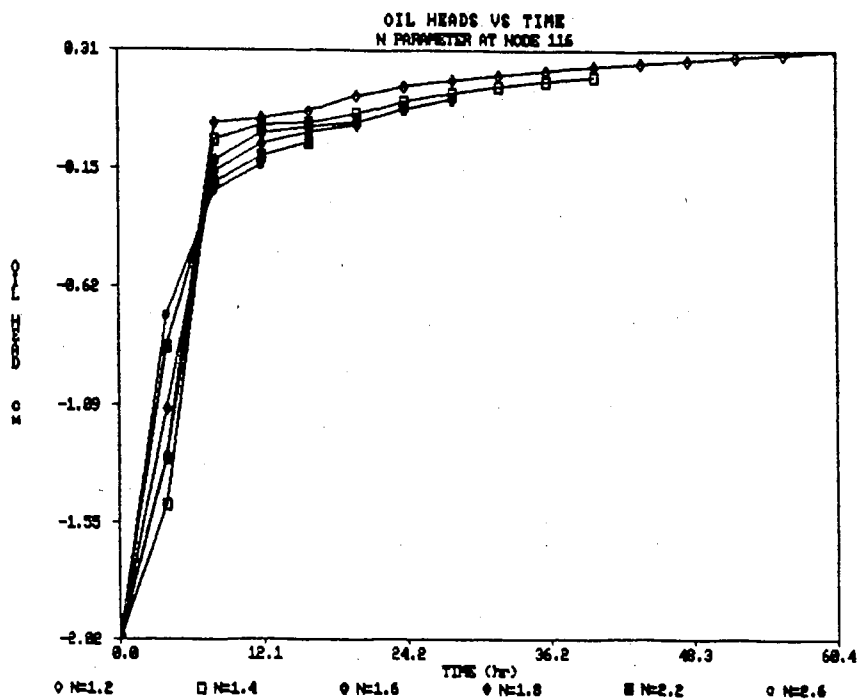


Figure 51. Oil Head vs Time For
N Parameter

of oil head increases for $.2/m$ and $.4/m$ and rises to a value of greater than zero. Oil heads at 4 hours for $\alpha = .2/cm$ and $1/cm$ vary 197% while, at 16 hours they vary only 61%.

N Parameter

The analysis of oil heads over time for the range of N values shows a relationship that is unique to the N parameter (Fig. 51) As the N values were increased, the rate of oil head increase during the first 4 hours of simulation time also increased. Yet, during the period after 4 hours this rate reverses. The rate of increase of oil head is greater for the lower N values than for the higher N values. There is no retardation in oil head response for the N parameter once the simulation starts. Oil heads at 4 hours for $N = 1.4$ and 2.6 vary 101%. At 12 hours the two extreme N values vary in value only 69%.

Porosity Parameter

Porosity values of 5%, 10%, and 20% all show a similar rate of increase of oil head with time (Fig. 52). At these values oil heads increase to above zero and approach a constant head of $.4$ cm. The general trend shows that as porosity is increased, the rate of increase for oil head decreases. Porosity values of 40% and 50% show an initial delay in oil head response which is not seen for the other

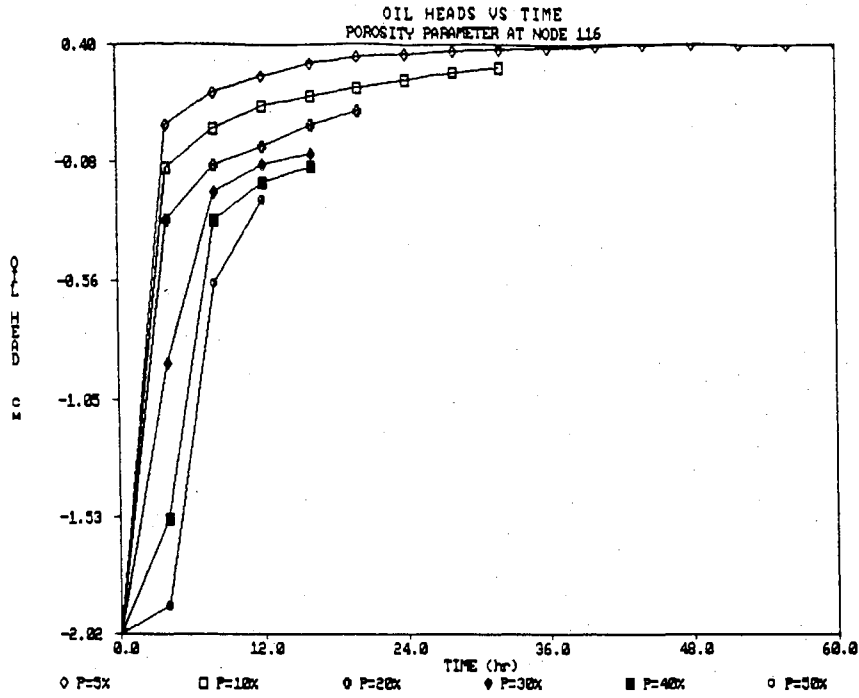


Figure 52. Oil Head vs Time For Porosity Parameter

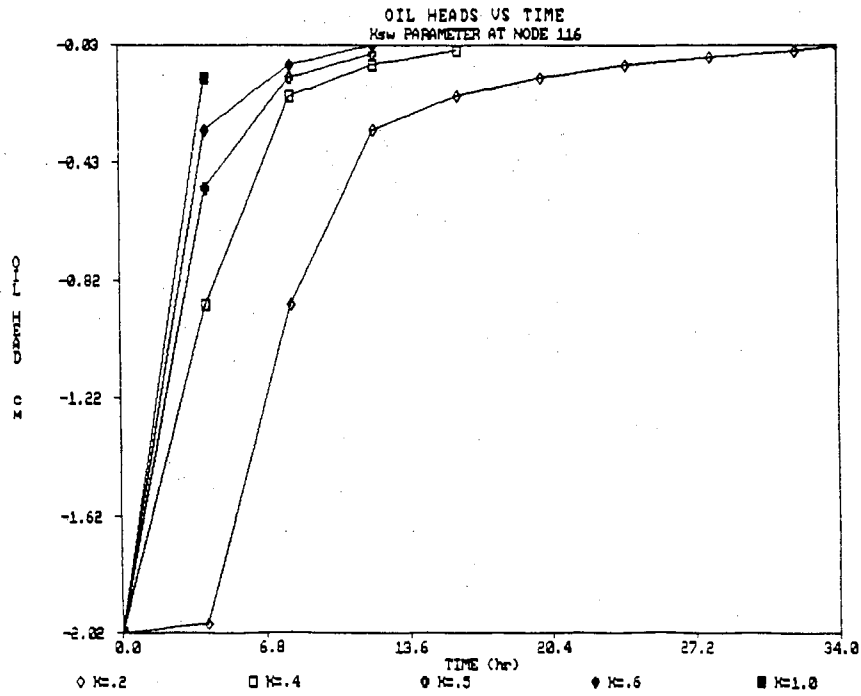


Figure 53. Oil Head vs Time For Ksw Parameter

values of porosity. Oil heads for the two extreme values of porosity (5% and 50%) show a 2,547% difference in value. At 12 hours this difference in oil head values decreases to only 16%.

Permeability (Ksw) Parameter

Oil heads at node 116 for the Ksw parameter exhibit a trend similar to the other parameters of increasing from an initial value of -2.02 cm to 0 cm of water equivalent head (Fig. 53). At $K_{sw} = .2$ m/day there is an initial delay in oil head increase. The rate of increase in oil head decreases with decreasing permeability. All oil heads asymptotically reach zero with time. Higher water saturated permeability values reach zero faster while lower permeability values reach zero oil head at a slower rate. A difference in oil heads values of 526% is seen between the values of $K_{sw}=.6$ and $K_{sw}=.2$ at 4 hours. Later at 8 hours there is only a 117% difference between oil head values for these values.

Density Parameter

Oil heads for each density parameter increase with time and asymptotically approach zero (Fig 54). As the density parameter is increased oil head increases as a greater rate with each increment of density. When the model was run with a density value of 1.6, the oil head is shown to decrease

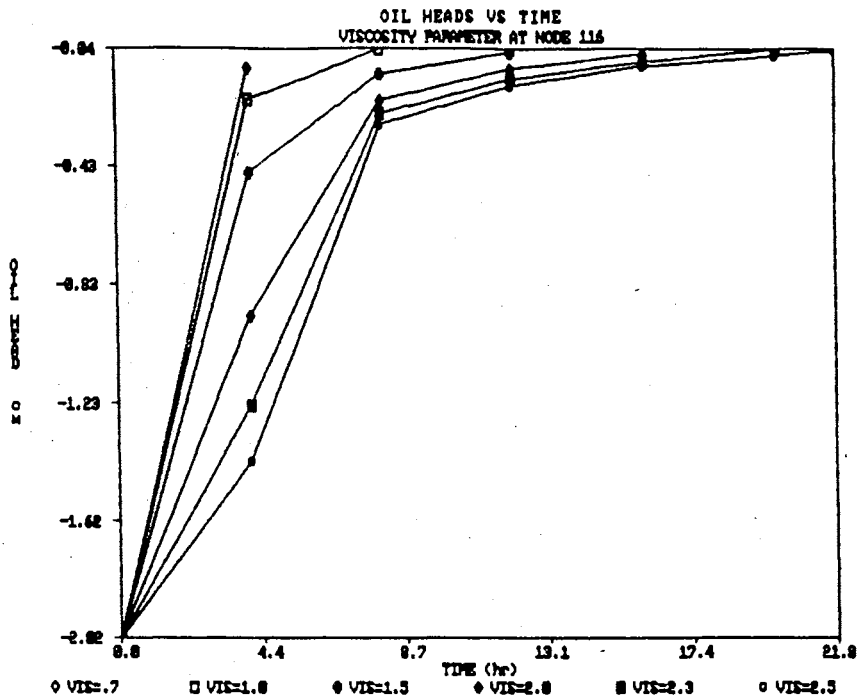


Figure 54. Oil Head vs Time For Viscosity Parameter

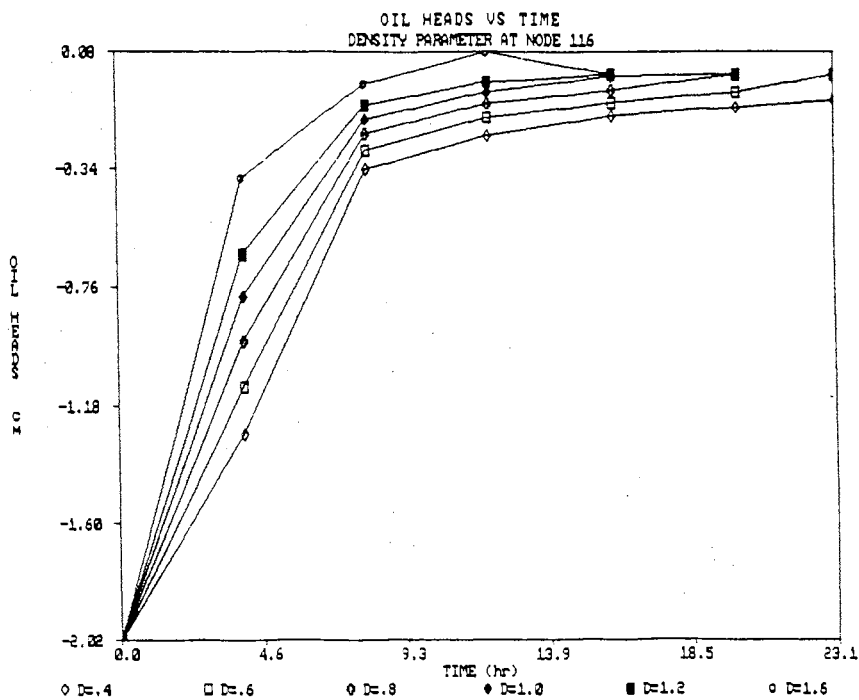


Figure 55. Oil Head vs Time For Density Parameter

slightly after reaching a value of near zero. This slight decrease is caused by the passage of the oil front past the node point and shows the decrease of oil head as the front travels away from node 116. Oil heads for the density parameter show a variation of 243% between oil density ratio values of .4 and 1.6. Later at 12 hours there is only a 185% difference.

Viscosity Parameter

Examination of oil heads with time at node 116 shows that as viscosity is increased the rate at which oil head increases is lower with increasing viscosity (Fig. 55). Oil heads at viscosity = .7 and 1.0 increase at the fastest rate and at nearly the same rate of .4 cm/hr during the first 4 hours of the simulation. At the higher viscosity values of 2.3 and 2.5, rates of increase are approximately -.19 and -.15 cm of water equivalent head respectively. At these higher values of viscosity, the rate of increase in oil head increases between 4 and 8 hours. The other values of viscosity show that the rate of increase of oil head decreases between 4 and 8 hours. The oil heads all asymptotically approach zero with time from the initial -2.02 cm of water equivalent head. The viscosity parameter shows a 582% change in oil head values between viscosity to oil ratios of 1.0 and 2.5 at 4 hours. At 12 hours this decreases to a 237% difference.

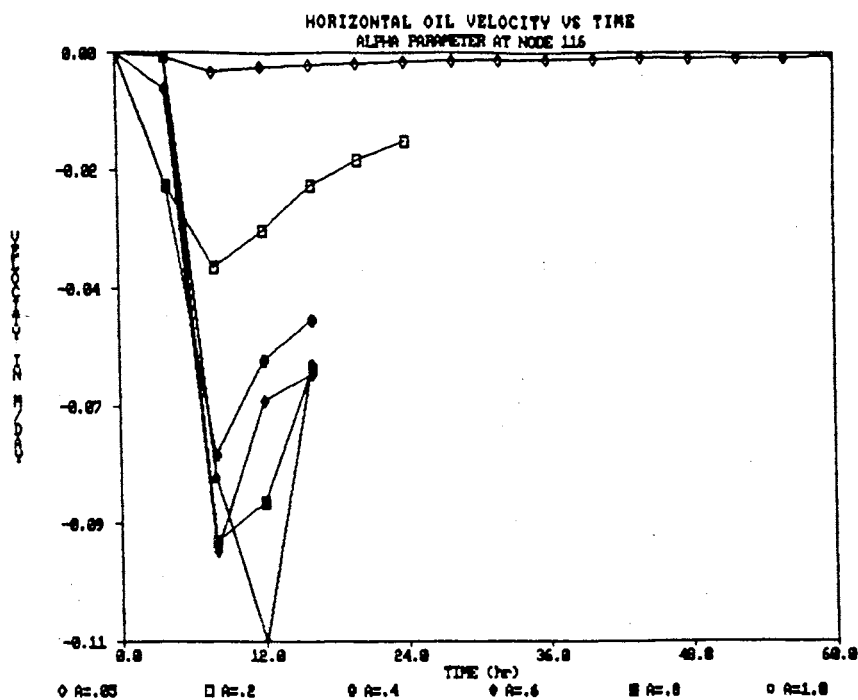


Figure 56. Horizontal Oil Velocity
Alpha Parameter

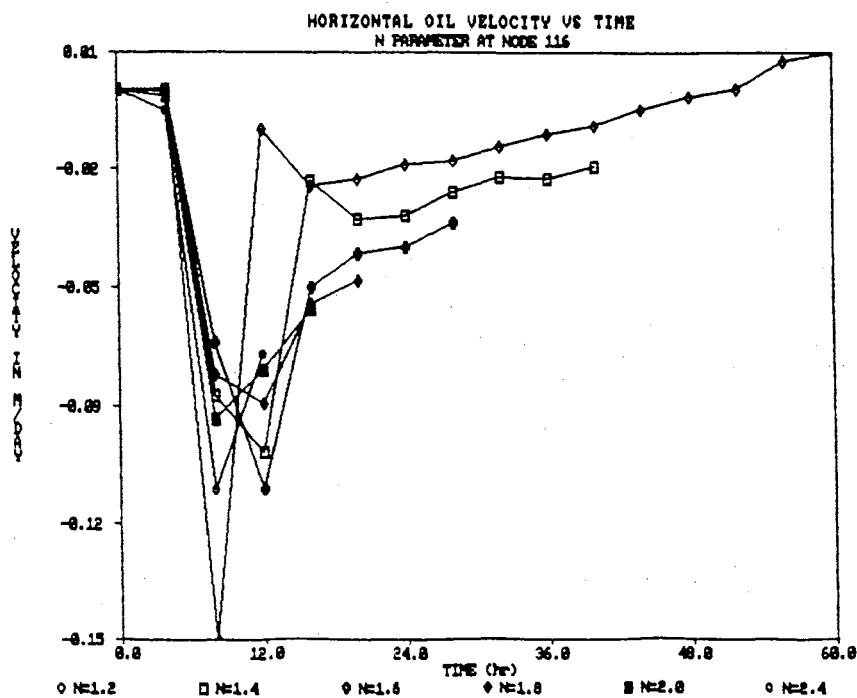


Figure 57. Horizontal Oil Velocity
N Parameter

Oil Velocities

Alpha Parameter

At $\alpha = .05/m$ there is very little increase in horizontal oil velocity over time (Fig. 56). As α is increased horizontal oil velocity reaches increasingly higher values. At $\alpha = 1.0/m$ horizontal oil velocity reaches $.11$ m/day at 12 hours. Vertical oil velocities exhibit a similar trend but at greater magnitudes. The maximum vertical oil velocity observed was 3.31 m/day at $\alpha = 1.0/m$. Once the horizontal oil velocities reach their greatest values of 8 to 12 hours, they decrease and appear to level off to more constant values.

N Parameter

Horizontal oil velocities at node 116 during the initial 4 hours act similar as the N parameter is varied (Fig. 57). $N = 1.2$ exhibits the fastest rate of increase in horizontal oil velocity and reaches a maximum value of $.15$ m/day. The other values of N act in a similar manner of increasing to approximately $.09$ m/day then decreasing over time. All values of N with the exception of $N=1.4, 1.6,$ and 1.8 maximum horizontal oil velocity is reached at 12 hours. A maximum vertical oil velocity of 3.38 m/day is reached at 12.8 hours for $N=2.6$. Therefore

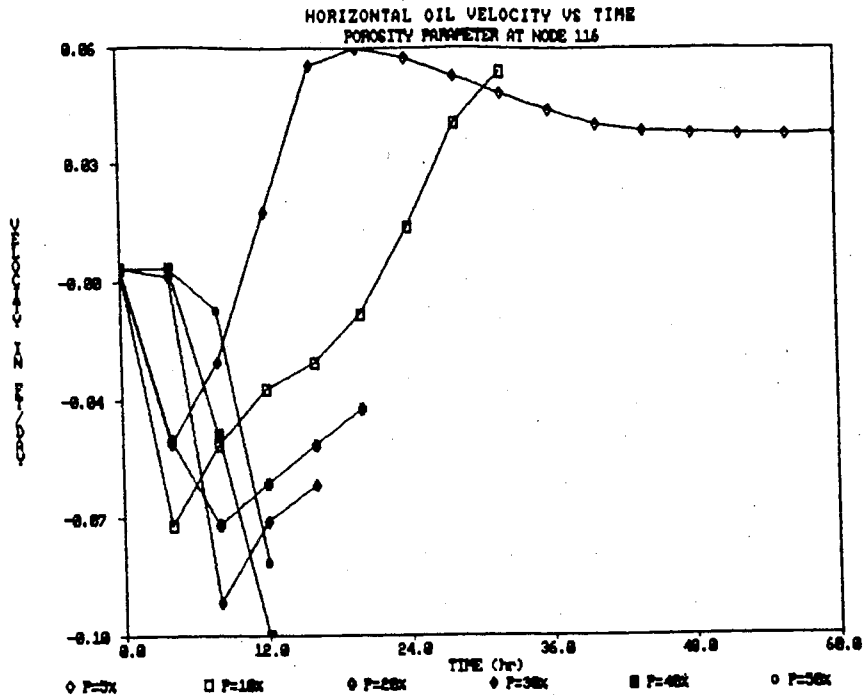


Figure 58. Horizontal Oil Velocity
Porosity Parameter

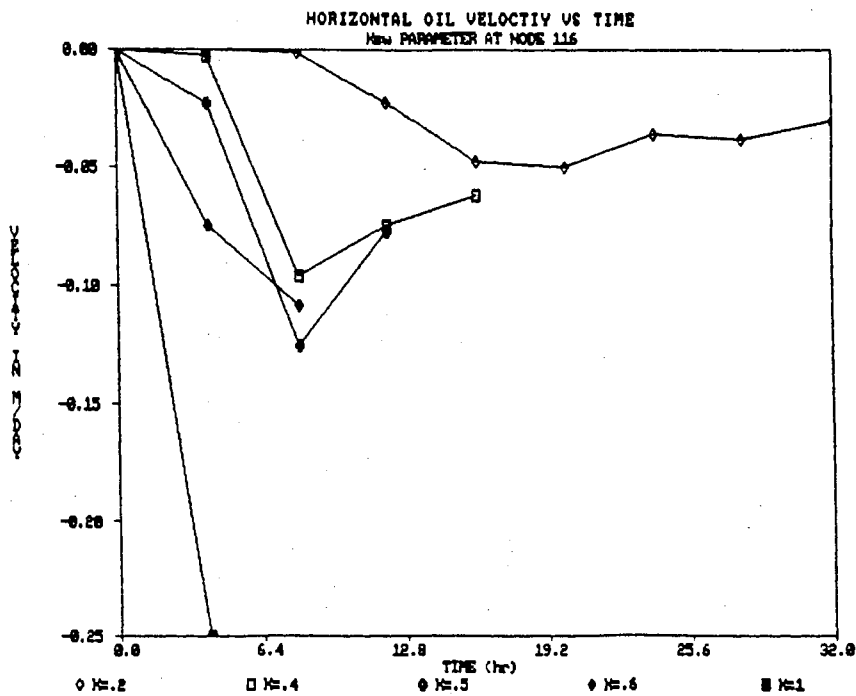


Figure 59. Horizontal Oil Velocity
Ksw Parameter

it is found that maximum horizontal oil velocity occurs at $N=1.2$ while maximum vertical oil velocity is found at $N=2.6$.

Porosity Parameter

At porosity = 5% and 10% there is a rapid increase of horizontal oil velocity within 4 hours after the simulation had started (Fig. 58). This is followed by a decrease in velocity and sequentially a slower increase in velocity in the x direction. Porosity values of 20%, 30%, 40% and 50% initially exhibit a delay in oil velocity response over the first 4 hours of simulation time. Yet, after 4 hours the velocities increase. As porosity is increased, horizontal oil velocity also increases but the rate of change in this velocity decreases. The maximum horizontal oil velocity seen for the porosity simulations was .10 m/day. Maximum vertical oil velocities observed during the simulation reached approximately 3 m/day at 20-30% porosity.

Permeability (Ksw) Parameter

At low permeability of .2 m/day a 8 hour delay in velocity response is observed (Fig. 59). As K_{sw} is increased the delay period shortens until $K_{sw} = .5$ m/day. The general trend for the permeability parameter shows that as permeability is increased of oil velocity rates also increase. At $K_{sw} = 1.0$ m/day horizontal oil velocity

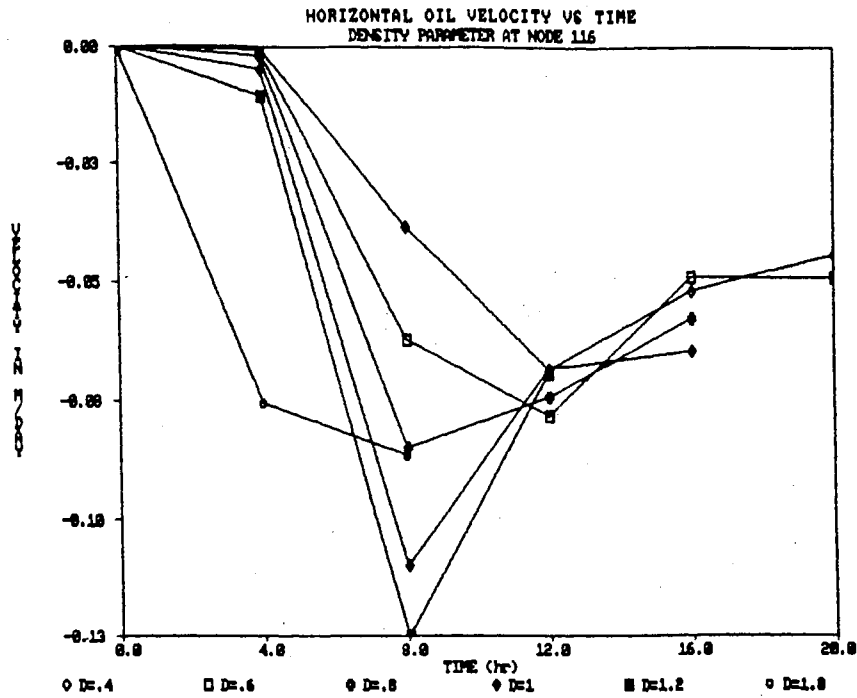


Figure 60. Horizontal Oil Velocity
Density Parameter

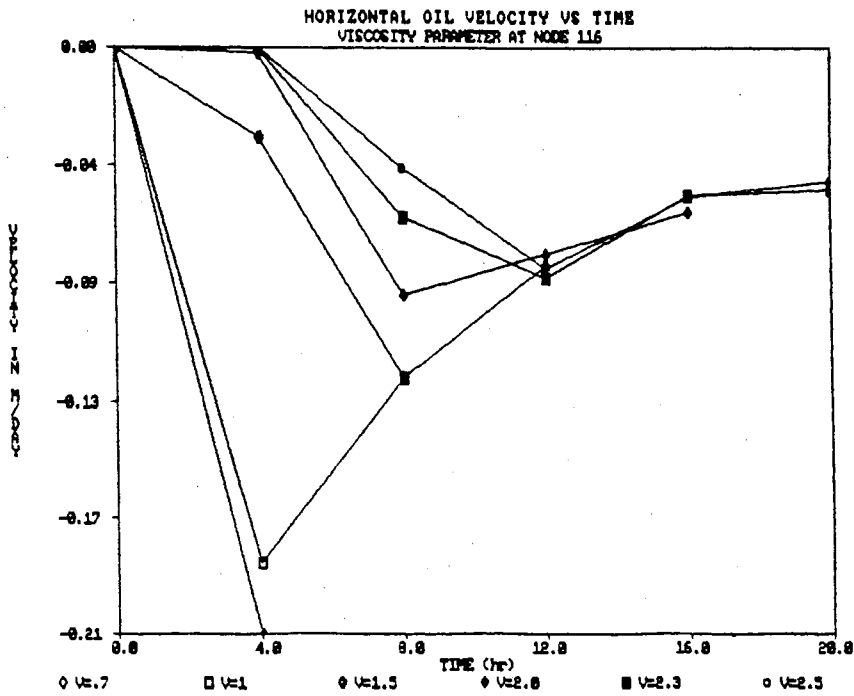


Figure 61. Horizontal Oil Velocity
Viscosity Parameter

increases rapidly over the first four hours to a value of .25 m/day. It is presumed that at Ksw values of greater than 1.0 m/day (i.e. 3, 5, or 7 m/day) oil velocities would reach even greater values than this. Vertical oil velocities show the same trend as the horizontal velocities of an initial increase in velocity followed by a decrease in velocity with time. The maximum vertical oil velocity observed for the simulations was 7.68 m/day for Ksw = 1.0 m/day at 7 hours.

Density Parameter

As density increases, sharper increases in horizontal oil velocity with time are observed (Fig. 60). Although, at density = 1.8 oil velocity does not show as high a value for horizontal velocity as at density = 1.0 and 1.2. The maximum horizontal oil velocity was observed to be .13 m/day at a density of 1.2. Maximum horizontal oil velocity for density = 1.8 was observed to be .09 m/day. Vertical oil velocities reached a maximum value of 6.5 m/day for a density of 1.8.

Viscosity Parameter

As viscosity is decreased, horizontal oil velocities at node 116 increase in rate (Fig. 61). At a viscosity of .7 oil velocity is observed to have the greatest value of -.21

m/day. Viscosities of 2.0, 2.3, and 2.5 show essentially no horizontal oil velocities during the first 4 hours. This is due to the fact that the oil front does not reach node 116 at that time. The oil horizontal velocities for viscosity equal to .7, 1.0, and 1.5, after an initial rapid increase, decrease and level off to approximately .05 to .06 m/day. All other values of viscosity level off to close to the same point. Maximum vertical oil velocity was found to be 8.4 m/day at viscosity = .7.

Plume Configuration

Alpha Parameter

Changes in the alpha parameter appear to have very little effect on the plume configurations. Plots of the plumes at time = 16 hours can be found in Appendix C. Plume size changes very little as the alpha parameter is changed over its range of values.

N Parameter

Plume configurations at 12 hours for the N parameter show little effect on N on the plume size. At $N = 1.2$ and 1.4 , plume size is approximately the same. At $N = 1.6$, the plume increases in size both laterally and vertically but not to a significant extent. From $N = 1.6$ to 2.6 plume size does not increase in size and remains in a similar configuration (see Appendix C).

Porosity Parameter

Plume configurations were plotted for porosity at time equal to 12 hours. Distinct changes in plume sizes is observed. As porosity is decreased the plume size enlarges dramatically especially at porosity = 5% and 10% (see Appendix C).

Permeability (Ksw) Parameter

Plots of the oil plume configurations for the various Ksw values used indicates that as expected at low Ksw values the plume is small and increases in size for higher Ksw values. Appendix C contains plots of the oil plumes for Ksw at 4 hours.

Density Parameter

Examination of the oil plumes for the density parameter at time = 8 hours shows that the plume expands downward further with each increasing step of density. Horizontal spread of the plume at the upper nodes is not observed with changing densities. Plume configurations for the density parameter at 8 hours can be found in Appendix C.

Viscosity Parameter

Examination of plume configurations for the viscosity parameter at 4 hours shows a marked decrease in plume size

both laterally and vertically as viscosity is increased. The most distinct change occurs between viscosity = 1 and 1.5. Little change is seen between 1.5 and 2.0 yet a distinct change occurs between 2.0 and 2.5 (see Appendix C).

Central Processing Unit (CPU) Time

One noted disadvantage of the MOFAT-2D model is its' requirements on central processing unit (CPU) time. Depending on the simulation, CPU times often exceeded 70 minutes and occasionally exceeded 90 minutes on the IBM mainframe (see Table IV). Analysis of alpha, N, and porosity show that as the parameter is increased in value the CPU time decreases in an exponential manner. Permeability and density show no distinct pattern in CPU time as compared to increasing values. No explanation for this inconsistent pattern is available. Viscosity shows a unique CPU time - parameter relationship. As viscosity increases CPU time also increases.

Time For Total Oil Infiltration

Figures 74 through 79 show the relationships between the values of the parameters and the time it takes for the total amount of oil at the surface to infiltrate. Parameters alpha, N, porosity and permeability show a exponential type relationship between increasing parameter values and total infiltration time. Density and viscosity

parameters show a linear type relationship between infiltration time and the increasing parameter values.

TABLE IV
CPU TIMES AND COMPUTER COSTS FOR PARAMETERS

Parameter	Value	CPU Time (Min)	Cost of Run (w/o discounts)
Alpha	.05	79.6	\$1,326.67
	.2	59.5	\$991.67
	.3	53.4	\$890.00
	.4	48.9	\$815.00
	.5	47.1	\$785.00
	.6	46.0	\$766.67
	.7	44.3	\$738.33
	.8	43.3	\$721.67
	.9	42.8	\$713.33
	1.0	43.0	\$716.67
N	2.6	40.20	\$670.00
	2.4	40.44	\$674.00
	2.2	42.06	\$701.00
	2.0	44.28	\$738.00
	1.8	48.65	\$810.83
	1.6	55.34	\$922.33
	1.4	66.19	\$1,103.16
	1.2	92.11	\$1,535.17
Ksw	0.2	44.12	\$735.33
	0.4	44.08	\$734.67
	0.5	42.31	\$705.17
	0.6	41.54	\$692.33
	1.0	33.56	\$559.33
	3.0	30.89	\$514.83
	5.0	23.07	\$384.50
Porosity	5%	99.03	\$1,650.50
	10%	63.90	\$1,065.00
	20%	55.01	\$916.83
	30%	48.21	\$803.50
	40%	44.20	\$736.67
	45%	42.49	\$708.17
	50%	43.71	\$728.50

TABLE V (Continued)

Parameter	Value	CPU Time (Min)	Cost of Run (w/o discount)
Density	.4	45.9	\$765.00
	.6	44.45	\$740.83
	.8	43.71	\$728.50
	1.0	44.06	\$734.33
	1.2	44.13	\$735.50
	1.6	45.43	\$757.16
	1.8	44.88	\$748.00
Viscosity	2.5	45.18	\$753.00
	2.3	44.68	\$744.67
	2.0	43.79	\$729.83
	1.7	42.85	\$714.16
	1.5	42.24	\$704.00
	1.0	38.82	\$647.00
	0.7	36.22	\$603.67

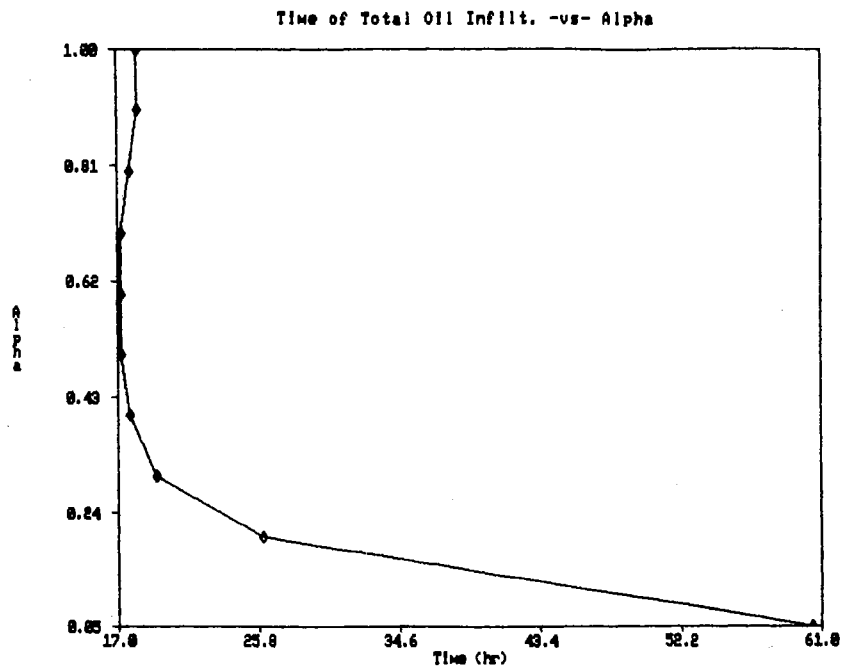


Figure 74. Total Time of Oil
Infil. vs Alpha

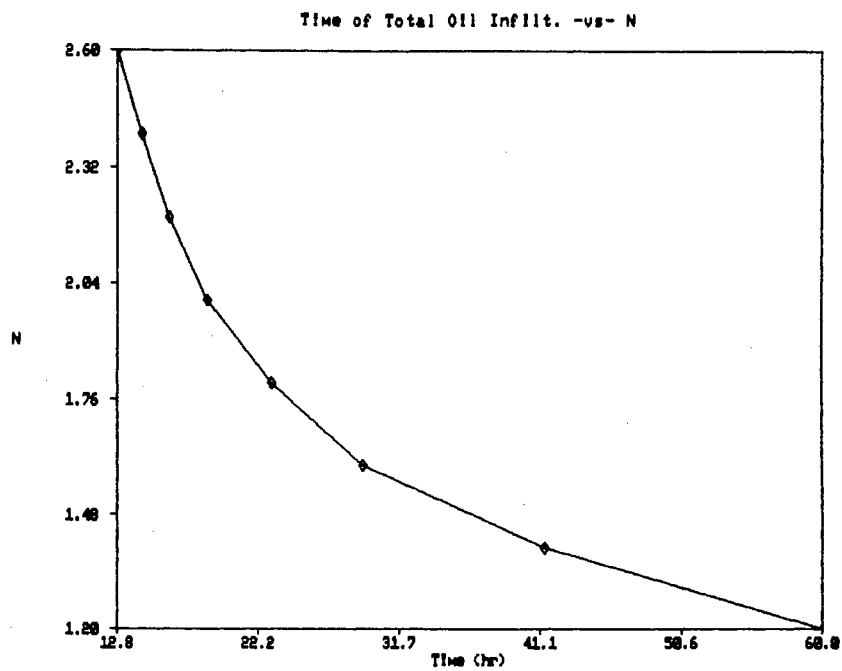


Figure 75. Total Time of Oil
Infil. vs N

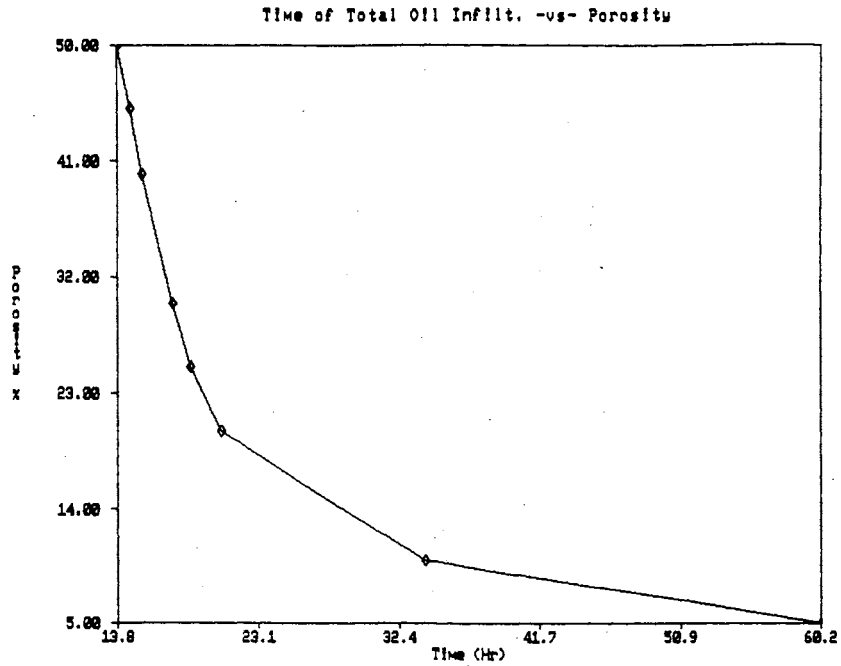


Figure 76. Total Time of Oil Infil. vs Porosity

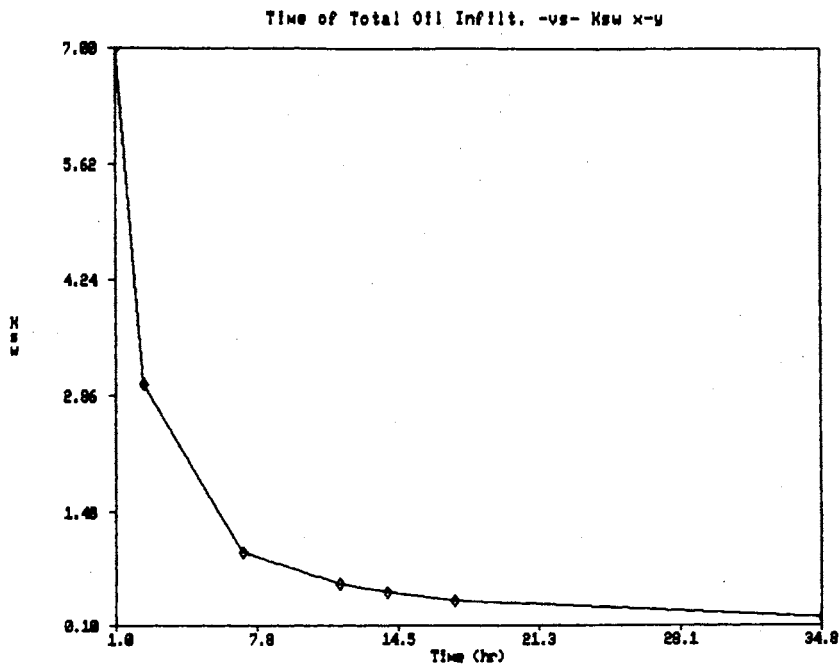


Figure 77. Total Time of Oil Infil. vs Ksw

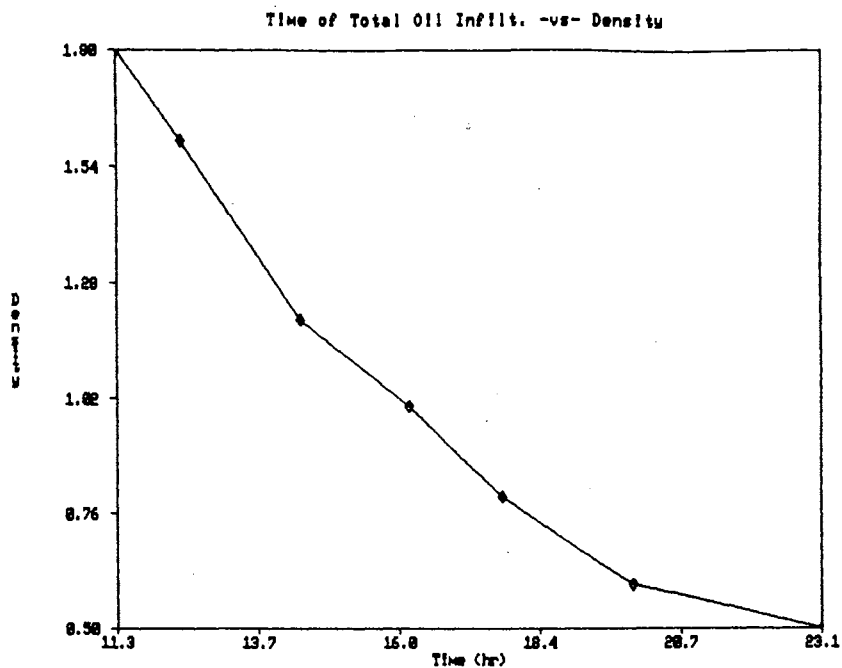


Figure 78. Total Time of Oil Infil. vs Density

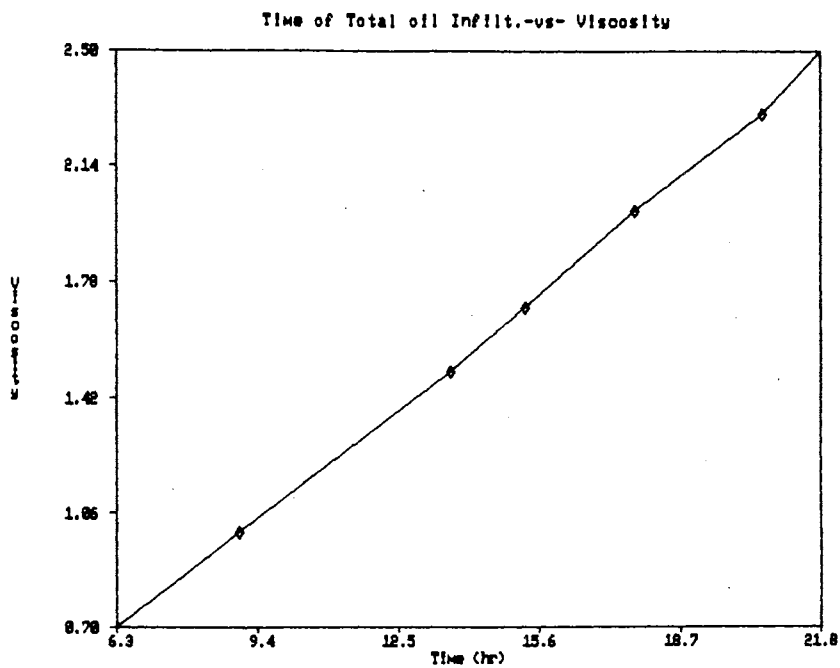


Figure 79. Total Time of Oil Infil. vs Viscosity

CHAPTER V

CONCLUSIONS

Analysis of the data pertaining to the sensitivity of each of the six parameters shows interesting results. One parameter may greatly affect a certain output value while not affecting other output values. It is the purpose of this study to determine how each parameter affects the individual output values.

The alpha parameter appears have a great affect on oil saturation values within the unsaturated zone. The greatest amount of variation in initial and final saturation values for the various parameters is observed with the alpha value. The N parameter is similar to alpha in its' affect on oil saturation values. For each increment in alpha there is a small change in oil saturation. For N there is a significant change in oil saturation for each increment of N. Therefore, MOFAT 2-D is more sensitive to N than alpha in its prediction of oil saturations. Alpha and N effect to a great extent the initial water saturation values that the model predicts. For alpha, initial water saturation values decrease 74% between alpha = .05/m and 1.0/m. Alpha is incorporated into the Van Genuchten soil equations used by

the model to determine water and total saturations (Table I). N is an exponential constant in the same equations.

Porosity appears to have a pronounced affect on oil and water saturation although, not as great as the alpha and N parameter. At high porosity values , the saturation of oil in the pore spaces in the unsaturated zone takes up to 6 hours while at porosity = 5% there is almost instantaneous saturation. The porosity term is incorporated into the fluid capacity term of the 2-D flow equations used by the model.

Permeability, incorporated into the Darcy velocity portion of the multiphase flow equations, has a small affect on the prediction of oil saturation in the unsaturated zone. Increases in the permeability parameter causes increased rates at which oil saturates the pore spaces.

Density, incorporated into directly into the Darcy velocity term of the multiphase flow equations, has very little effect on predicted oil saturation rates in the unsaturated zone. As predicted by MOFAT 2-D, low density hydrocarbons take a greater amount of time to saturate the pore spaces over the more dense hydrocarbons.

Viscosity, also incorporated into the Darcy velocity equation through the phase conductivity term, has little affect on the prediction of oil saturation rates within the unsaturated zone. As viscosity is increased, oil saturation rates decrease and exhibit substantial retardation of 2

hours at high values.

Oil heads in the unsaturated zone indicate a trend of increasing oil heads from an initial value of -2.02 cm of water equivalent head to a near constant level. For all of the parameters, the oil head values during the initial 0 to 8 hours have the greatest amount of variation. With increasing time, the oil head values within the unsaturated zone for each of the parameter values approach each other and have a smaller range of variation.

Oil heads in the unsaturated zone for the alpha parameter at 4 hours vary 197% from -.456 cm for alpha = .2/cm to -1.355 cm for alpha = 1.0/cm. At 16 hours, oil heads at alpha = .2/cm and 1.0/cm vary only 61%.

Oil heads in the unsaturated zone for the N parameter at 4 hours, vary 101% from -1.48 cm at N=1.4 to -.734 at N=2.6. At 12 hours, oil heads only vary 69% between the two extreme values of N=1.2 and N=2.6. As N values are increased, the rate of oil head increase during the first four hours also increases. This trend reverses at 8 hours.

Oil heads for the porosity parameter show a large difference in values during the initial 8 hours of simulation time. At 4 hours, there is a 2,574% difference between oil head values of -.071 cm and -1.899 cm at 5% and 50% respectively. At 12 hours, the percentage of difference in oil heads decreases to only 16% from -.273 cm for 5% porosity to -.234 cm for 50% porosity.

Oil heads for the permeability parameter within the unsaturated zone show a large variation in values at 4 hours. A difference of 526% is seen between the value of oil head for $K_{sw}=.6$ and $K_{sw}=.2$ at 4 hours. Later at 8 hours there is a 117% difference between oil head values for $K_{sw}=.6$ and $K_{sw}=.2$.

Oil head for the density parameter has a variation of 243% in oil head values from predicted oil head for oil to water density ratios of .4 and 1.6 at 4 hours. Later at 12 hours there is only a 185% difference in values.

The viscosity parameter shows a 582% change in oil head values between viscosity to oil ratios of 1.0 and 2.5 at 4 hours. At 12 hours this decreases to a 237% difference.

Oil velocities are affected slightly by the alpha and N parameter. This is due to the fact that both alpha and N are utilized in the Van Genuchten soil saturation equations and are not incorporated into the Darcy velocity portion of the multiphase flow equations. Horizontal oil velocities for the alpha parameter vary from 0 m/day to .11 m/day during the first 12 hours of time. Horizontal oil velocities for N vary from 0 to .15 m/day during the same period.

The affect of porosity, permeability, viscosity and density on horizontal oil velocity is difficult to distinguish although, viscosity and permeability appear to

have the most pronounced effect. Horizontal oil velocity values for the porosity parameter ranged between 0 and .10 m/day. In the unsaturated zone, both viscosity and permeability had the greatest range of horizontal and vertical oil velocity values of all of the parameters. Both had horizontal oil velocities reach values of up to .2 m/day.

CPU times for the alpha, N, porosity and permeability parameters increase with decreasing values. Density shows an irregular trend in CPU time. Viscosity, demonstrates a opposite relationship of increasing CPU time with increasing values. Table V shows the CPU times and costs required to run the simulation for each parameter based on a class 1 and class 2 rate of \$1000.00 per CPU hour.

The time for the total 7.5 cubic meters per square meters of oil to infiltrate as compared to the parameters appears to be affected to the greatest extent by permeability. Increases in the permeability values causes significantly increased infiltration rates and oil velocities. Density shows a direct relationship between increase in infiltration rate and increasing density. Viscosity shows an inverse relationship between infiltration rate and increasing viscosity. Appendix E contains the approximate curve equations that describe the infiltration time versus the parameter values.

Plume configurations within the unsaturated zone show

that porosity, density and viscosity have the most pronounced affect on the plume sizes. Porosity appears to cause the greatest variation in plume size especially at low porosities between 5% and 10%. Very little skew in the direction of water flow gradient is observed for any of the plumes.

REFERENCES

- Abriola, Linda M., Pinder George F., A Multiphase Approach to the Modeling of Porous Media Contamination by Organic Compounds, (1.) Equation Development. Water Resources Research, Vol. 21, No.1, pages 11-18, January 1985.
- Abriola, Linda M., Pinder George F., A Multiphase Approach to the Modeling of Porous Media Contamination by Organic Compounds, (2.) Numerical Simulation. Water Resources Research, Vol. 21, No.1, pages 19-26, January 1985.
- Baehr, Aurthur., Immicible Contaminant Transport in Soils With an Emphasis on Gasoline Hydrocarbons, PH.D. Dissertation. Dept. of Civil Eng., University of Delaware. Newark 1984, p.403.
- Bridie, A.L.A.M., Groenewould, W.M., Van Der Waarden, M., Transport of Mineral Oil Components to Groundwater-I, Model Experements on the Transfer of Hydrocarbons From a Residual Oil Zone to Trickling Water. Water Research. Pergamon Press 1971. Vol. 5, Great Britian. pp.213-226.
- Bridie, A.L.A.M., Groenewould, W.M., Van Der Waarden, M., Transport of Mineral Oil Components To Groundwater-II, Influence of Lime, Clay and Organic Soil Components on the Rate of Transport. Water Research. Pergamon Press 1977. Vol. 11, pp.359-365. Great Britian.
- Brooks, R.H., and Corey, A.T., Properties of Porous Media Affecting Fluid Flow, ASCE Journal, Irrigation Drainage Division, IR2, Vol. 92, 1966.
- Burcik, Emil J., Properties of Petroleum Reservoir Fluids, John Wiley and Sons, Inc., New York, 1961. 190pp.
- Byer, H.G., Blankenship, W., and Allen R., Groundwater Contamination by Chlorinated hydrocarbons: Causes and Prevention, ASCE, 54-55, March 1981.

- Casulli, V., Greenspan, D. Numerical Simulation of Miscible and Immiscible Fluid Flows in Porous Media. Society of Petroleum Engineers Journal, Vol. 22, No. 5, pages 635-649, 1971.
- Corapcioglu, M. Yavuz , Baehr , Aurthur L., A Compositional Multiphase Model for Groundwater Contamination by Petroleum Products. (1.) Theoretical Considerations. Water Resources Research, Vol. 23, No.1, pages 191-200, January 1987.
- Corapcioglu, M. Yavuz, Baehr, Aurthur L., A Compositional Multiphase Model for Groundwater Contamination by Petroleum Products. (2.) Numerical Solution Water Resources Research, Vol. 23, No.1, pages 201-213, January 1987.
- Corey, A.T., The Iterrelation Between Gas and Oil Relative Permeability, Producers Monthly, Vol. 19, No. 1, 1954.
- Dibble, J.T., and Bartha, H., Effect of Environmental Parameters on the Biodegradation of Oil Sludge, Applied Environmental Microbiology, Vol. 37, No. 4, pp. 729-738 1979.
- Douglas, J., Peaceman, D.W. and H. H. Rachford, A Method for Calculating Multi-dimensional Immiscible Displacement, Trans., American Institute of Mining, Metallurgical and Petroleum Engineering, Soc. of Petroleum Eng., Vol. 216 pp. 297-305, 1959.
- Duffey, J.J., E. Peake, and M.F. Mohtadi, Oil Spills on Land as Potential Sources of Groundwater Contamination. Environmental International, Vol. 3, pp. 107-120, 1980, Great Britian.
- Dumas, Alex., Brooklyn Spill : 17 Million Gallons under the Side Walks of New York, National Petroleum News, Jan 1980. pp. 34,35.
- Faust, Charles R., Transport of Immiscible Fluids Within and Below the Unsaturated Zone: A Numerical Model, Water Resources Research, Vol. 21, No. 4, Pages 587-596, April 1985.
- Fried, J.J., P. Muntzer, and L. Zilliox., Ground-Water Pollution By Transfer Of Oil Hydrocarbons., Groundwater, Vol. 17, No. 6, Nov-Dec. 1979.

- Goodger, E. M., Hydrocarbon Fuels - Production, Properties and Performance of Liquids and Gases, The Macmillian Press Ltd. New York, pp.270 1975.
- Gudin, C., W.J. Syrratt, Biological Aspects of Land Rehabilitation Following Hydrocarbon Contamination. Environmental Pollution, (8) Applied Science Publishers. England, pp. 107-112, 1975.
- Hochmuth, David P., Sunada, Daniel K., Ground-Water Model of Two-Phase Immiscible Flow in Coarse Material. Ground Water, Vol. 23, No. 5, Sept-Oct 1985. pp. 617-625.
- Hoffman, B., Dispersion of Soluble Hydrocarbons in Groundwater Streams Advances in Water Pollution Research, Ed. S. H. Jenkins, pp. HA/7 (b)/ 1-8, 1970.
- Holzer, Thomas L., Application of Ground-Water Flow Theory to a Subsurface Oil Spill. Ground Water, Vol. 14, No. 3, May-June 1976. pp. 138-145.
- Huyakorn, P.S., S.D. Thomas, J.W. Mercer, and B.H. Lester, SATURN: A Finite Element Model For Simulating Saturated-Unsaturated Flow And Radionuclide Transport, report prepared for Electric Power Research Institute, Geo Trans., Herndon, VA., 1983.
- Kaluarachchi, J.J. and J.C. Parker, User Guide to MOFAT-2D Version 1.2 - A Two Dimensional Vertical Section Finite Element Code for Flow and Multispecies Transport in Three Fluid Phase Porous Media Systems, Virginia State University, Blacksburg Va., 1988.
- Kovski, John R. P.E., Physical Transport Process for Hydrocarbons in the Subsurface. Second International Conference on Groundwater Quality Research. National Center for Groundwater Research., pp. 127-128.
- Mackay, Donald and Aaron W. Wolkoff., Rate of Evaporation of Low-Solubility Contaminants From Water Bodies to Atmosphere. Environmental Science and Technology, Vol. 7, No. 7, 1973, pp.611-614.
- Matis, John R., Petroleum Contamination of Ground Water in Maryland. Ground Water, Vol. 9, No. 6, Nov-Dec 1971, pp.57-61.

- McAuliffe, C., Solubility in Water of Paraffin, Cycloparaffin, Olefin, Acetylene, Cycloolefin and Aromatic Hydrocarbons, Journal Physical Chemistry, Vol. 70, No. 4 ,1267-1275, 1966.
- McKee, J.E., F.B. Laverty, and R.M. Hertel, Gasoline in Groundwater. Journal Water Pollution Control Federation, Vol. 44, No. 2, 293-302 1972.
- Mull, R., The Migration of Oil-Products in the Subsoil with Regard To Ground-Water-Pollution by Oil. Advances in Water Pollution Research pp. HA-7(a)/1, 1970.
- Neuman, S.P., R.A. Feddes, and E. Bresler, Finite Element Simulation of Flow in Saturated-Unsaturated Soils Considering Water Uptake By Plants, Development of Methods, Tools, and Solutions For Unsaturated Flow, Third Annual Report., Technion, Haifa, Israel, 1974.
- Osborne M., Sykes J., Numerical Modeling of Immiscible Organic Transport at the Hyde Park Landfill. Water Resources Research, Vol 22, No. 1, Pages 25-33, January 1986.
- Osgood, J.O., Hydrocarbon Dispersion in Ground Water: Significance and Characteristics, Groundwater, Vol 12, No. 6, Nov-Dec 1974. pp427-428.
- Peaceman, D.W., Fundamentals of Numerical Reservoir Simulation, Elsevier, New York, 1977.
- Roberts, P., M. Reinhard, and A. Valocchi, Movement of Organic Contaminants in Groundwater: Implications for Water Supply, Journal Water Works Association, pp. 408-413, 1982.
- University Computer Center User Manual, Oklahoma State University Computer Center, 3rd ed., November 1985.
- Williams, Dennis E., Wilder, Dale G., Gasoline Pollution of a Ground Water aquifer - A Case History. Ground Water, Vol. 9, No. 6, Nov-Dec 1971. pp. 50-56.

- Van Dam, J., The Joint Problems of Oil and Water Industries, The Institute of Petroleum, London, pp. 55-88, 1967.
- Van Genuchten, M. Th., A Closed-Form Equation for Predicting the Hydraulic Conductivity of Unsaturated Soils. Soil Science Society Am. J. vol. 44, pp. 892-898, 1980.

APPENDIXES

APPENDIX A

MOFAT-2D: RECOMENDED JCL SAMPLE FOR IBM 3081K

```
//U12877G JOB(12877,446-45-5579),'NAME',TIME=(90,59),CLASS4,
//MSGCLASS X
//*PASSWORD SUSY
//*JOBPARM ROOM=M
//EXEC FORTVCLG
//FORT.SYSIN DD *
*
*
(FORTRAN PROGRAM)
*
*
//GO.FT09F001 DD UNIT=SYSDA,DISP=(NEW,CATLG),
// SPACE=(6160,(40,10),RLSE),
// DCB=(LRECL=80,BLKSIZE=6160,RECFM=FB),
// DSN=U12877G.SIM.DATA
//GO.FT10F001 DD UNIT=SYSDA,
// SPACE=(9040,(40,10),RLSE),
// DCB=(RECFM=U,LRECL=32760)
//GO.FT11F001 DD UNIT=SYSDA,
// SPACE=(9040,(40,10),RLSE),
// DCB=(RECFM=U,LRECL=32760)
//GO.FT12F001 DD UNIT=SYSDA,
// SPACE=(9040,(40,10),RLSE),
// DCB=(RECFM=U,LRECL=32760)
//GO.SYSIN DD *
*
*
(INPUT DATA)
*
*
//
```

APPENDIX B

INPUT DATA USED FOR MOFAT-2D SIMULATION

Line

Line	MOFAT.SIM	2D FLOW & INFITRATION									
1											
2	0	0	0								
3	0	2	1	2	1	1	0				
4	0	308	345	15	23	4	1	18	0	9	0
6a	2	5	23								
6c	1	0.0									
	2	2.0									
	8	5.0									
	11	8.0									
	15	10.0									
6d	0.0	2.0	3.0	4.0	5.0	6.0	7.0				
	8.0	9.0	10.0	11.0	12.0	13.0	14.0				
	15.0	16.0	17.0	18.0	19.0	20.0	21.0				
	22.0	23.0									
8	0.7	0.02	2.1	0.45	0.04	0.04					
9	1.2	0.5	1.83	2.2							
10f	3	23	-10.0								
10h	1	15	5.0								
	16	30	4.83								
	31	45	4.74								
	46	60	4.65								
	61	75	4.57								
	76	90	4.45								
	91	105	4.39								
	106	120	4.30								
	121	135	4.22								
	136	150	4.13								
	151	165	4.04								
	166	180	3.96								
	181	195	3.87								
	183	196	3.58								
	196	210	3.78								
211	225	3.70									
226	240	3.61									
241	255	3.52									
256	270	3.43									
271	285	3.35									

Line

APPENDIX B (Continued)

10h	286	300	3.26				
	301	315	3.17				
	316	330	3.09				
	331	345	3.0				
	3						
12a	1	1					
13	0.0	0.001	60.0	0.001	0.4	1.0300	2.00
14	1000	4	15	0	0.005	0.001	0.001
15	0.5		0.5				
16	2	0.0	7.5				
17	1	1	0				
	2	2	0				
	3	3	0				
	4	4	0				
	5	5	0				
	6	6	0				
	7	7	0				
	8	8	0				
	90	0	9				
	105	0	9				
	120	0	9				
	135	0	9				
	150	0	9				
	165	0	9				
331	2	0					
332	6	0					
333	7	0					
334	8	8					
19a	1	0.0	400.0	5.0	5.0		
	1	0.0	400.0	3.0	3.0		
	1	0.0	400.0	2.5	2.5		
	1	0.0	400.0	2.0	2.0		
	1	0.0	400.0	1.5	1.5		
	1	0.0	400.0	1.0	1.0		
	1	0.0	400.0	0.5	0.5		
	1	0.0	400.0	0.0	0.0		
	1	0.0	400.0	0.02	0.02		

APPENDIX B (Continued)

Line	Variable	Format	Description
1	TITLE	72A1	Description or title of the problem.
2	KAXIS	I5	Index to describe 2D radial problem: = 1 if radial = 0 otherwise
	KGAS	I5	Index to include gas convection to the flow problem: = 1 with gas convection = 0 otherwise
	KTRANS	I5	Index to include transport module: = 1 with transport = 0 otherwise
3	INPUT	I5	Index for execution control: = 0 executes the problem = 1 reads and prints a detailed version of input data
	ICAP	I5	Index to prescribe type of capacity computation for the flow problem: = 0 default option. = 1 modified analytical functions = 2 chord-slope approximation = 3 mid-pressure analytic scheme
	IELMT	I5	Index for nonlinear analysis: = 1 for Picard method = 2 for Newton-Raphson method
	IDIM	I5	Index to specify the units of linear dimensions: = 1 for cm = 2 for meters
	IMASS	I5	Index to specify mass fraction calculations: = 1 computes volume fraction of each phase for flow and mass of each species for transport = 0 otherwise
	ISOIL	I5	Index to described the type of soil constitutive relationship model used: = 1 van Genuchten = 2 Brooks and Corey

APPENDIX B (Continued)

Line	Variable	Format	Description
4	IMESH	I5	Index for mesh geometry: = 0 for a regular mesh (Fig. 2) = 1 for an irregular mesh (Fig. 3) = 2 for 1D mesh (Fig. 4)
	NEL	I5	Number of elements (only if IMESH > 0)
	NNOD	I5	Number of nodes (only if IMESH > 0)
	NROW	I5	Number of rows (only if IMESH=0)
	NCOL	I5	Number of columns (only if IMESH=0)
	NOR	I5	Number of data lines describing the connectivity of elements for IMESH=1
	NMAT	I5	Number of material types
	NNTO	I5	Number of nodes with type-1 boundary conditions for both water or oil phases
	NBEL	I5	Number of elements with type-2 boundary conditions for both water and oil phases
	NNTOP	I5	Number of cycles describing the time-dependence of the type-1, and -2 boundary conditions for both water and oil phases
	MSEEP	I5	Number of seepage faces (max = 2) and used with KGAS = 0
6A	NPP	I5	Index describing coordinate data: = 1 nodes are assumed to be equally spaced between given data and linearly interpolated using either X or Y coordinates = 2 Y-coordinates of the first vertical block of nodes are given and assumed to repeat at given X coordinates = 3 X-coordinates of the first horizontal block of nodes are given and assumed to repeat at given Y coordinates

APPENDIX B (Continued)

Line	Variable	Format	Description
	NRR	I5	Number of data lines describing the coordinates of the first vertical or horizontal block of nodes with NPP = 2 or 3
	NLL	I5	Number of data lines describing the vertical or horizontal distances of the repeating block of nodes with NPP = 2 or 3
	NCOR	I5	Number of data lines describing the coordinates of the nodes with NPP = 1
6C	NCM(I,1)	I5	Node number along the first block of nodes
	ECORD(I,1)	F10.4	X or Y coordinate of the node depending on the NPP value

Note:

Line 6C should be entered only if NPP = 2 or 3 and repeated NRR times.

6D	ECORD(I,2) I=1,NLL	7F10.4	X or Y distances of the repeating block of nodes
----	-----------------------	--------	--

Note:

Line 6D should be entered only if NPP = 2 or 3 and after line 6C.

8	PROP(I,1)	F10.4	Parameter α of VG model or h_d of BC model
	PROP(I,2)	F10.4	Parameter S_m
	PROP(I,3)	F10.4	Parameter n of VG model or λ of BC model
	PROP(I,4)	F10.4	Total porosity
	PROP(I,5)	F10.4	K_{sw} in the X - direction
	PROP(I,6)	F10.4	K_{sw} in the Y - direction

Note:

Line 8 should be repeated NMAT times.

APPENDIX B (Continued)

Line	Variable	Format	Description
9	DENR	F10.4	Ratio of oil to water density
	VISR	F10.4	Ratio of oil to water viscosity
	BAO	F10.4	Scaling parameter β_{ao}
	BOW	F10.4	Scaling parameter β_{ow}
10F	LPRW	I5	Index describing uniformity of initial water heads for 2D cases: = 1 uniform initial water head equal to PRHTW = 2 non-uniform case = 3 pressure heads interpolated along transects parallel to the y-axis
	LNPRW	I5	Number of transects for the case LPRW = 3
	PRHTW	F10.4	Uniform initial water head for the case LPRW = 1

Note:

Line 10F should be entered only if IMESH \neq 2 and IRES = 0.

10H	N1	I5	First node of the transect towards the y-axis.
	N2	I5	Second " " "
	YB	F10.4	Y-coordinate of the water table location along the transect

Note:

Line 10H should be repeated LNPRW times provided IRES = 0 and LPRW = 3.

12A	LPROP	I5	Index describing the uniformity of soil properties in the medium: = 1 uniform soil in the medium and given by material type LTYPE = 1 material distribution non-uniform
	LTYPE	I5	Uniform material type for the medium

APPENDIX B (Continued)

Line	Variable	Format	Description
13	TIME	F10.4	Starting time of the simulation. Usually zero unless a restart problem
	DELT	F10.4	Starting time increment
	TMAX	F10.4	Maximum simulation time
	DETFI	F10.4	Minimum time increment allowed
	DETFX	F10.4	Maximum time increment allowed
	DETRA	F10.4	Incremental factor for time steps (1.0 ≤ DETRA ≤ 1.1)
	PRT	F10.4	Time interval for results printouts
14	MAXTI	I5	Maximum number of time steps allowed
	ITRFI	I5	Minimum " " iterations "
	ITRFX	I5	Maximum " " "
	IPRCO	I5	Index to control additional printouts at each iterations of each time step providing details on convergence: = 0 no details required = 1 details printed
	RELCO	F10.4	Relative convergence error with respect to previous iteration values.
	ABSW	F10.4	Absolute convergence limit for the water phase
	ABSO	F10.4	Absolute convergence limit for the oil phase
15	ALI	F10.4	Upstream weighting parameter should be between 0 and 1.0
	WF	F10.4	Weighting factor for material properties and recommended value is 0.5

APPENDIX B (Continued)

Line	Variable	Format	Description
16	ITERM	I5	Index to control execution based on on flow simulation: = 0 uninterrupted simulation = 1 run terminated when total accumulated water in the system \geq TOTW = -1 same as for ITERM = 1 except when total water \leq TOTW = 2 run terminated when total accumulated oil in the system \geq TOTO = -2 same as ITERM = 2 except when total oil \leq TOTO
	TOTW	F10.4	Total volume of water prescribed under ITERM index and required if only ITERM = * 1
	TOTO	F10.4	Total volume of oil prescribed under ITERM index and required only if ITERM = * 2
17	IBTO(I,1)	I5	Nodal number of the node with type-1 boundary condition
	IBTO(I,2)	I5	Index for type-1 boundary condition for the water phase: = 0 type-1 does not apply; corresponds to zero-flux type = L type-1 applicable and the time dependent value given by cycle L
	IBTO(I,3)	I5	Same as for IBTO(I,2) but applicable for the oil phase

Note:

Line 17 should be entered only if NNTO $>$ 0

and repeated NNTO times (I=1, NNTO)

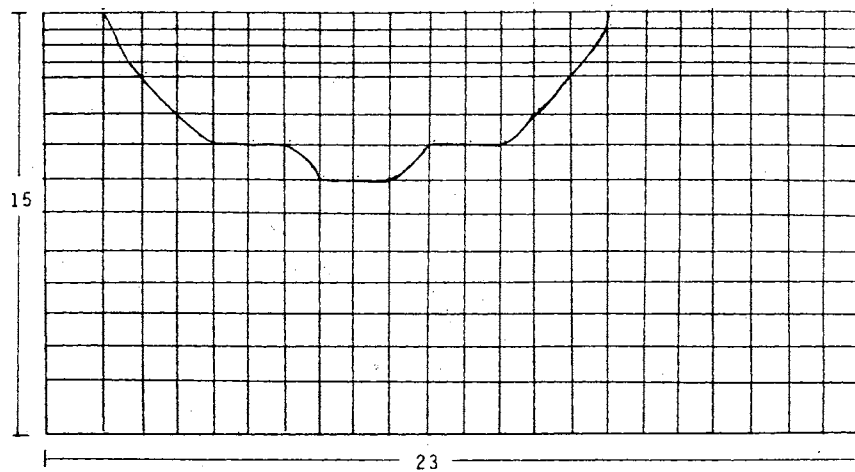
APPENDIX B (Continued)

Line	Variable	Format	Description
19A	IPRTO(L)	I5	Number of subcycles in cycle L
	PRTO(I,1,L)	F10.4	Starting time of the boundary condition of subcycle I of cycle L
	PRTO(I,2,L)	F10.4	Ending time of the boundary condition of subcycle I of cycle L
	PRTO(I,3,L)	F10.4	Starting value of subcycle I of cycle L
	PRTO(I,4,L)	F10.4	Ending value of subcycle I of cycle L

APPENDIX C

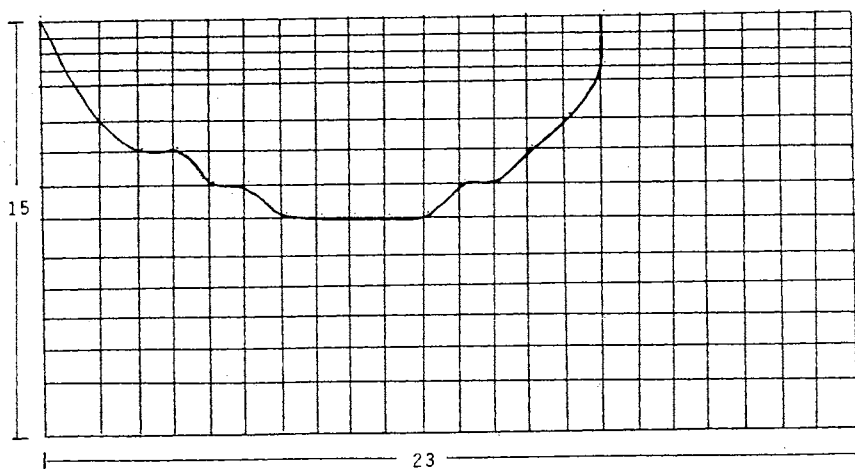
PLOTS OF HYDROCARBON PLUMES FOR
MOFAT 2-D SIMULATIONS

MOFAT 2-D
FINITE ELEMENT GRID



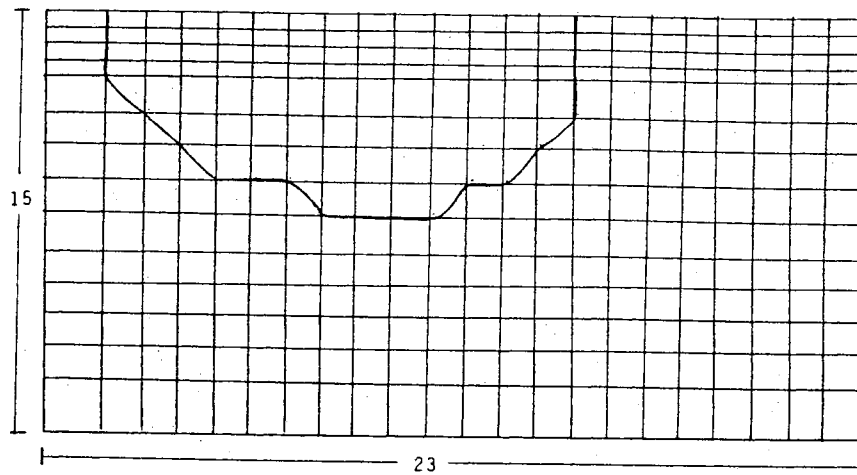
ALPHA=.05/m AT TIME=16HR

MOFAT 2-D
FINITE ELEMENT GRID



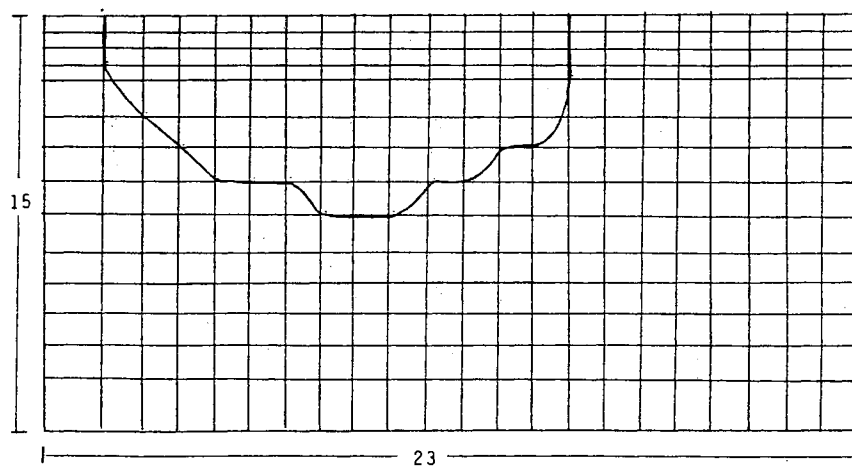
ALPHA=.2/m AT TIME=16HR

MOFAT 2-D
FINITE ELEMENT GRID



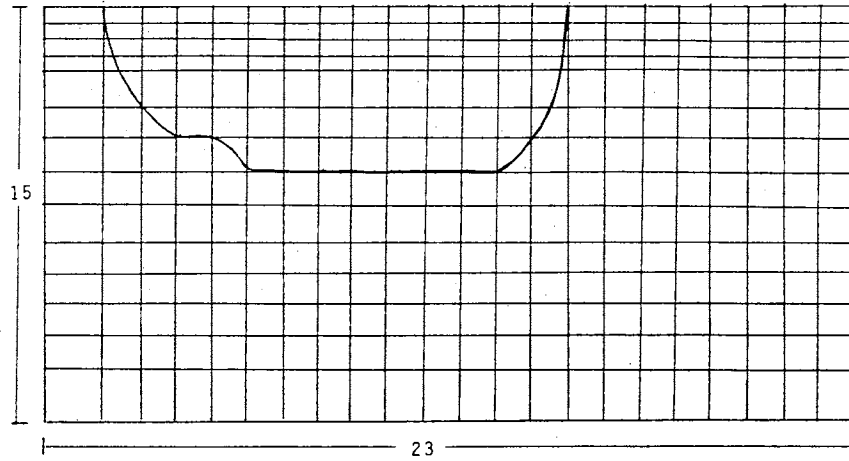
ALPHA=.3/m AT TIME=16HR

MOFAT 2-D
FINITE ELEMENT GRID



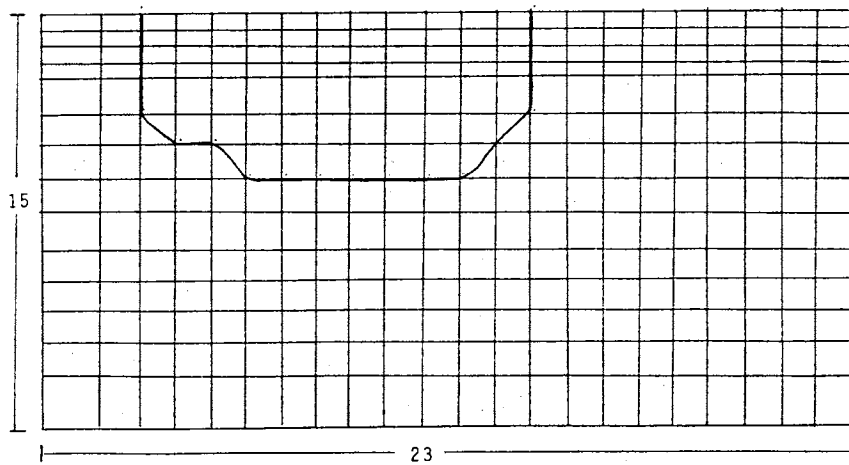
ALPHA=.4/m AT TIME=16HR

MOFAT 2-D
FINITE ELEMENT GRID



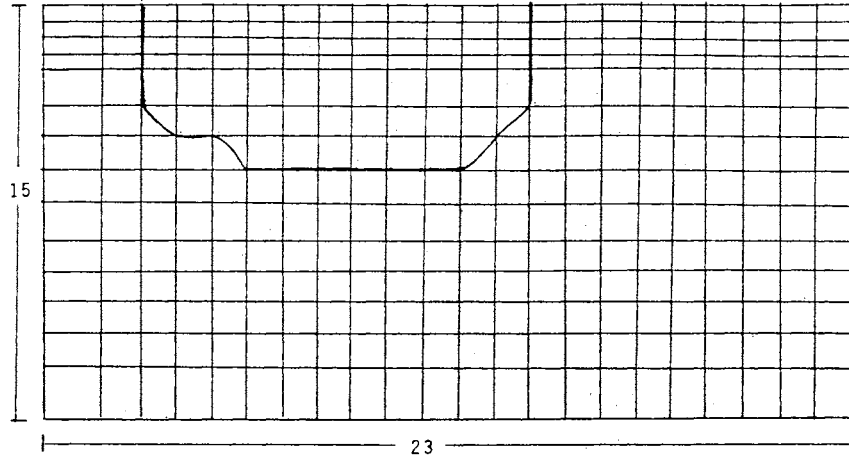
ALPHA=.5/m AT TIME=16HR

MOFAT 2-D
FINITE ELEMENT GRID



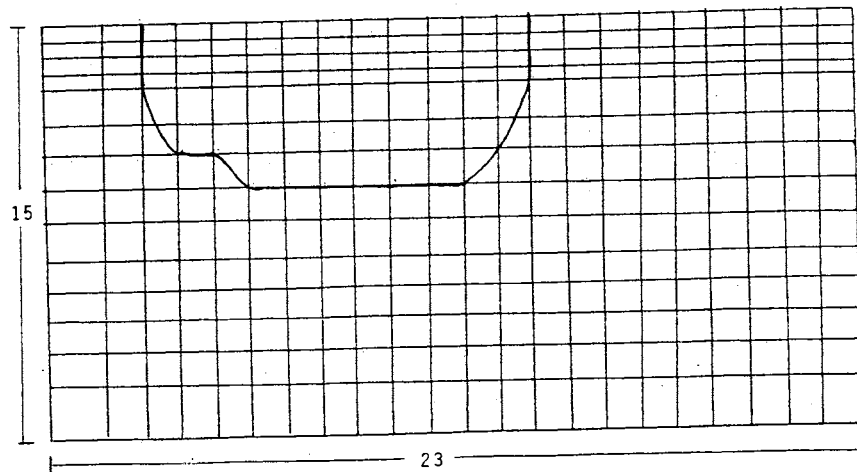
ALPHA=.6/m AT TIME=16HR

MOFAT 2-D
FINITE ELEMENT GRID



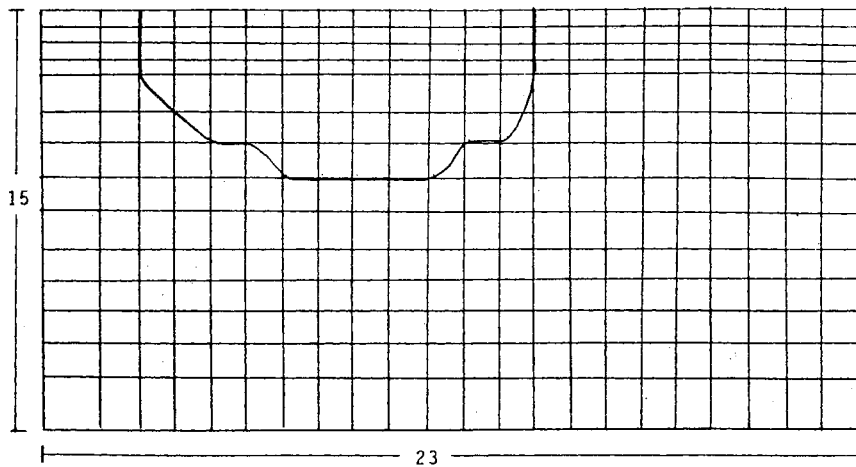
ALPHA=.7/m AT TIME=16HR

MOFAT 2-D
FINITE ELEMENT GRID



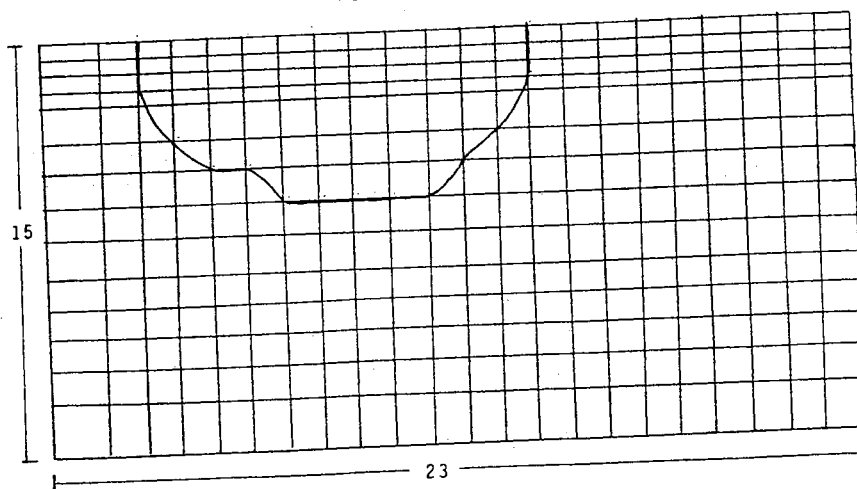
ALPHA=.8/m AT TIME=16HR

MOFAT 2-D
FINITE ELEMENT GRID



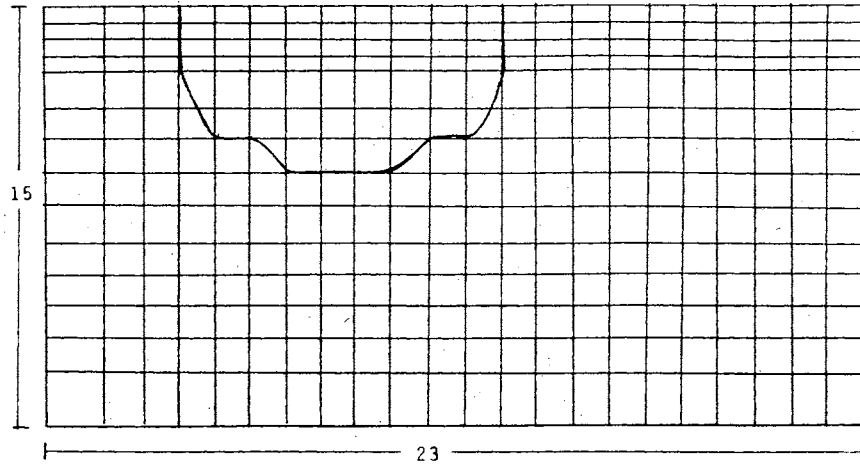
ALPHA=.9/m AT TIME=16HR

MOFAT 2-D
FINITE ELEMENT GRID



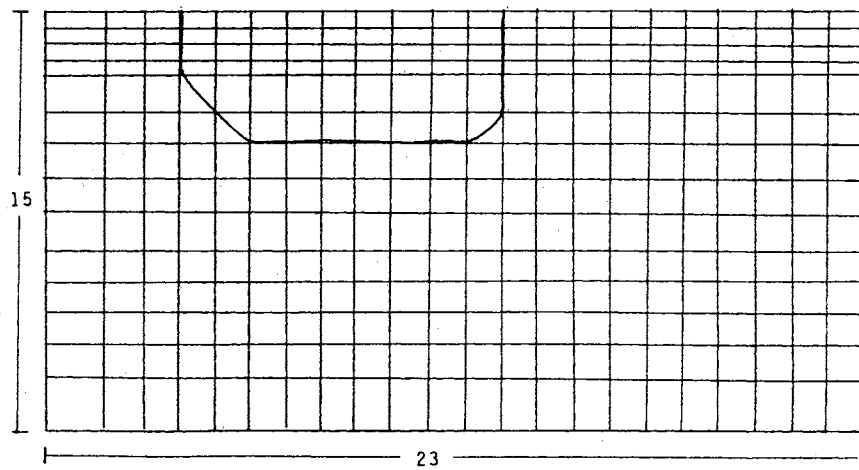
ALPHA=1.0/m AT TIME=16HR

MOFAT 2-D
FINITE ELEMENT GRID



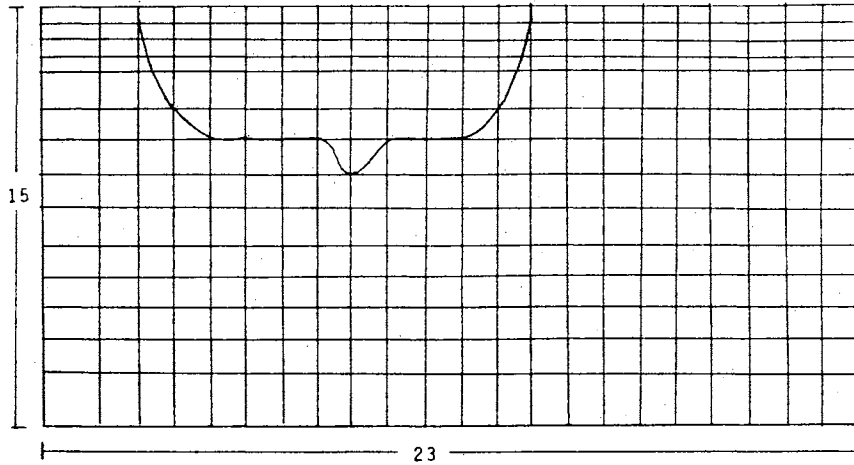
N=1.2 AT TIME=12HR

MOFAT 2-D
FINITE ELEMENT GRID



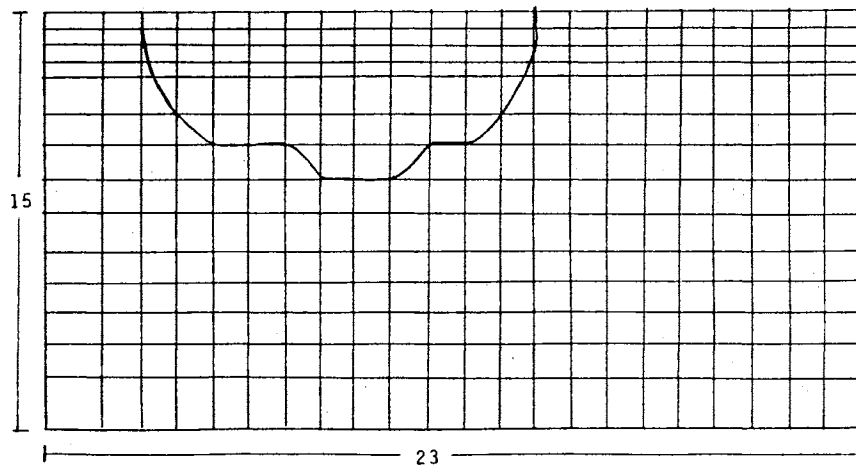
N=1.4 AT TIME=12HR

MOFAT 2-D
FINITE ELEMENT GRID



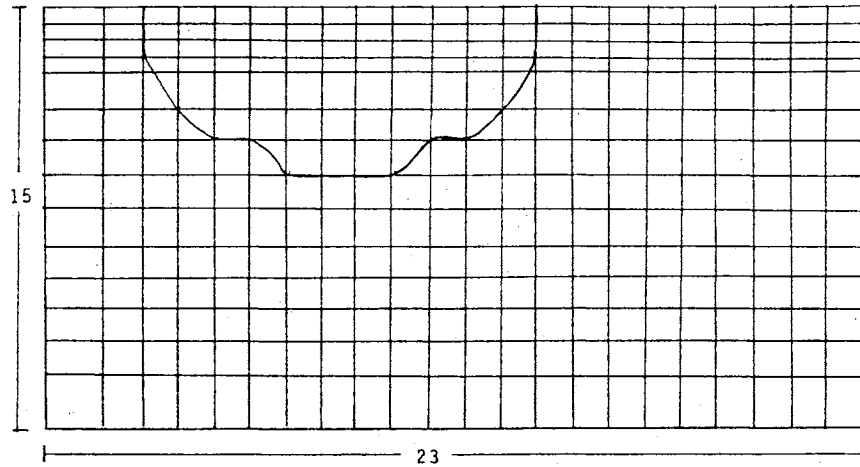
N=1.6 AT TIME=12HR

MOFAT 2-D
FINITE ELEMENT GRID



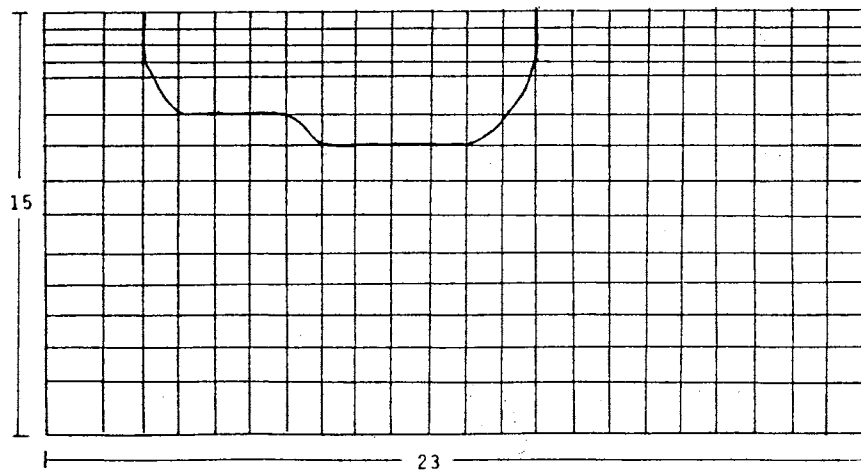
N=1.8 AT TIME=12HR

MOFAT 2-D
FINITE ELEMENT GRID



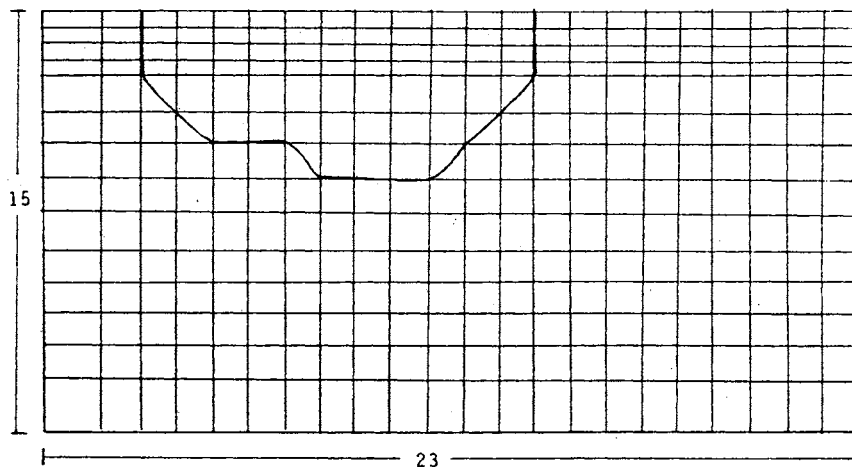
N=2.0 AT TIME=12HR

MOFAT 2-D
FINITE ELEMENT GRID



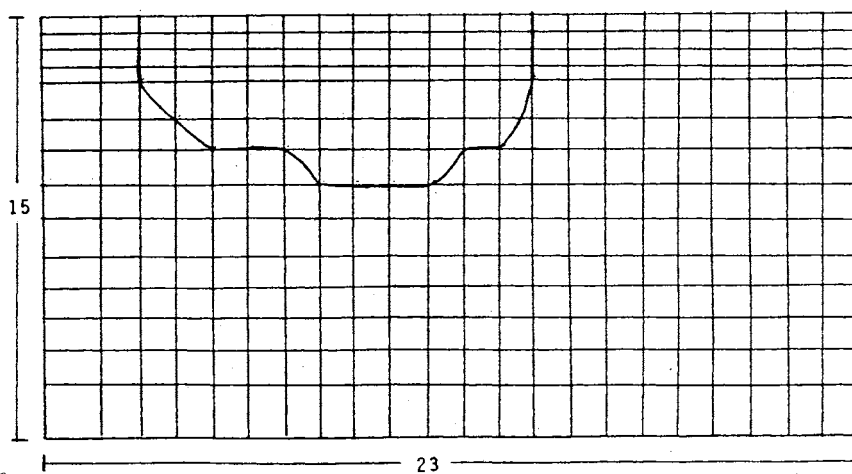
N=2.2 AT TIME=12HR

MOFAT 2-D
FINITE ELEMENT GRID



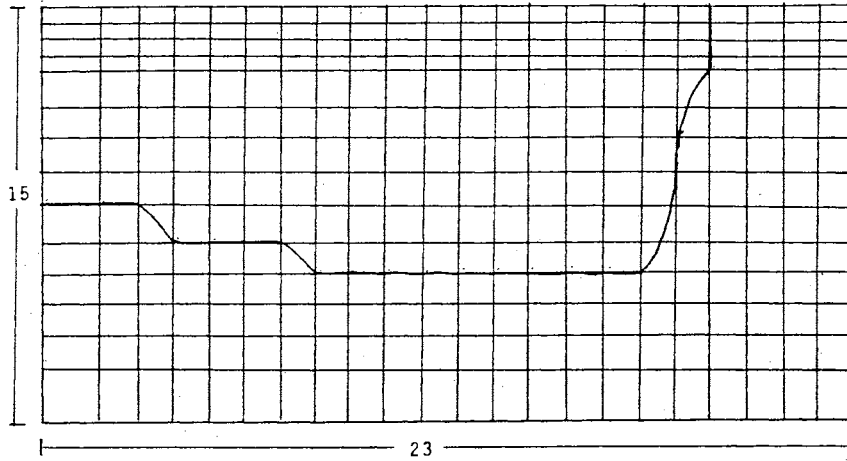
$N=2.4$ AT TIME=12HR

MOFAT 2-D
FINITE ELEMENT GRID



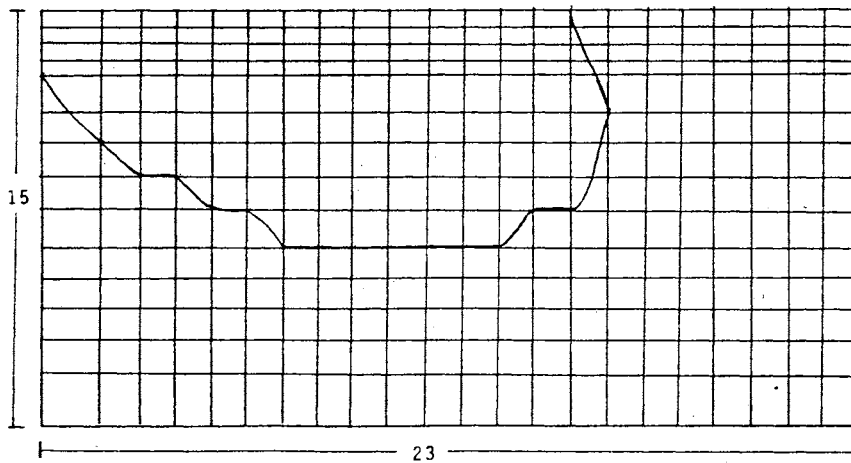
$N=2.6$ AT TIME=12HR

HOFAT 2-D
FINITE ELEMENT GRID



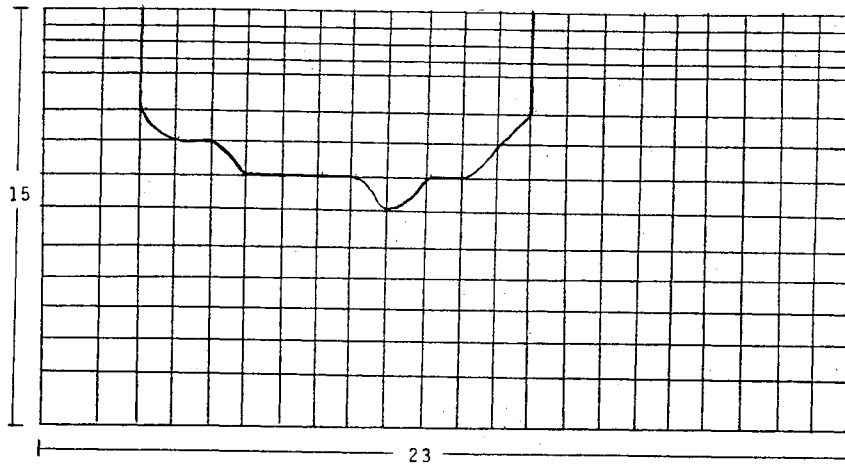
POROSITY=5% AT TIME=12HR

HOFAT 2-D
FINITE ELEMENT GRID



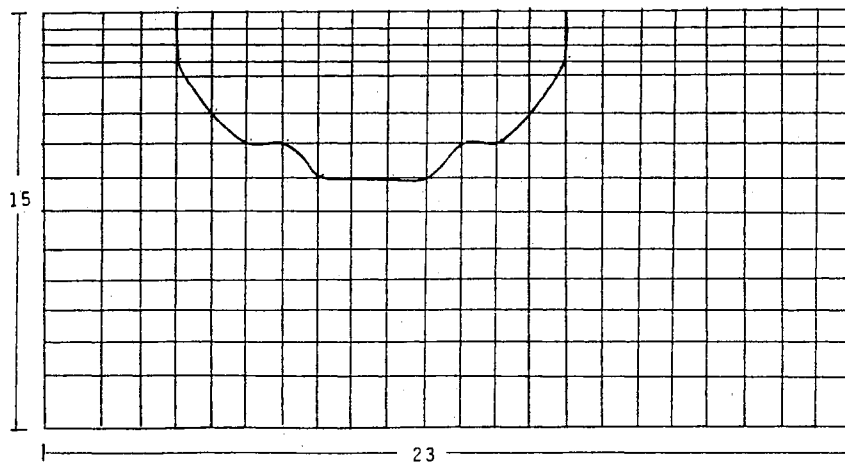
POROSITY=10% AT TIME=12HR

MOFAT 2-D
FINITE ELEMENT GRID



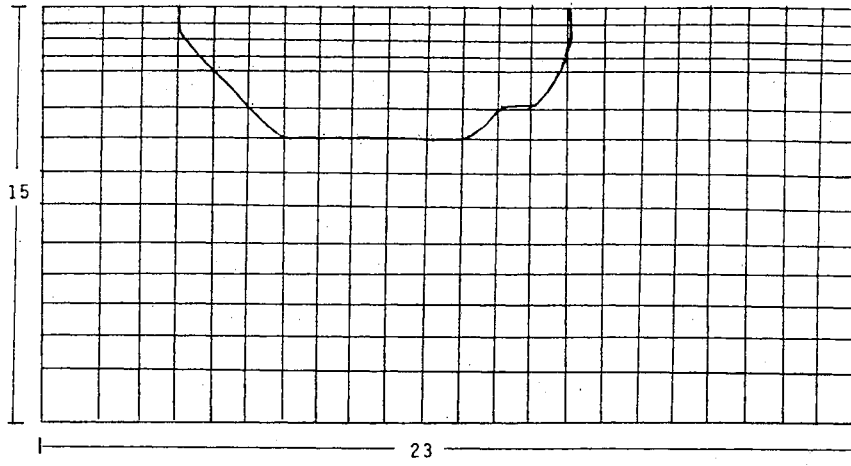
POROSITY=20% AT TIME=12HR

MOFAT 2-D
FINITE ELEMENT GRID



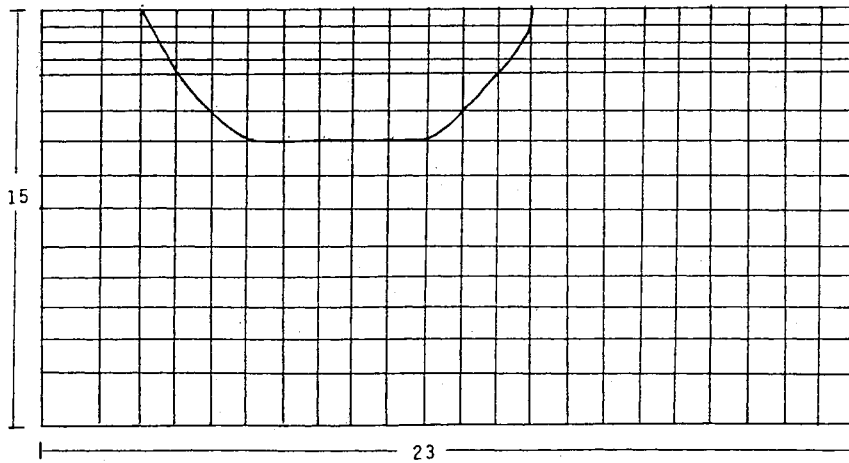
POROSITY=30% AT TIME=12HR

HOFAT 2-D
FINITE ELEMENT GRID



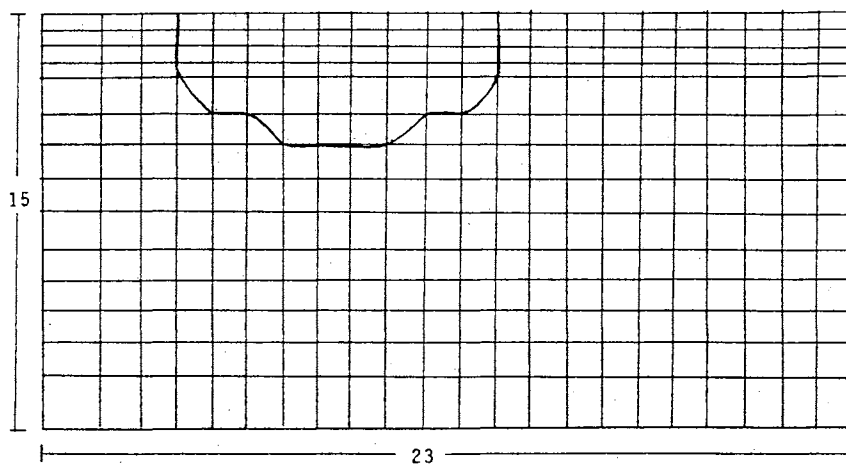
POROSITY=40% AT TIME=12HR

HOFAT 2-D
FINITE ELEMENT GRID



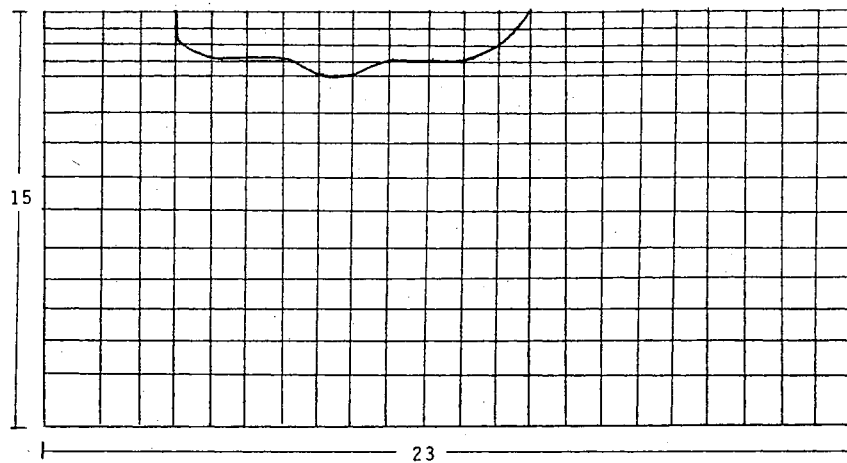
POROSITY=45% AT TIME=12HR

MOFAT 2-D
FINITE ELEMENT GRID



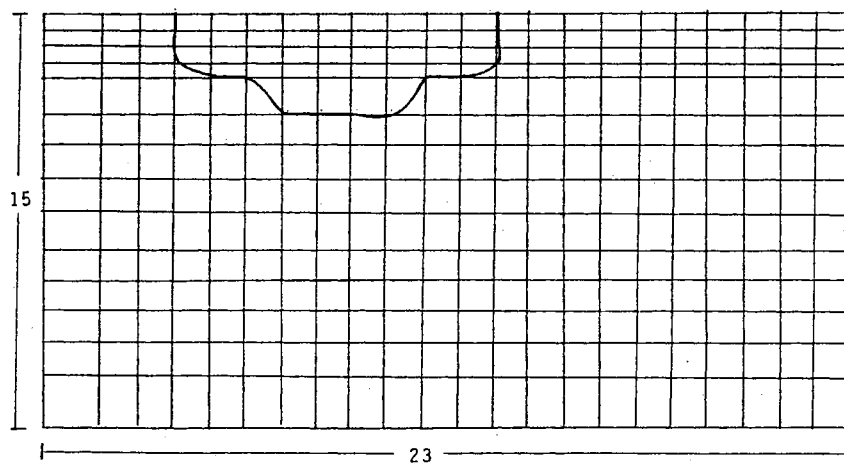
POROSITY=50% AT TIME=12HR

MOFAT 2-D
FINITE ELEMENT GRID



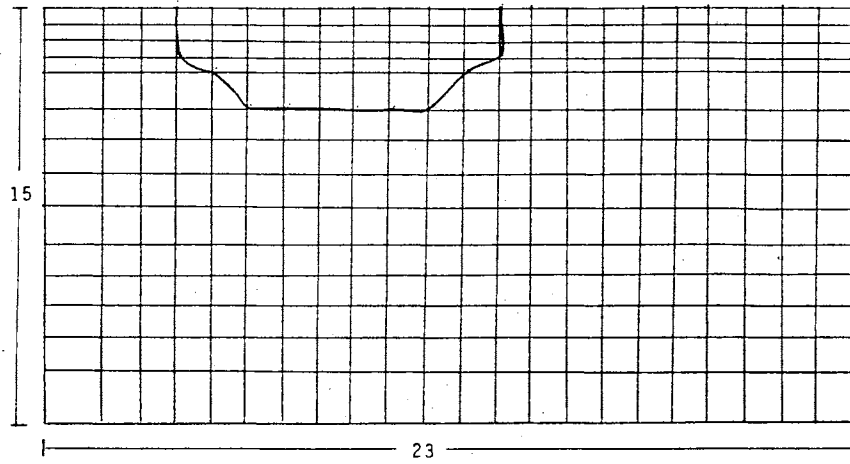
$K_{sw} = .2$ AT TIME=4HR

MOFAT 2-D
FINITE ELEMENT GRID



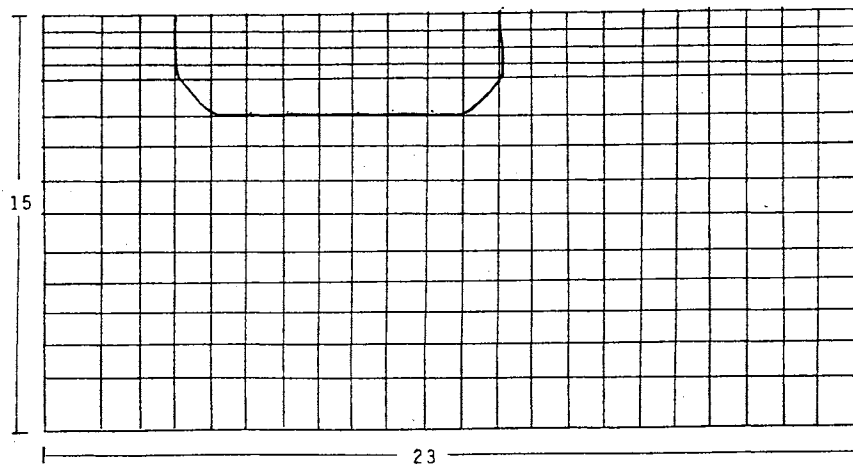
$K_{sw} = .4$ AT TIME=4HR

MOFAT 2-D
FINITE ELEMENT GRID



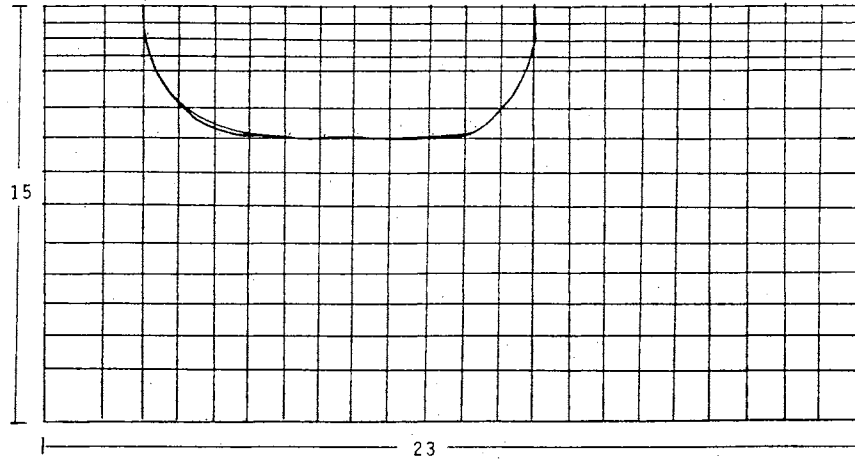
$K_{sw} = .5$ AT TIME=4HR

MOFAT 2-D
FINITE ELEMENT GRID



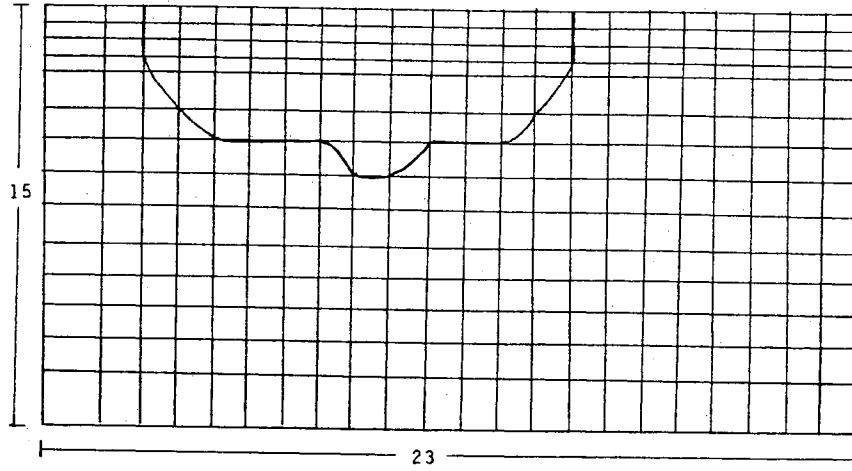
$K_{sw} = .6$ AT TIME=4HR

MOFAT 2-D
FINITE ELEMENT GRID



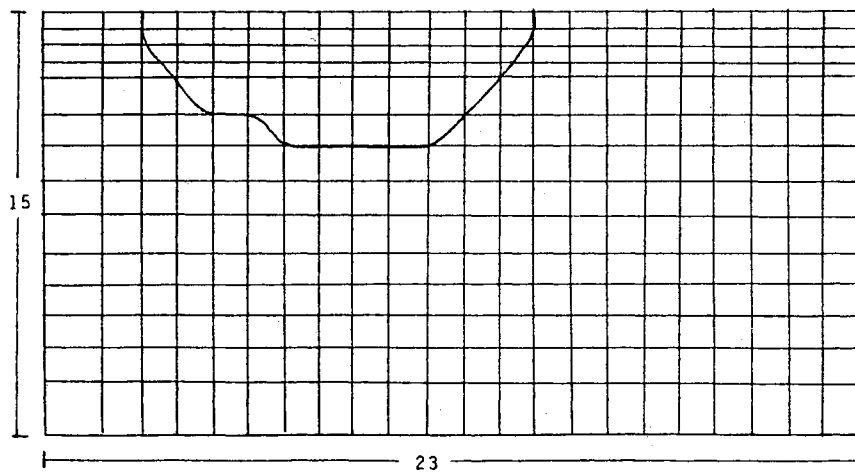
Ksw=1.0 AT TIME=4HR

MOFAT 2-D
FINITE ELEMENT GRID



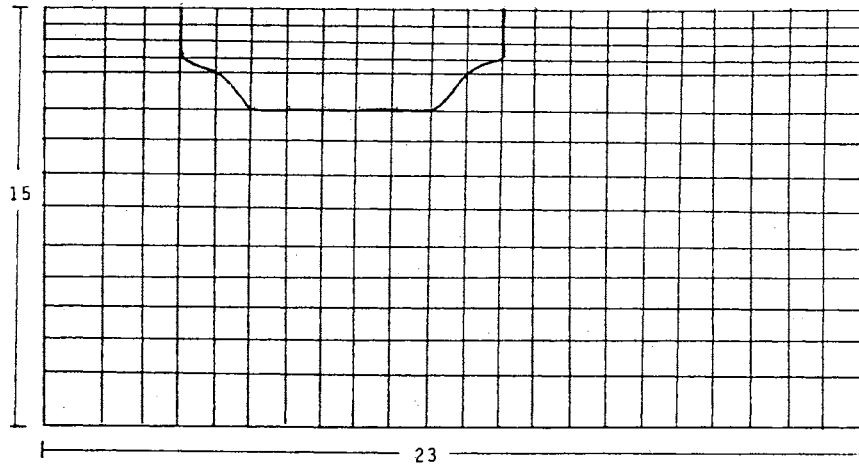
VISCOSITY=.7 AT TIME=4HR

MOFAT 2-D
FINITE ELEMENT GRID



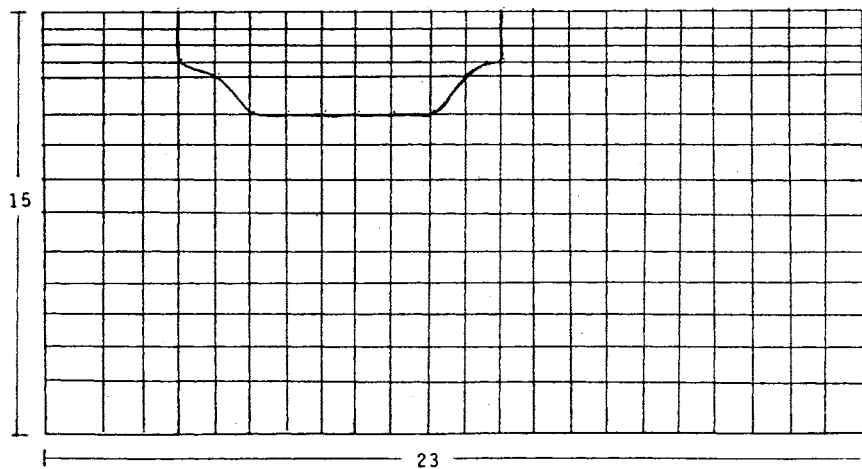
VISCOSITY=1.0 AT TIME=4HR

MOFAT 2-D
FINITE ELEMENT GRID



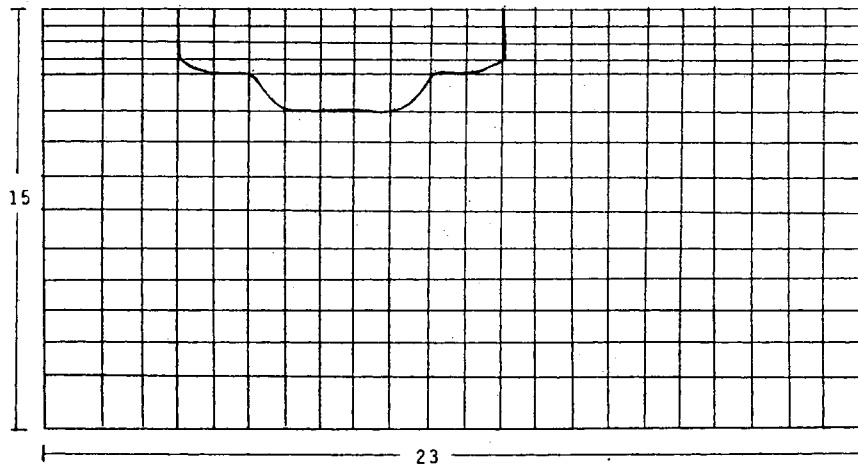
VISCOSITY=1.5 AT TIME=4HR

MOFAT 2-D
FINITE ELEMENT GRID



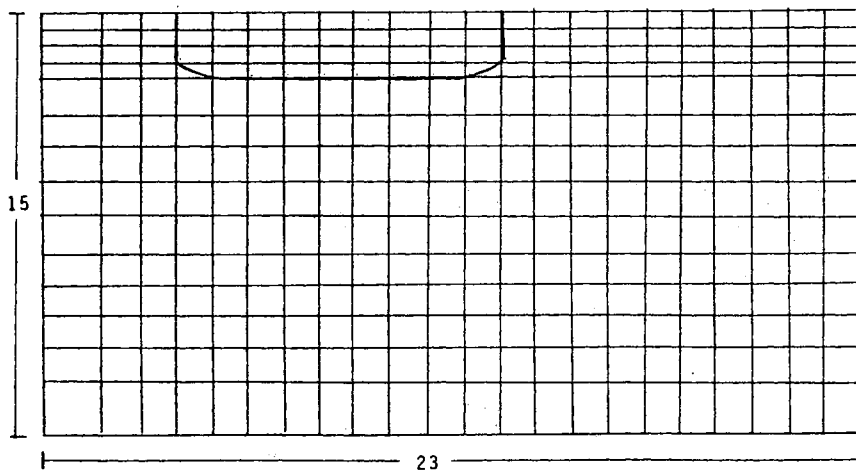
VISCOSITY=1.7 AT TIME=4HR

MOFAT 2-D
FINITE ELEMENT GRID



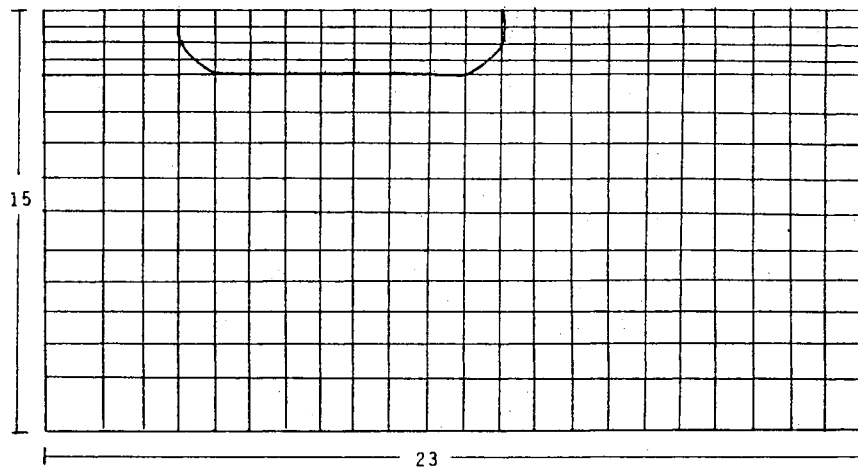
VISCOSITY=2.0 AT TIME=4HR

MOFAT 2-D
FINITE ELEMENT GRID



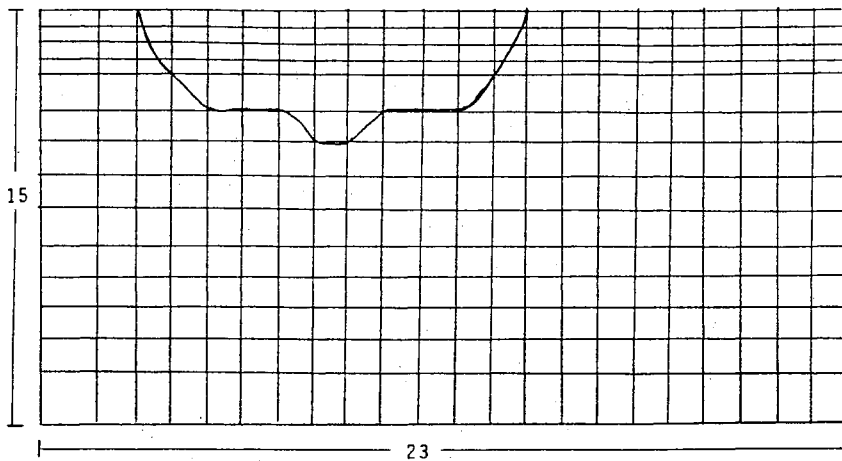
VISCOSITY=2.3 AT TIME=4HR

MOFAT 2-D
FINITE ELEMENT GRID



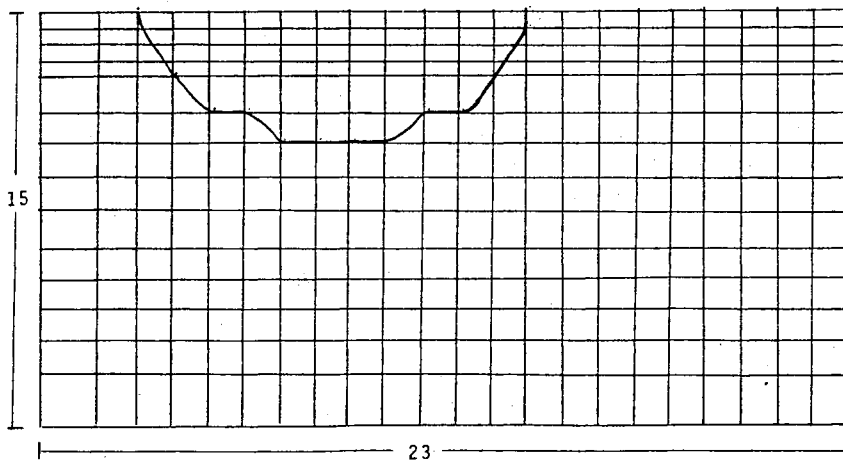
VISCOSITY=2.5 AT TIME=4HR

HOFAT 2-D
FINITE ELEMENT GRID



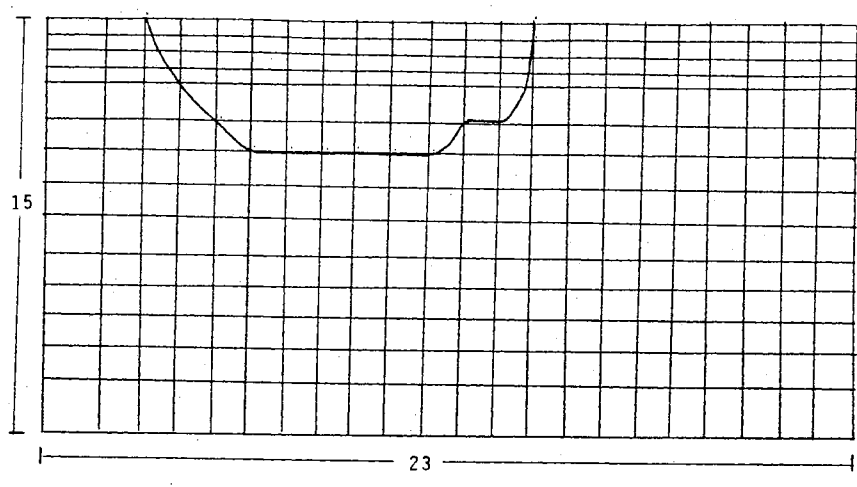
DENSITY=.4 AT TIME=8HR

HOFAT 2-D
FINITE ELEMENT GRID



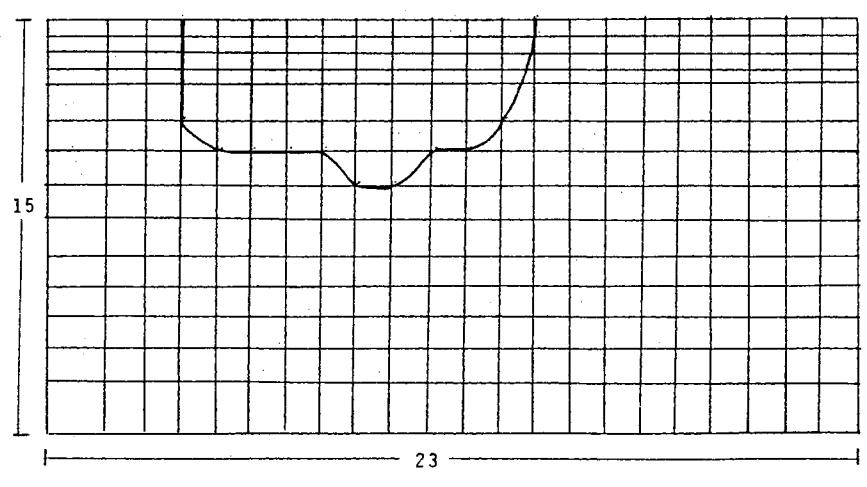
DENSITY=.6 AT TIME=8HR

MOFAT 2-D
FINITE ELEMENT GRID



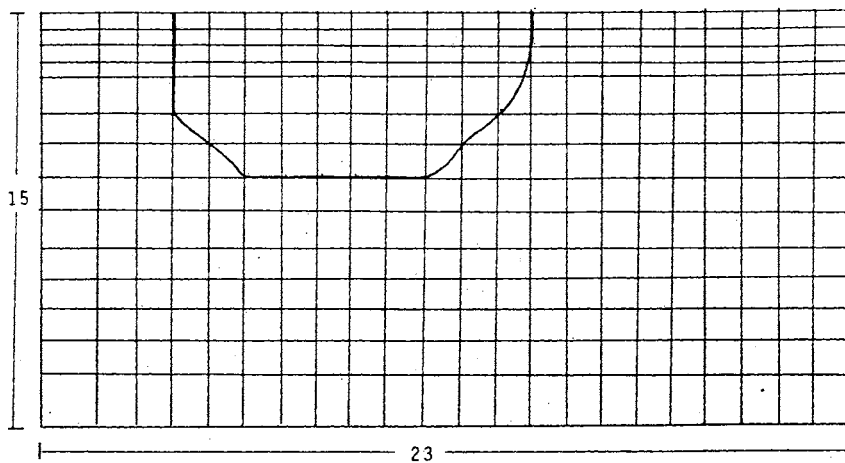
DENSITY=1.2 AT TIME=8HR

MOFAT 2-D
FINITE ELEMENT GRID



DENSITY=1.6 AT TIME=8HR

HOFAT 2-D
FINITE ELEMENT GRID



DENSITY=1.8 AT TIME=8HR

APPENDIX D

CURVE EQUATIONS FOR INFILTRATION TIME
VS PARAMETER

Alpha Parameter:

COEF A	COEF B	COEF C	R ²	R ^{2C}	EQUATION
-.5871D+1	.4274	0	.9880	.9865	Y=1/(A+B+X)

N Parameter:

COEF A	COEF B	COEF C	R ²	R ^{2C}	EQUATION
.2827D+1	.7093D+3	-.2345	.9994	.9992	Y=A*B ^(1/X) *X ^C

Porosity Parameter:

COEF A	COEF B	COEF C	R ²	R ^{2C}	EQUATION
-.5778D-05	-.3733D+3	.7662	.9996	.9994	Y=1/(A*(X+B) ² +C)

Permeability Parameter:

COEF A	COEF B	COEF C	R ²	R ^{2C}	EQUATION
.7468D-02	.6877D+1	.1146	1.000	1.000	Y=A+B/X+C/X*X

Density Parameter:

COEF A	COEF B	COEF C	R ²	R ^{2C}	EQUATION
.5326D+1	-.4086	.8638D-2	.9985	.9978	Y=A+B*X+C*X*X

Viscosity Parameter:

COEF A	COEF B	COEF C	R ²	R ^{2C}	EQUATION
-.2918D-2	.8968+1	0	.9997	.9997	Y=X/(A*X+B)

VITA

James E. Martell

Candidate for the Degree of
Master of Science

Thesis: FINITE ELEMENT MODELING OF IMMISCIBLE
HYDROCARBONS IN GROUNDWATER SYSTEMS

Major Field: Civil Engineering

Biographical:

Personal Data: Born in Idaho Falls, Idaho, May 30,
1964, son of Paul J. and Patricia Martell,
moved to Bartlesville, Oklahoma, 1967.

Education: Graduated from Sooner High School,
Bartlesville, Oklahoma, May 1982; Received
Bachelor of Science Degree in Geology from
Oklahoma State University in December, 1986;
completed requirements for the Master of
Science degree at Oklahoma State University in
July, 1989.

Professional Experience: Research Assistant,
Department of Civil Engineering, Oklahoma
State University, January, 1986 to December,
1988; Engineer for Hydrologic Inc. Engineering
Consultants, August, 1986 to August, 1988.
Currently employed by the Tulsa District Corp
of Engineers.

Professional Affiliations: Member of Association
of Groundwater Scientist and Engineers, student
member of American Association of Petroleum
Geologists, Student Member of American Society
of Civil Engineers.